Neutron Scattering Measurements

Y. Danon

Professor and Director Gaerttner LINAC Center
Nuclear Engineering Program Director
Department of Mechanical, Aerospace and Nuclear Engineering
Rensselaer Polytechnic Institute, Troy, NY, 12180

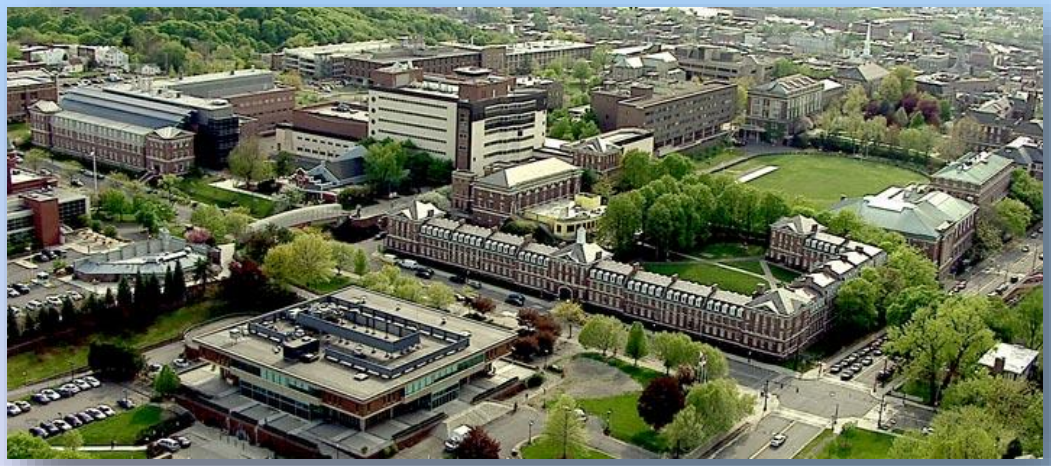

Joint ICTP-IAEA School on "Nuclear Data Measurements for Science and Applications", October 26, 2015, Trieste, Italy

Outline

- **Introduction**
  - Why we need nuclear data
  - The RPI nuclear data program
- **Neutron Scattering**
  - Why it is important
  - Basic physics
  - Types of neutron scattering phenomena
- **Examples of different experiments**
  - Thermal neutron scattering
  - Resonance neutron scattering
  - Fast neutron scattering

Why Should We Care About Nuclear Data?

Reactor Physics Calculations

Nuclear Data (Uncertainty)

Geometry Data

Computational Methods (Physics) (Uncertainty??)

Results
Accuracy??

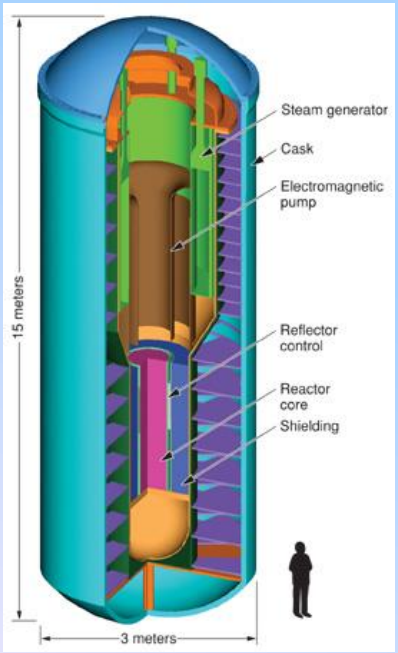

www.llnl.gov

The Shippingport Reactor (Critical in 1957)
http://www.pabook.libraries.psu.edu/palitmap/Shippingport.html

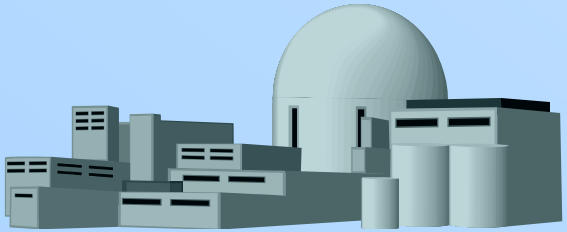

- Effective neutron Multiplication factor
- Neutron flux
- Burnup
- Kinetics

Nuclear Data Lifecycle (Danon's view)

Application Driven

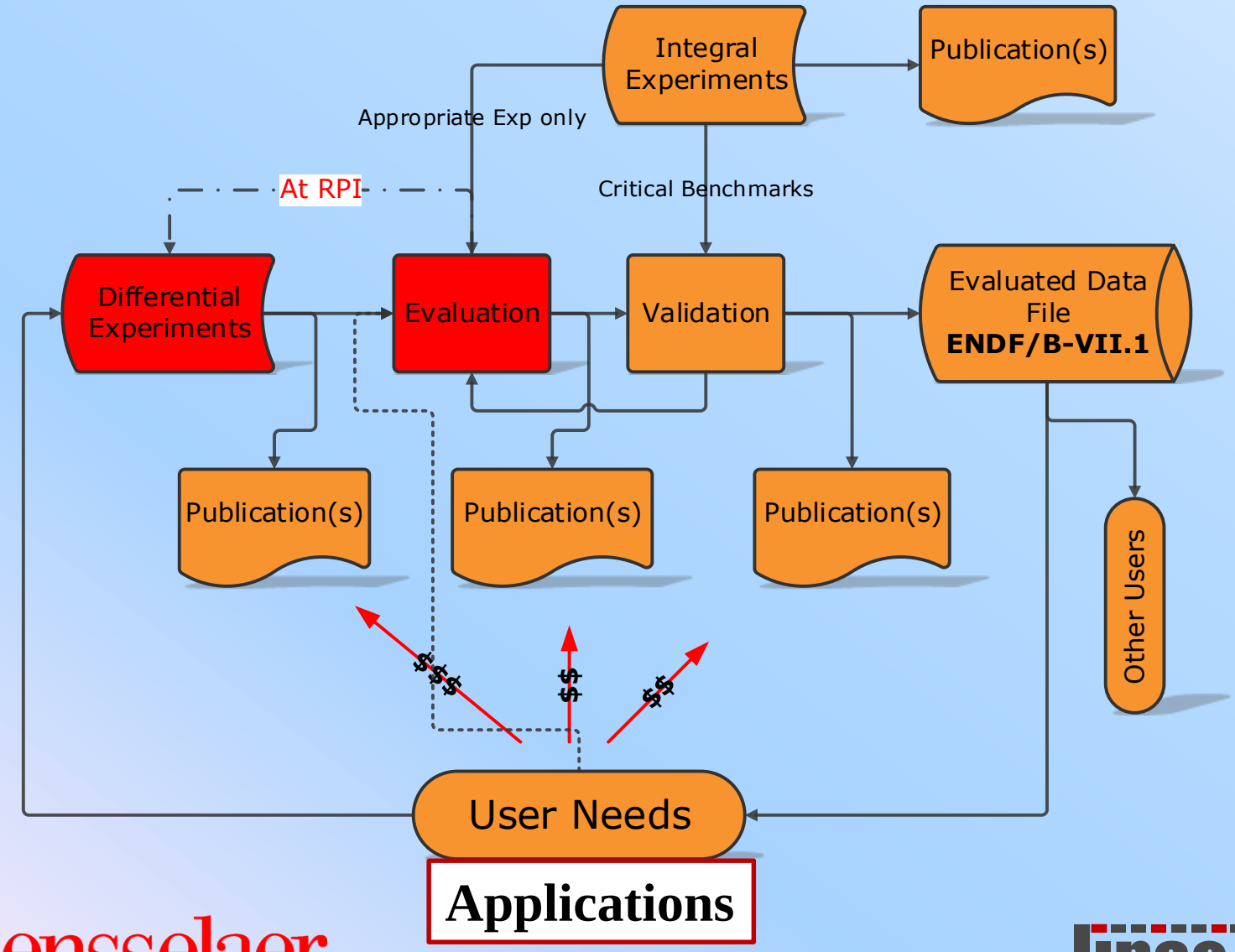

Where is the RPI LINAC ?

- It is on the highest point in Troy, NY

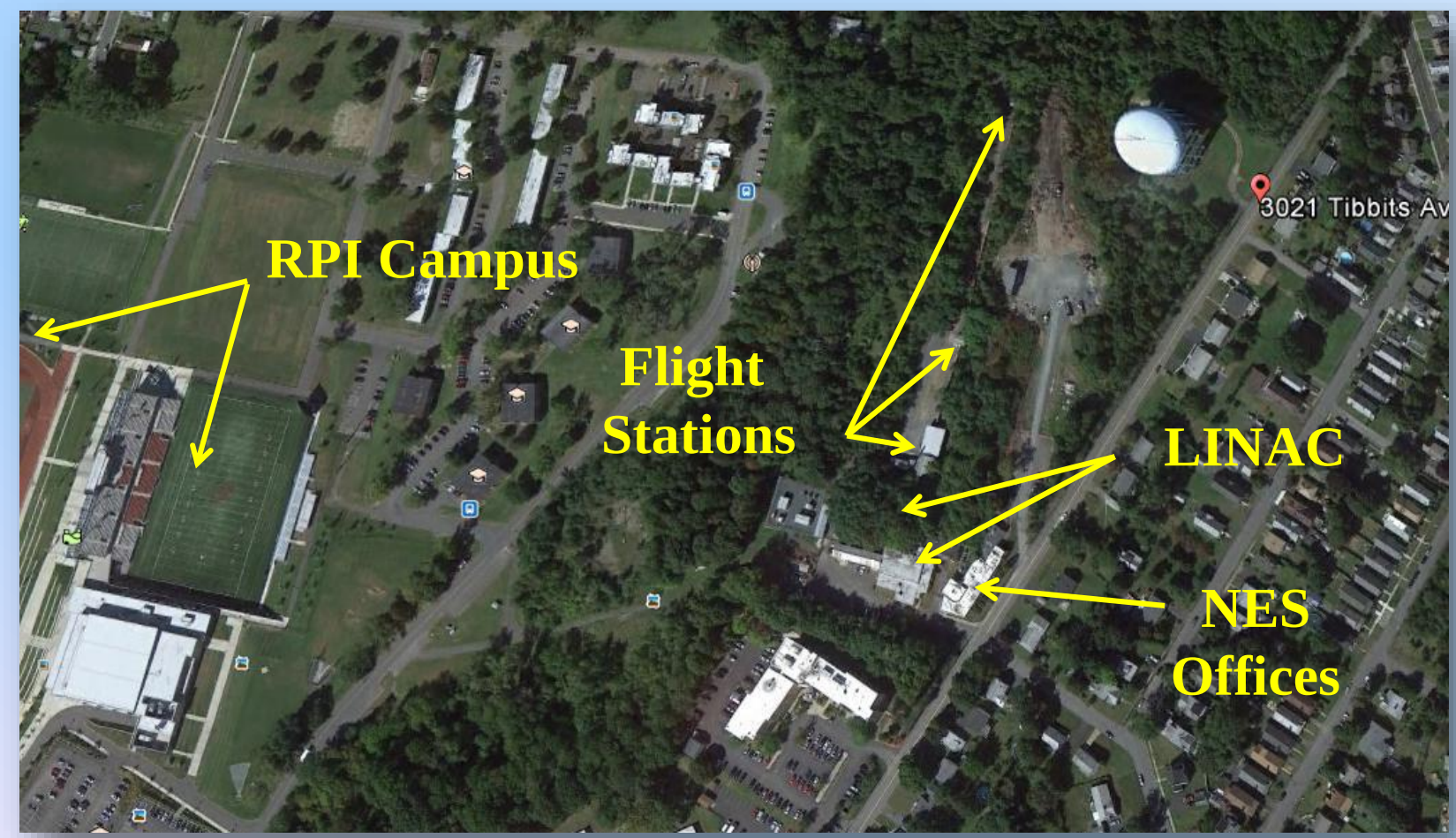

The RPI LINAC Facility

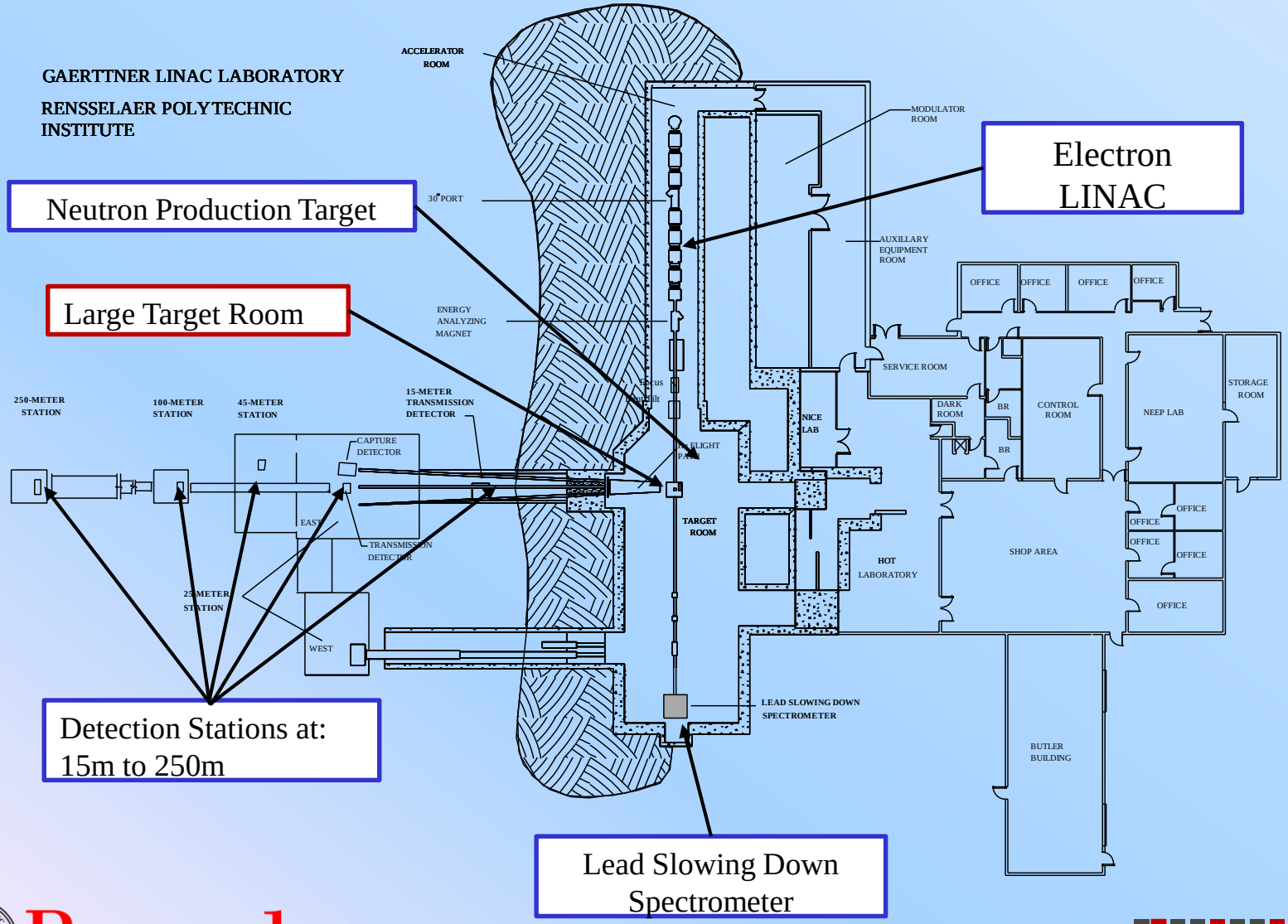

Neutron Production Target

Large Target Room

Detection Stations at:
15m to 250m

Electron LINAC

Lead Slowing Down Spectrometer

Rensselaer

linac The Gaerttner LINAC Center

Current Activity

- **Time of flight measurements**
  - Resonance Region
    - Capture (0.01 eV – 2 keV)
    - Transmission (0.001 eV – 100 KeV)
    - Capture to fission ratio (alpha)
    - keV capture detector
    - Neutron scattering (E<0.5 MeV)
  - High energy (0.4-20MeV)
    - Scattering (30 m flight path)
    - Transmission (100m and 250m flight path)
    - Prompt Fission Neutron Spectra
  - High accuracy total cross section measurements using filtered beam
- **Lead Slowing Down Spectrometer**
  - Simultaneous measurement of fission cross sections and fission fragment mass and energy distributions using the RPI lead slowing down spectrometer
  - Measurements of energy dependent (n,p) and (n,α) cross sections of nanogram quantities of short-lived isotopes. (collaboration with LANL).
  - Capture cross section measurements
- **Other**
  - Research on medical isotope production
  - S(α,β) measurements (at SNS in ORNL)

Neutron Production Targets

Bare Bounce Target (BBT)

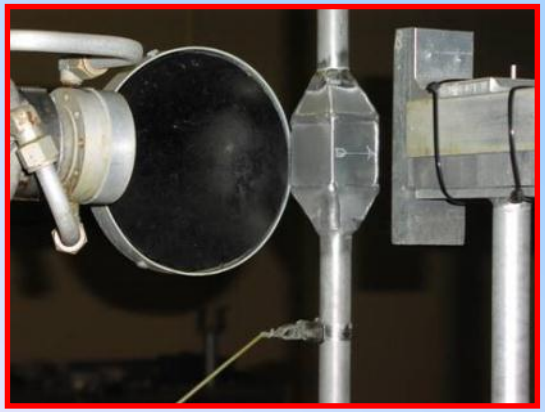

Enhanced Thermal Target (ETT)

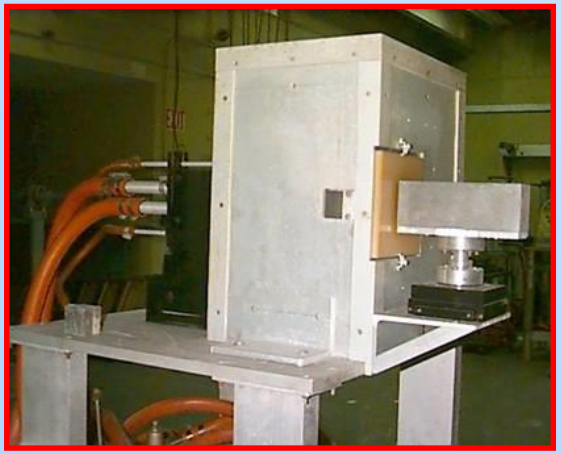

PACMAN Target

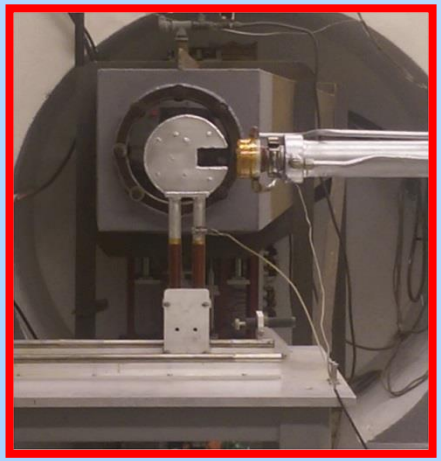

Detectors

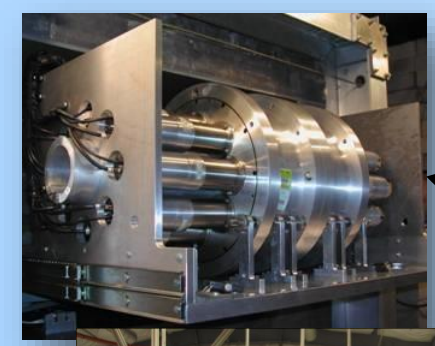

25m

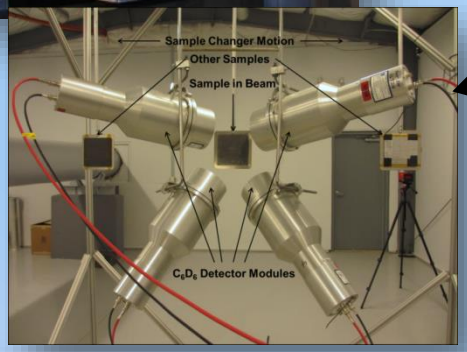

Capture/multiplicity

45m

Transmission

15m- 30m

100m

250m

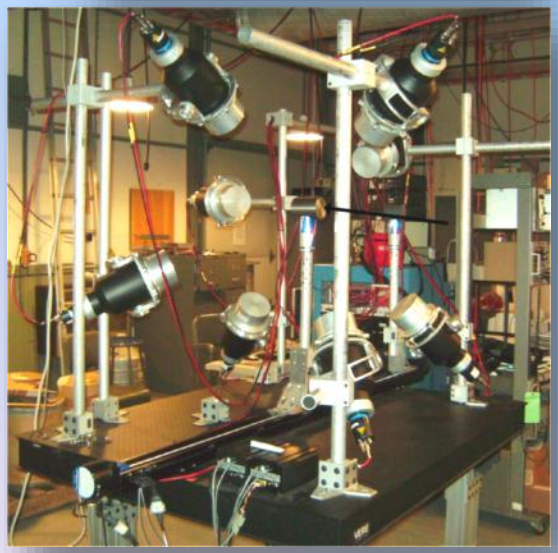

Scattering

PFNS

30m

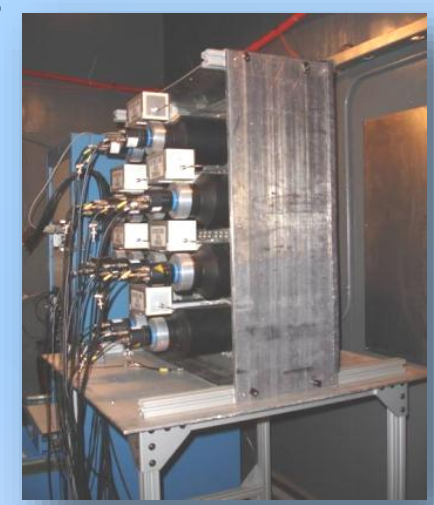

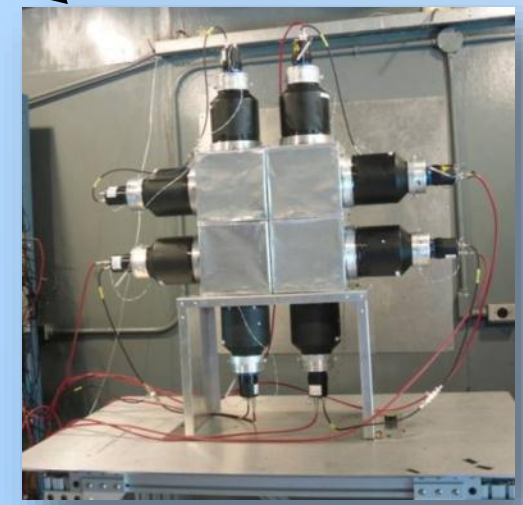

Capability Matrix and Development

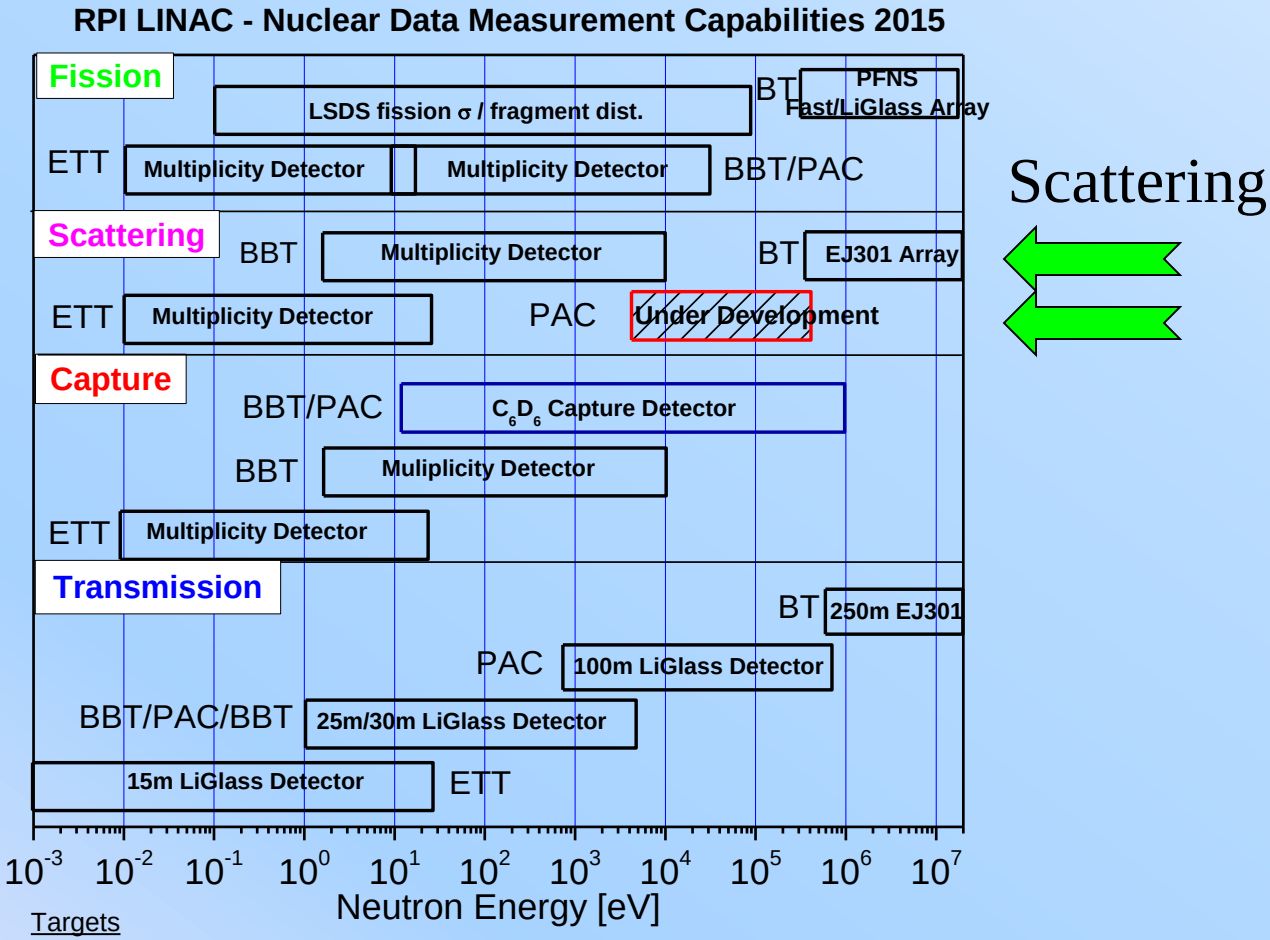

Scattering

Targets
ETT- Enhanced Thermal Traget
BBT - Bare Bounce Target
BT- Bare Target on Axis
PAC - PacMan Target

Motivation
The Neutron Transport Equation

- The scattering term appears in the neutron transport equation:
  - Double differential scattering
  - Total scattering is part of the total cross section
- Important for characterizing neutron slowing down from fission energy spectrum to the thermal spectrum
- Quantifies probability to scatter from:
  - Energy *E*' to *E*
  - Solid angle Ω' to Ω

$$\frac{1}{v}\frac{\partial\phi(\mathbf{r},E,\Omega,t)}{\partial t}+\Omega\cdot\nabla\phi(\mathbf{r},E,\Omega,t)+\Sigma_t(\mathbf{r},E)\phi(\mathbf{r},E,\Omega,t)=$$

$$\int_{4\pi}d\Omega'\int_0^\infty dE'\Sigma_s(E'\rightarrow E,\Omega'\rightarrow\Omega)\phi(\mathbf{r},E,\Omega,t)+s(\mathbf{r},E,\Omega,t)$$

The Concept of Compound Nucleus

- The neutron incident on a target material first creates a compound nucleus.
- The probability to form a compound nucleus increases near energy levels in the compound nucleus.
  - The magnitude of this increase is determined by the lifetime of the compound nucleus state.
  - There are several decay modes resulting in different interaction rates.

$$n + {}^{A}_{z}A \rightarrow {}^{A+1}_{Z}B^{*}$$

$n + {}^{A}_{z}X$ **Elastic Scattering**

$n + {}^{A}_{z}X^{*}$ **Inelastic Scattering**

${}^{A+1}_{z}X + \gamma$ Radiative Capture

${}^{A1}_{z1}X + {}^{A2}_{z2}X + \nu n$ Fission

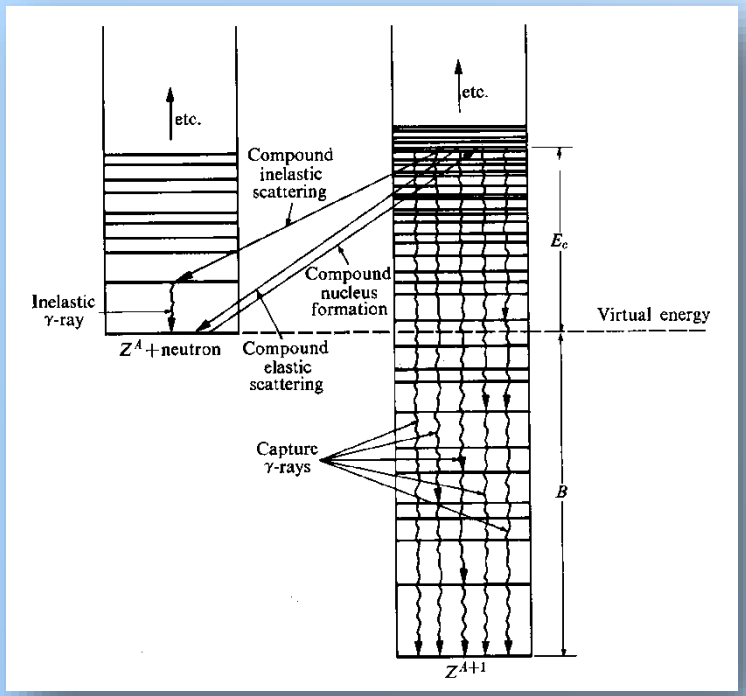

Types of neutron scattering

- **By collision type:**
  - Elastic
  - Inelastic (usually results in gamma emission)
- **By incident energy range:**
  - Thermal Scattering (E < 1 eV)
    - Molecular structure is important
    - Vibration rotational modes results in up scattering
  - Resonance Scattering
    - Similar to the thermal scattering effect
    - Small energy change → neutrons can scatter in/out of a resonance
  - Epi-thermal / fast neutron scattering
    - Elastic/inelastic collisions

Simple kinematics (Target at Rest)

- For target at rest the kinematic is usually done in center of mass system.
- For a given excitation state Q (this is a negative number) and a given scattering angle cosine μ, the relation between cm and lab is given by:

$$\mu_L = \frac{\gamma + \mu_c}{\left(1 + 2\gamma\mu_c + \gamma^2\right)^{1/2}} \qquad \text{where} \qquad \gamma = \left(A^2 + \frac{A(A+1)Q}{E}\right)^{-1/2}$$

- The neutron energy following a scattering collision is give by:

$$E' = \frac{1}{2}E(1+\alpha) + \frac{1}{2}(1-\alpha)E\sqrt{1+\Delta}\mu_c + Q\frac{A}{A+1}$$

where $\alpha = \left(\frac{A-1}{A+1}\right)^2$ $\Delta = \frac{Q}{E}\frac{A+1}{A}$

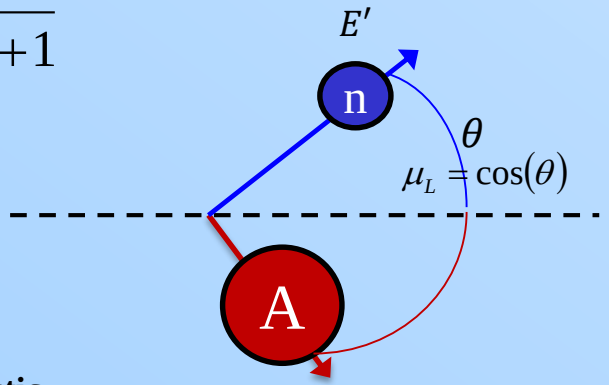

- **For elastic scattering Q=0 and thus E`$_{inelastic}$<E`$_{elastic}$**

Example: ^{56}Fe scattering cross section

Exited levels start at about 847 keV

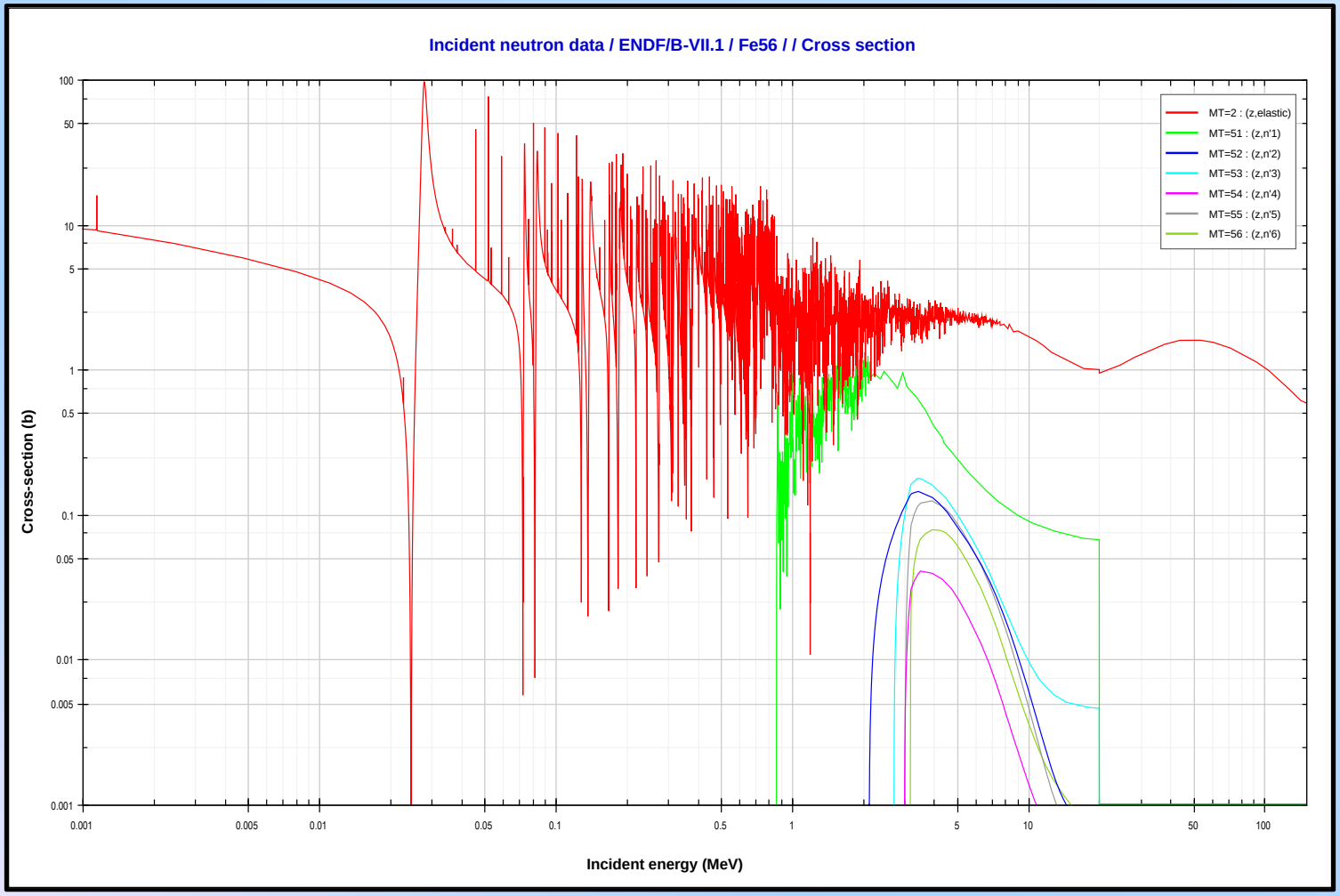

Example: ^{238}U scattering cross section

Exited levels start at about 45 keV

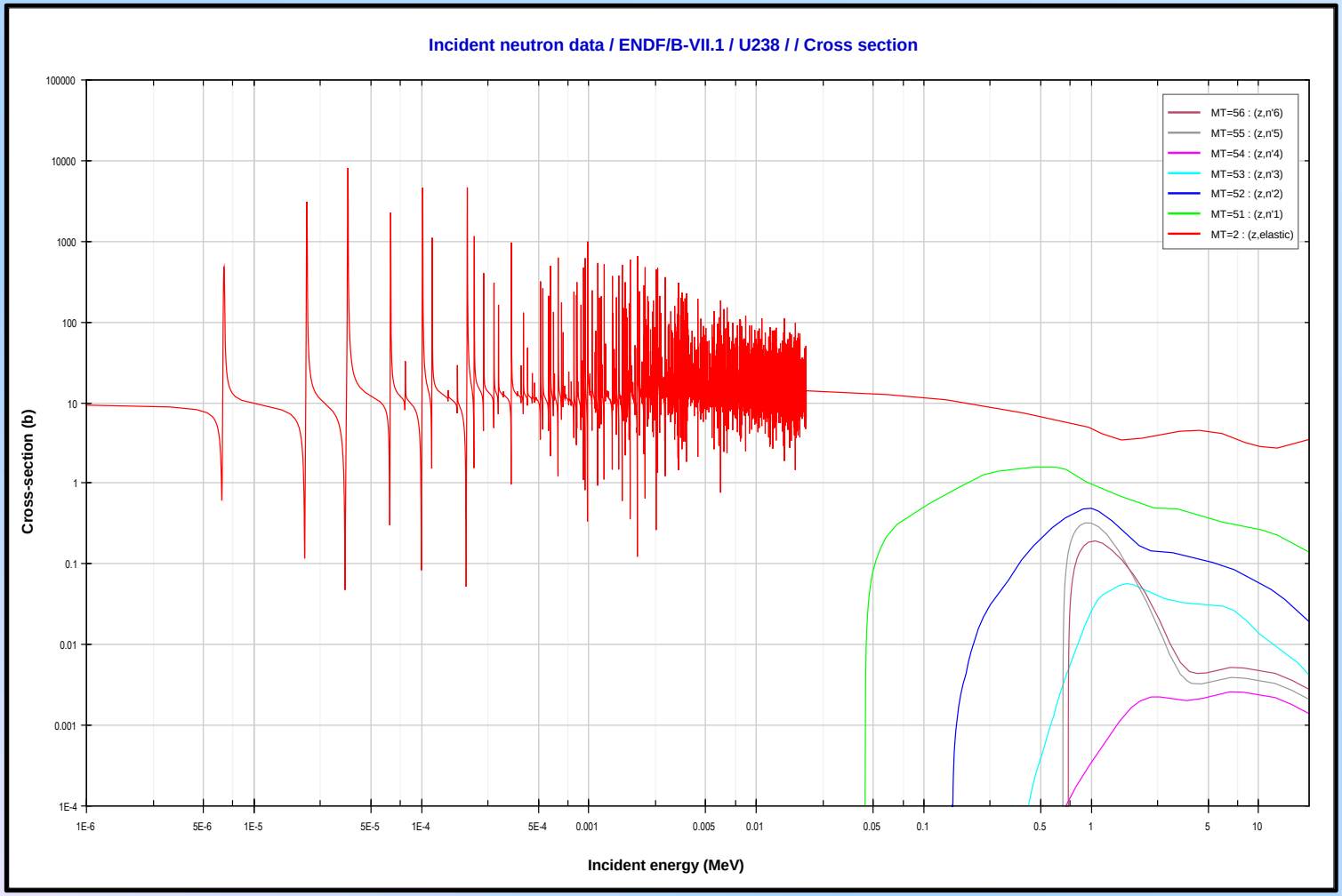

Angular Distribution of the scattered neutron

- The probability that a particle of incident energy E will be scattered into the interval dμ about an angle whose cosine is μ as defined in the ENDF manual is:

$$f(\mu,E)=\frac{2\pi}{\sigma_s(E)}\sigma(\mu,E)=\sum_{l=0}^{NL}\frac{2l+1}{2}a_l(E)P_l(\mu)$$

Where

μ	=cosine of the scattered angle in either the laboratory or the center of mass system
E	=energy of the incident particle in the laboratory system
$\sigma_s(E)$ =	=the scattering cross section, e.g., elastic scattering at energy E as given in File 3 for the particular reaction type (MT)
l	=order of the Legendre polynomial
$\sigma(\mu,E)$	=differential scattering cross section in units of barns per steradian
a_l	=the l^{th} Legendre polynomial coefficient and
$P(\mu)$	= Legendre polynomial of order l

The differential cross section is given by:

$$\sigma(\mu,E)=\frac{\sigma_s(E)}{2\pi}f(\mu,E)$$

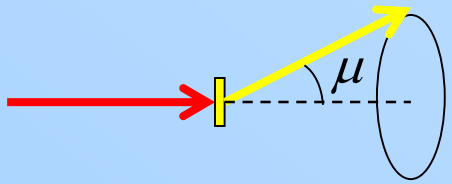

In the lab system scattering is symmetric around μ

Example: ^{238}U Elastic Scattering

- The angular distribution strongly dependent on the incident energy

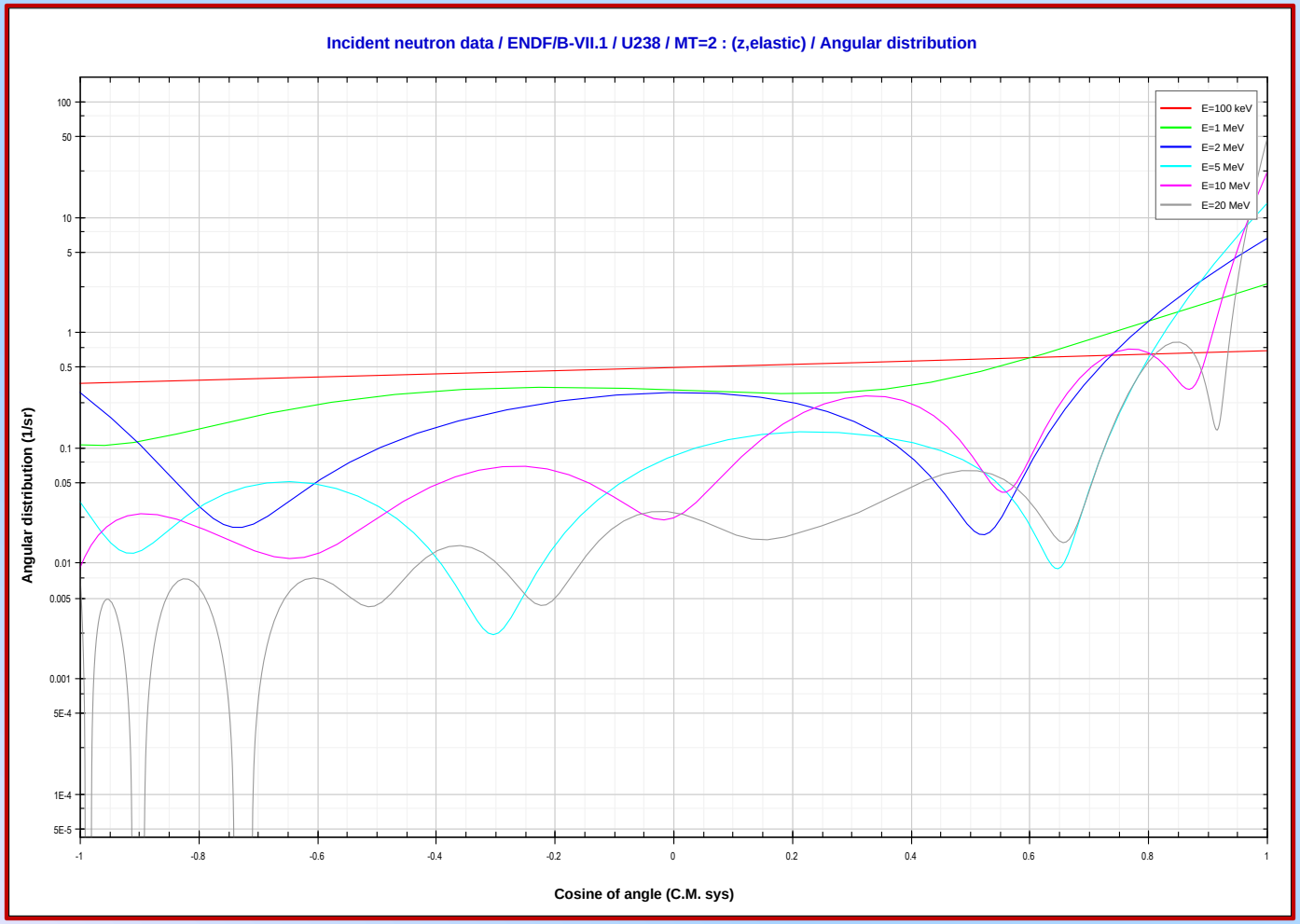

How to measure scattering reactions

- Observable include:
  - Neutrons
  - Gamma – for inelastic scattering
- Type of measurements
  - Total scattering cross section
    - Elastic only (Fe is might be an exception)
      - Can be obtained from resonance parameter analysis for transmission and capture measurements
      - Can similarly be obtained in the URR
    - Inelastic cross section
      - Measure the excitation gamma
      - Measure the scattered neutron
    - Double differential scattering cross section (DDS)
      - Measure the scattered neutron at different angles, need:
        - » Incident neutron energy
        - » Scattered neutron energy
        - » Scattering angle

Thermal Scattering

Overview

- Thermal scattering refers to scattering of thermal neutrons
  - The neutron energy is of the order of thermal motion of the scattering atoms
  - The neutron energy is of the order of rotational and vibrational molecular bond
  - **Results in down and up scattering**

- Experiments were done at the Spallation Neutron Source (SNS) at Oak Ridge National Laboratory (ORNL)

- Performed thermal scattering experiments at various temperatures and using different instruments for water, high density polyethylene (HDPE), and quartz (SiO_2).

SNS Spectrometers

Fine Resolution Fermi Chopper Spectrometer (SEQUOIA)

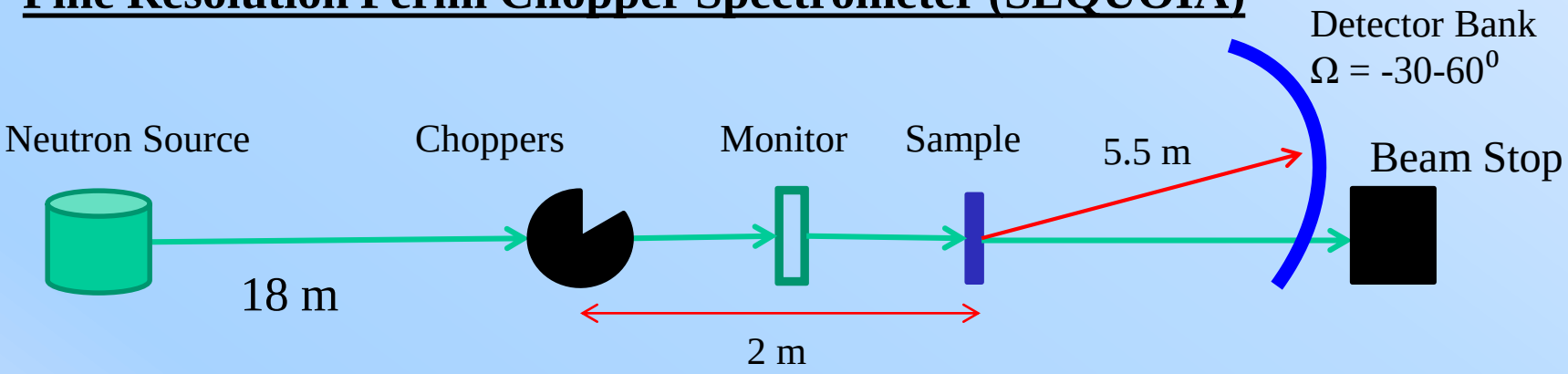

Wide-Angular Range Chopper Spectrometer (ARCS)

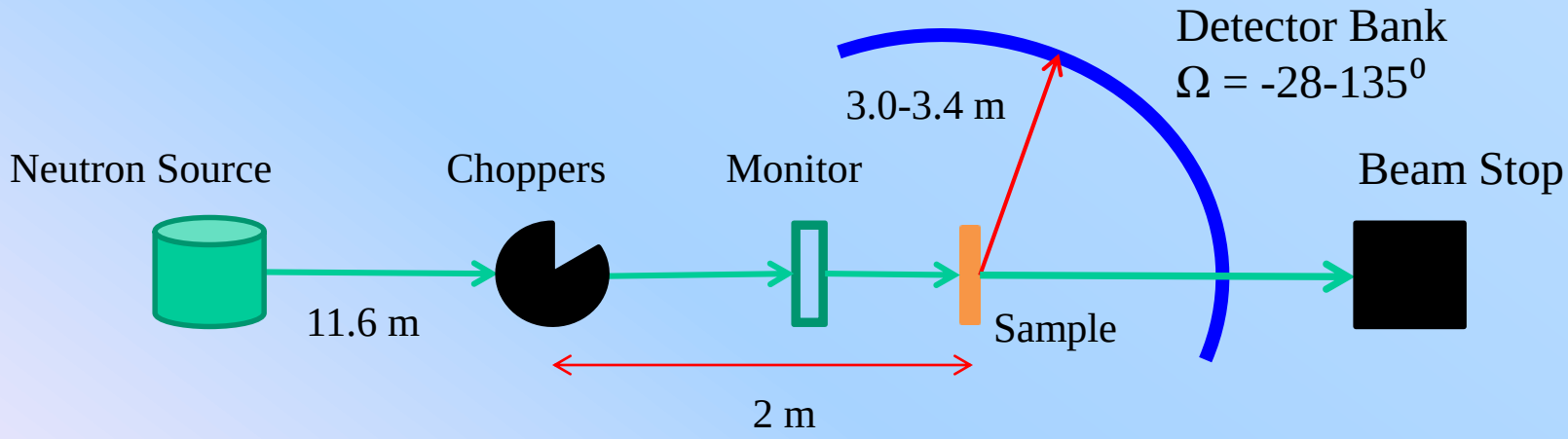

SNS spectrometers

Fine Resolution Fermi Chopper Spectrometer (SEQUOIA)

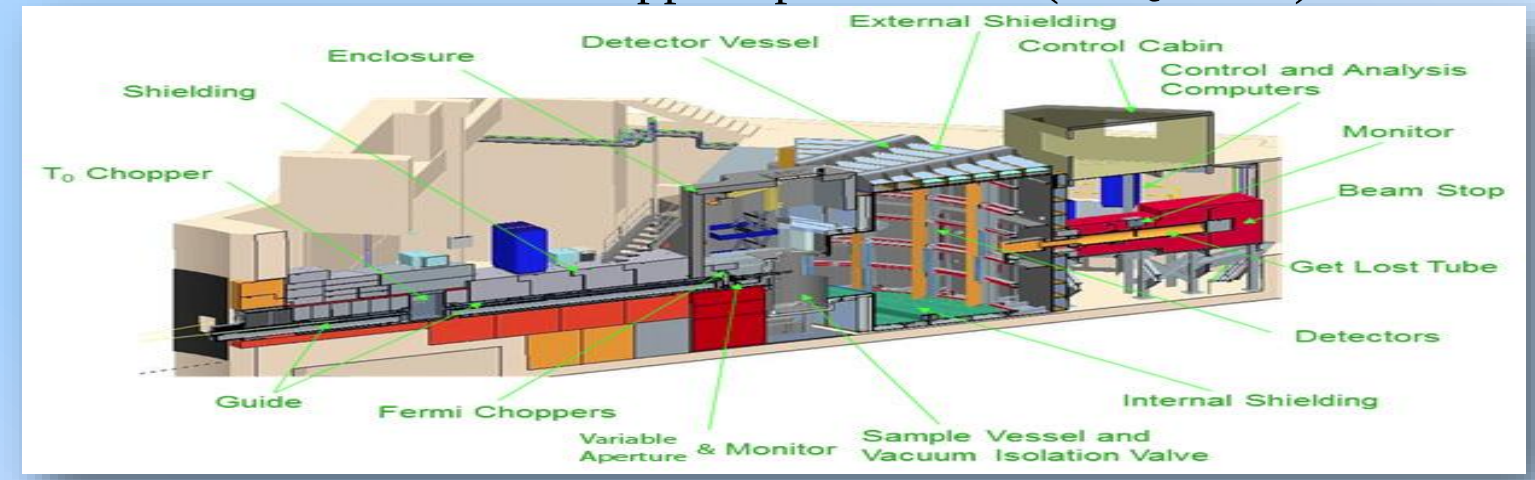

Wide-Angular Range Chopper Spectrometer (ARCS)

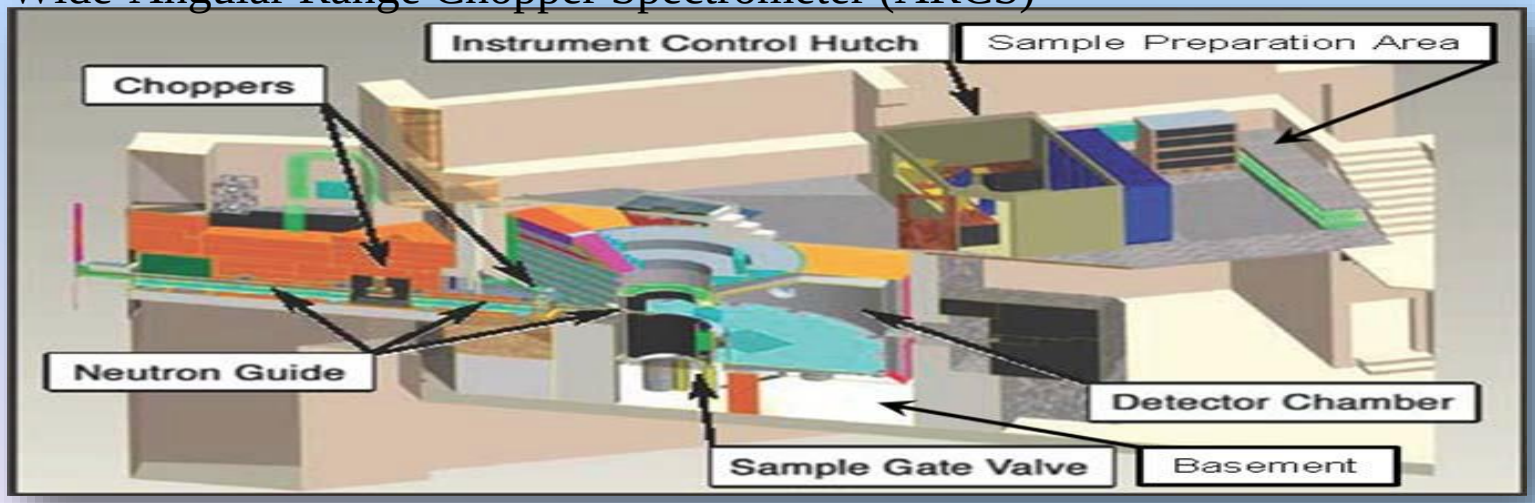

Thermal Neutron Scattering Geometry

$\text{momentum} = \hbar\mathbf{k}$ $\quad \text{energy} = (\hbar\mathbf{k})^2/2m$

$\text{energy} = 2\pi/\lambda$

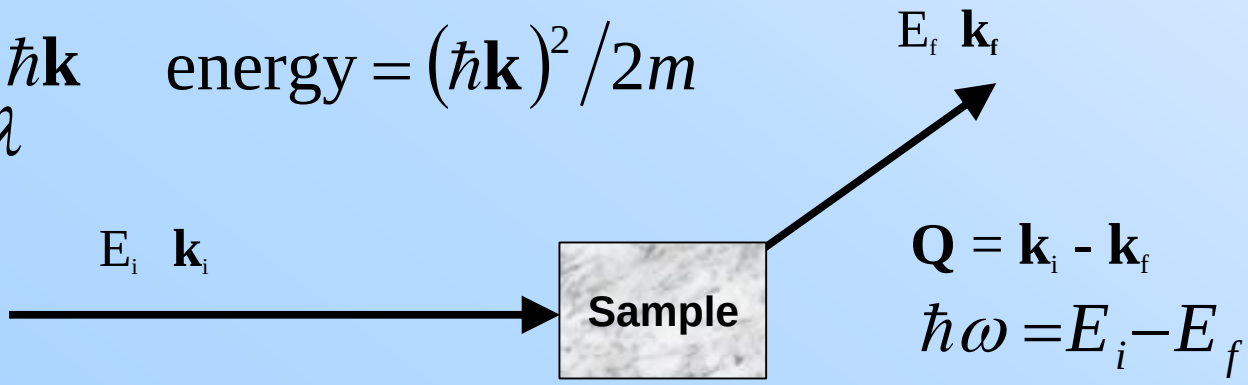

Measure the number of scattered neutrons as a function of Q and ω

=> S(Q,ω) (the scattering function for inelastic scattering)

depends ONLY on the sample

DDSCS $\quad \dfrac{d^2\sigma_H}{d\Omega d\omega} = 2N\dfrac{\sigma_H}{4\pi}\dfrac{k_f}{k_i}S_{inc}(Q,\omega)\otimes R(\omega)$

In our study:

- Neutron Scattering experimental plot: Double differential cross section (instead of S(Q,ω)) vs. scattered energy (E_f, instead of ω)

Scattering Kernel

Scattering Probability

- Double Differential Scattering Cross Section (DDSCS)
- Inelastic scattering

$$\sigma(E \to E', \Omega) = \frac{\sigma_b}{2kT}\sqrt{\frac{E'}{E}}\, e^{-\beta/2}\boldsymbol{S}(\boldsymbol{\alpha}, \boldsymbol{\beta})$$

$$\beta = \frac{E' - E}{kT} \qquad \alpha = \frac{E' + E - 2\mu\sqrt{EE'}}{AkT}$$

Thermal Scattering Measurements Overview

- Preformed measurements at SNS
  - SEQUOIA
    - Water
    - Medium Density Polyethylene (MDPE)
  - ARCS
    - High Density Polyethylene (HDPE) 295 °K and 5 °K
    - Quartz (SiO_2) at 20, 300 550, 600 °C
  - VISION (measures $S(\omega)$)
    - Lucite, Lexan, Polyethylene at 5 °K and 295 °K
- The double differential scattering data (DDSD) can be used to benchmark thermal scattering evaluations
- Method to generate $S(\alpha,\beta)$ from the experimental data are under development:
  1. Convert the data ($S(Q,\omega)$) to phonon spectrum (use low values of Q to limit multiple phonon scattering)
  2. Remove the elastic peak from the DDSD and convert the inelastic part directly to $S(\alpha,\beta)$
- Developed capabilities to use LAMMPS code to calculate the phonon spectrum and scattering kernel.

Scattering from Water

- For 160 meV incident energy where older RPI data exists:
  - The SNS experimental data is in agreement with the older RPI data
  - The simulation is in agreement with experiments
- For lower incident energy (55 meV) the simulation shows structure that is not visible in the data

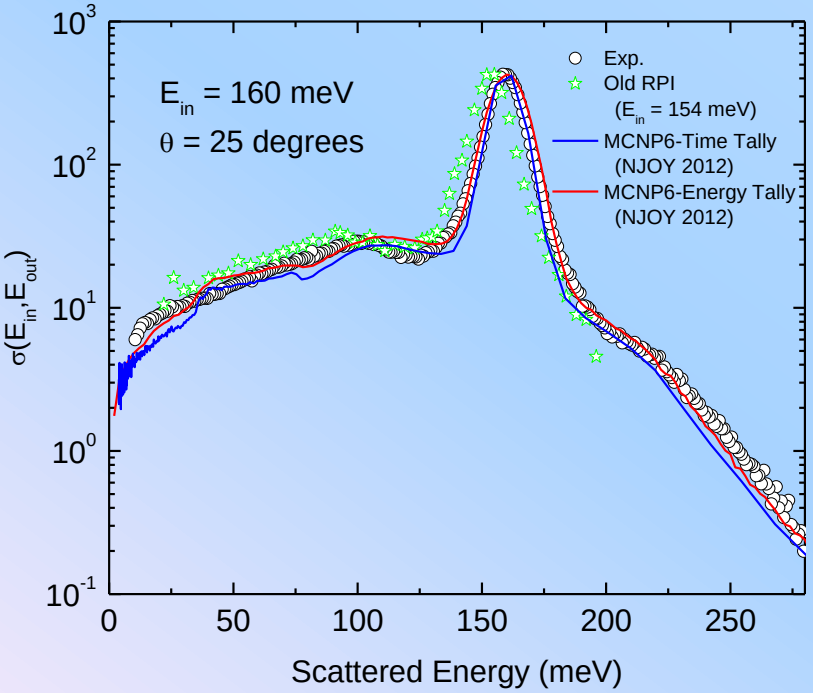

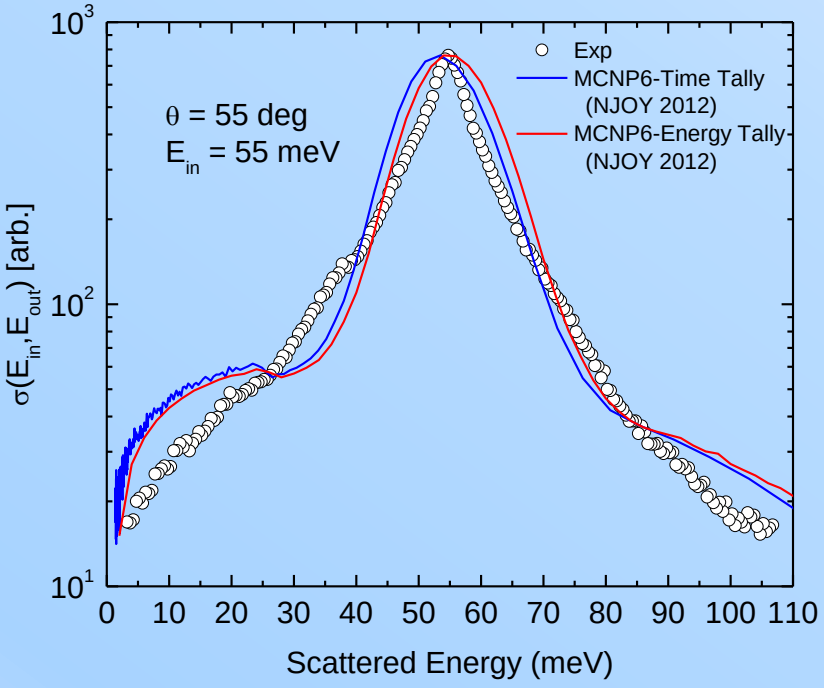

ARCS vs SEQUOIA

- 250 meV incident energy
- ARCS shows slightly better energy resolution compared to SEQUOIA
  - ARCS sample: CH_2 Sheets
  - SEQUOIA sample: CH_2 powder
- Sheets allow for coherent elastic scattering

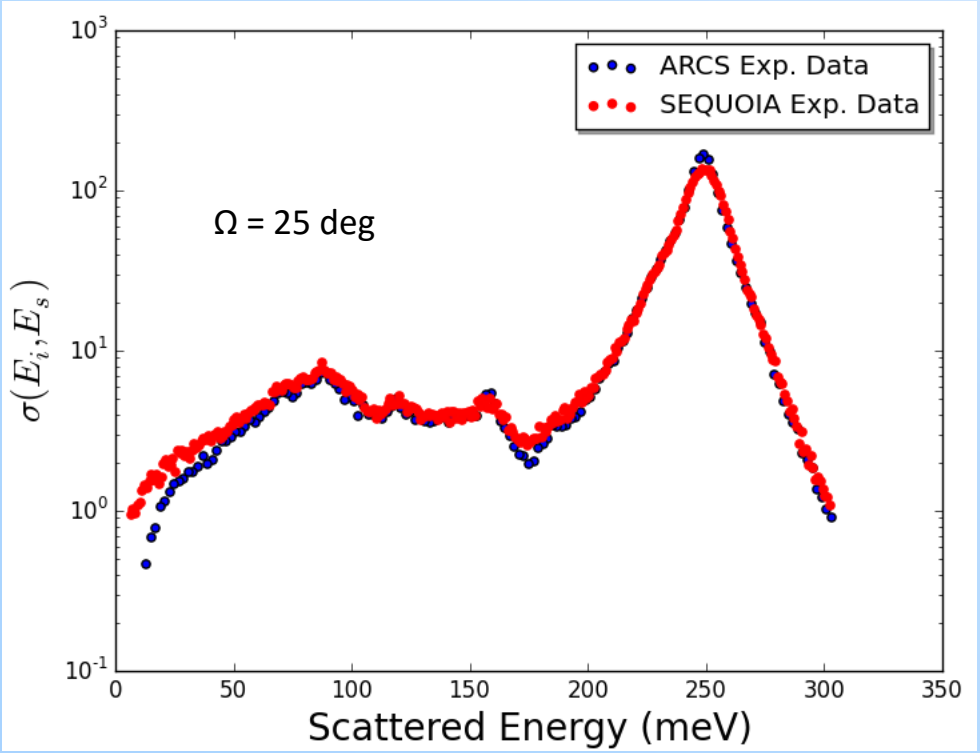

New Raw Experimental Data

- Polyethylene using ARCS-Wide Angle Spectrometer at SNS
- Low temperature reveals the vibrational/rotational modes

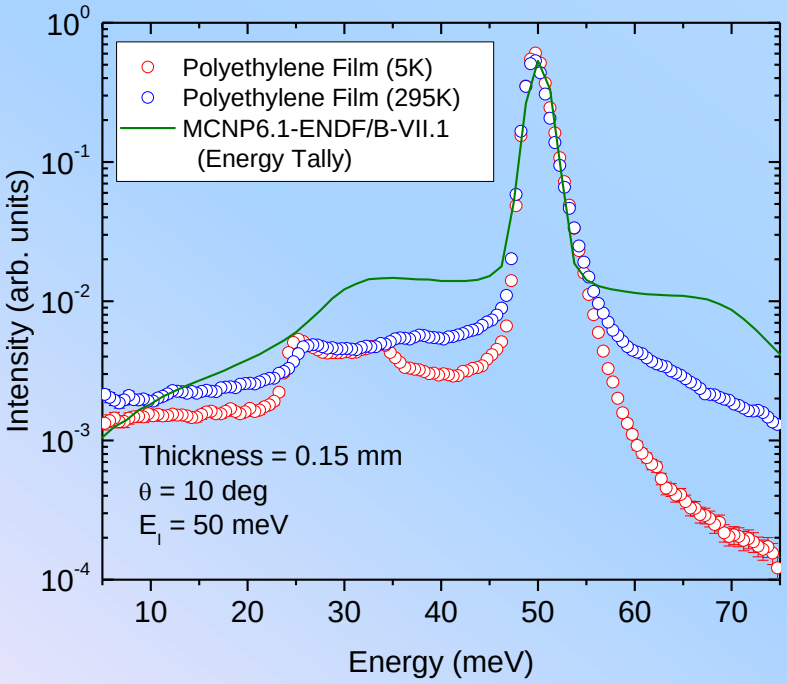

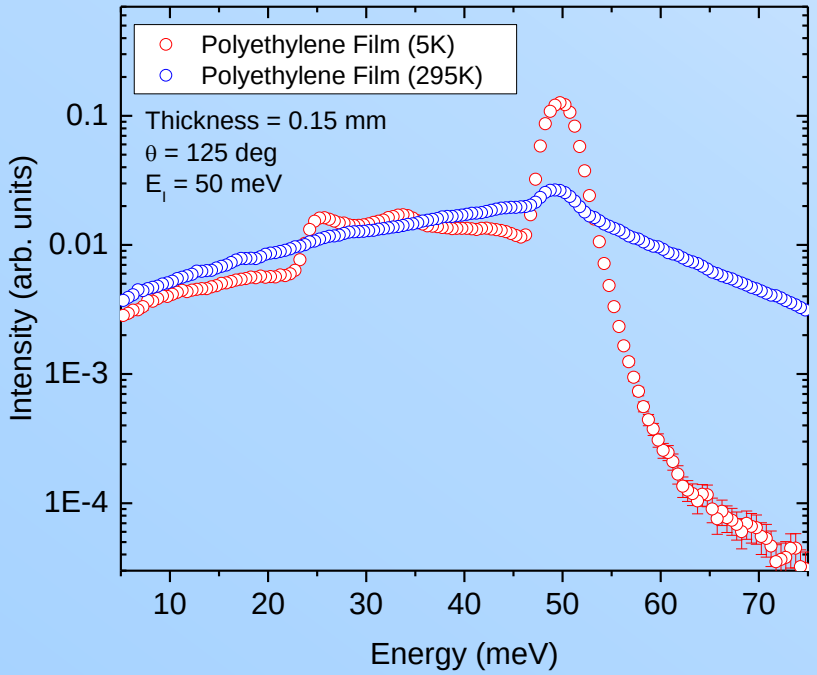

Phonon spectrum from measured $S(Q,E)$

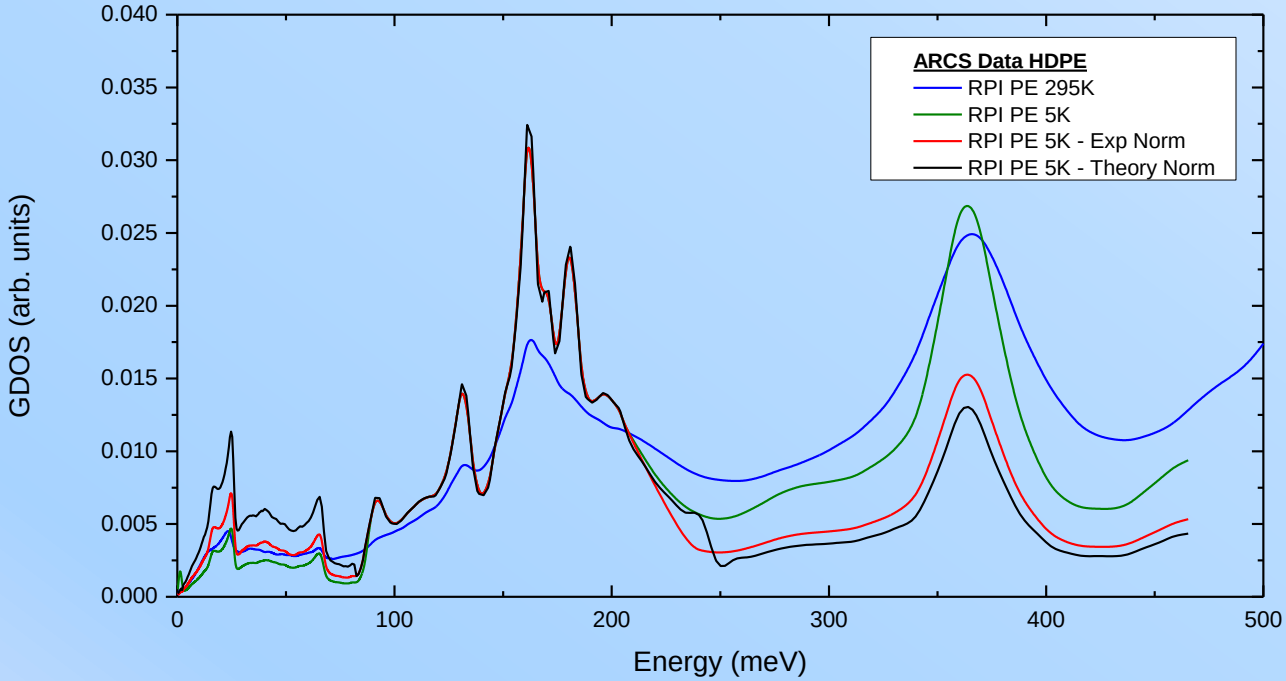

- Low temperature measurements are essential in order to resolve the structure.
- Convert the measured $S(Q,E)$ data for phono spectrum using the SNS DAVE code:

$$S(Q,E) = \frac{\hbar^2 Q^2}{6ME}\exp(-\langle u^2\rangle Q^2)G(E)[n(E,T)+1] \qquad n(E,T) = \frac{1}{\exp\left(\frac{E}{k_B T}\right)-1}$$

$G(E)$ - generalized phonon density-of-states(GDOS)

Q - wave vector transfer,

$S(Q,E)$ - structure dynamics factor.

M - mass of the atom,

$\langle u^2 \rangle$ - mean square displacement.

Example for HDPE

Experiment Normalized GDOS

- The phonon spectrum was processed with NJOY 2012
- The experimental response simulated with MCNP 6
- The agreement with the experiment is improved

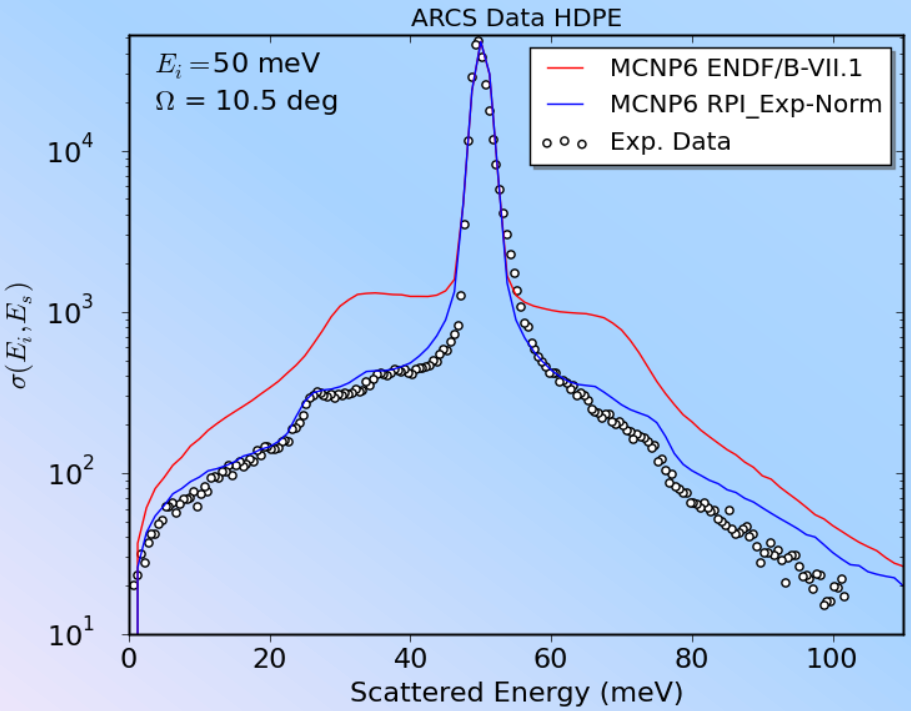

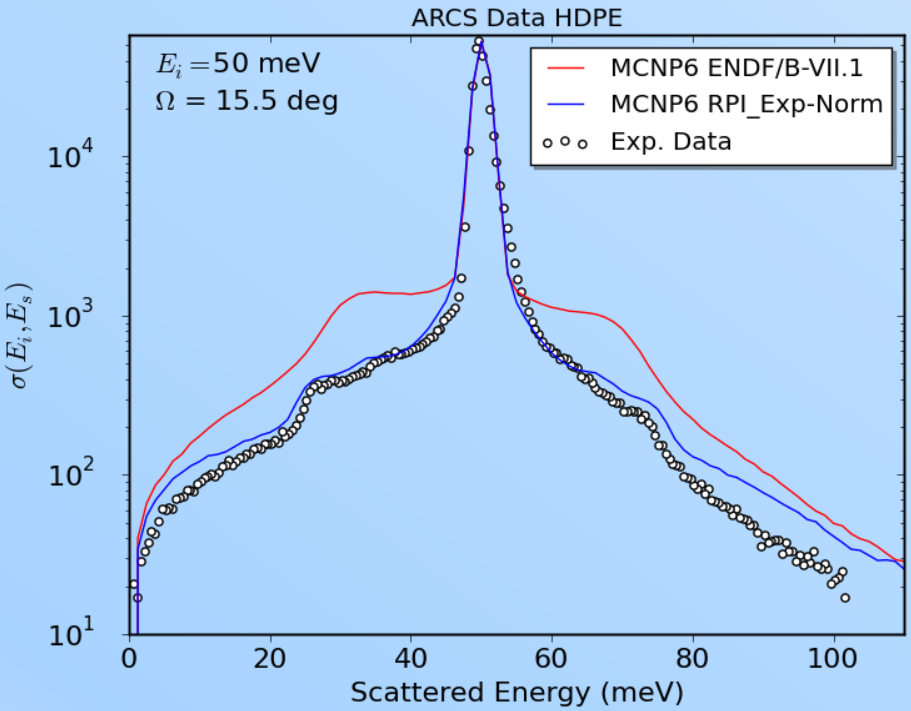

Example for HDPE other angles Experiment Normalized GDOS

- Similar improvements
- Other incident energies and angels available

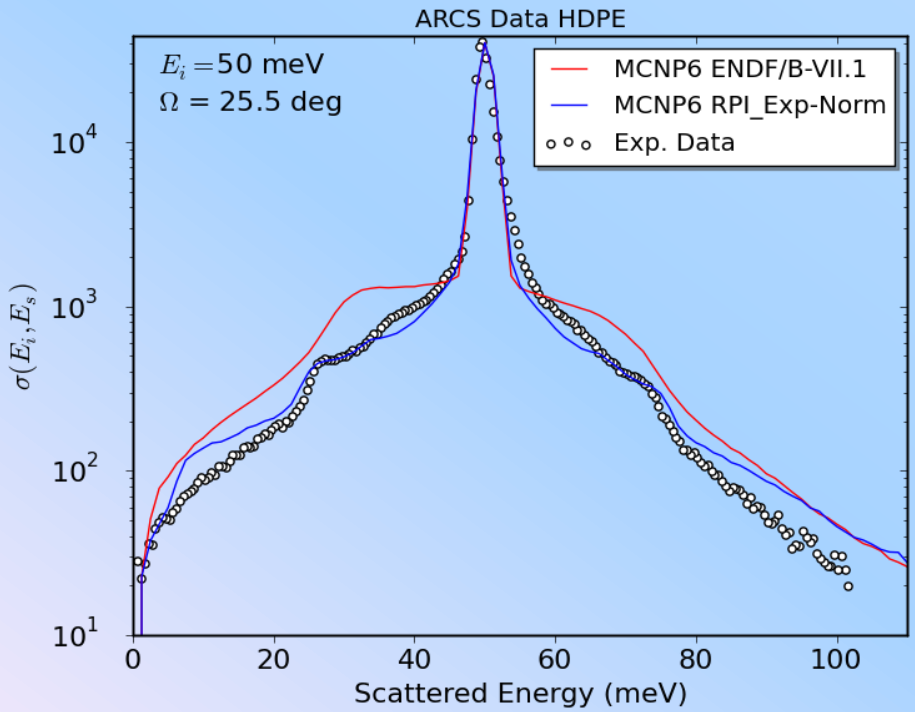

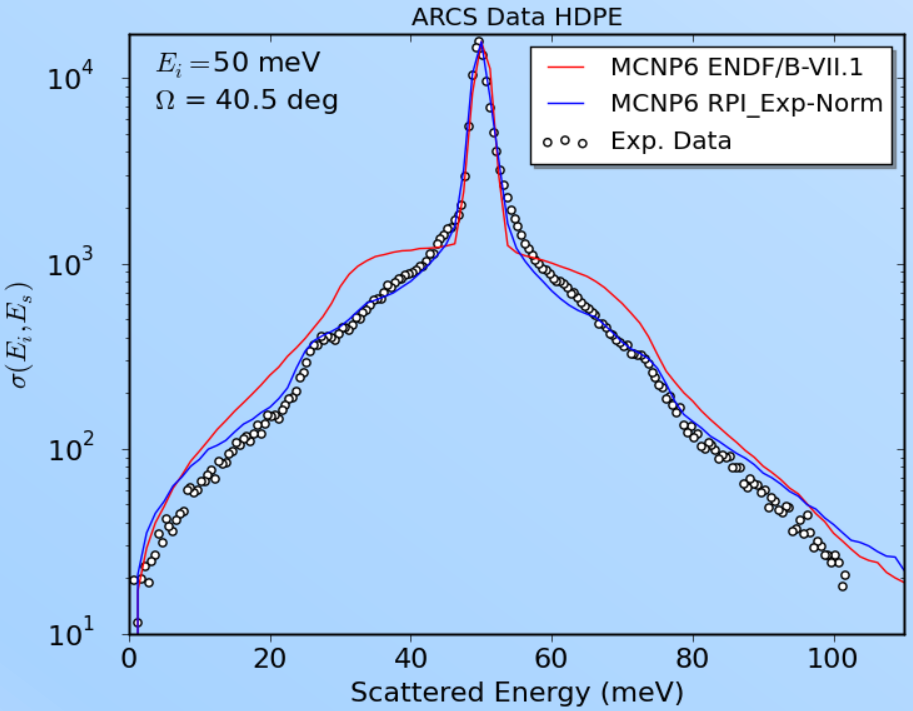

Polyethylene Total Cross Section

- The experimentally derived phonon spectrum is in good agreement with the total cross section measurement.
- The Experimental vs theory driven measurement give slightly different results

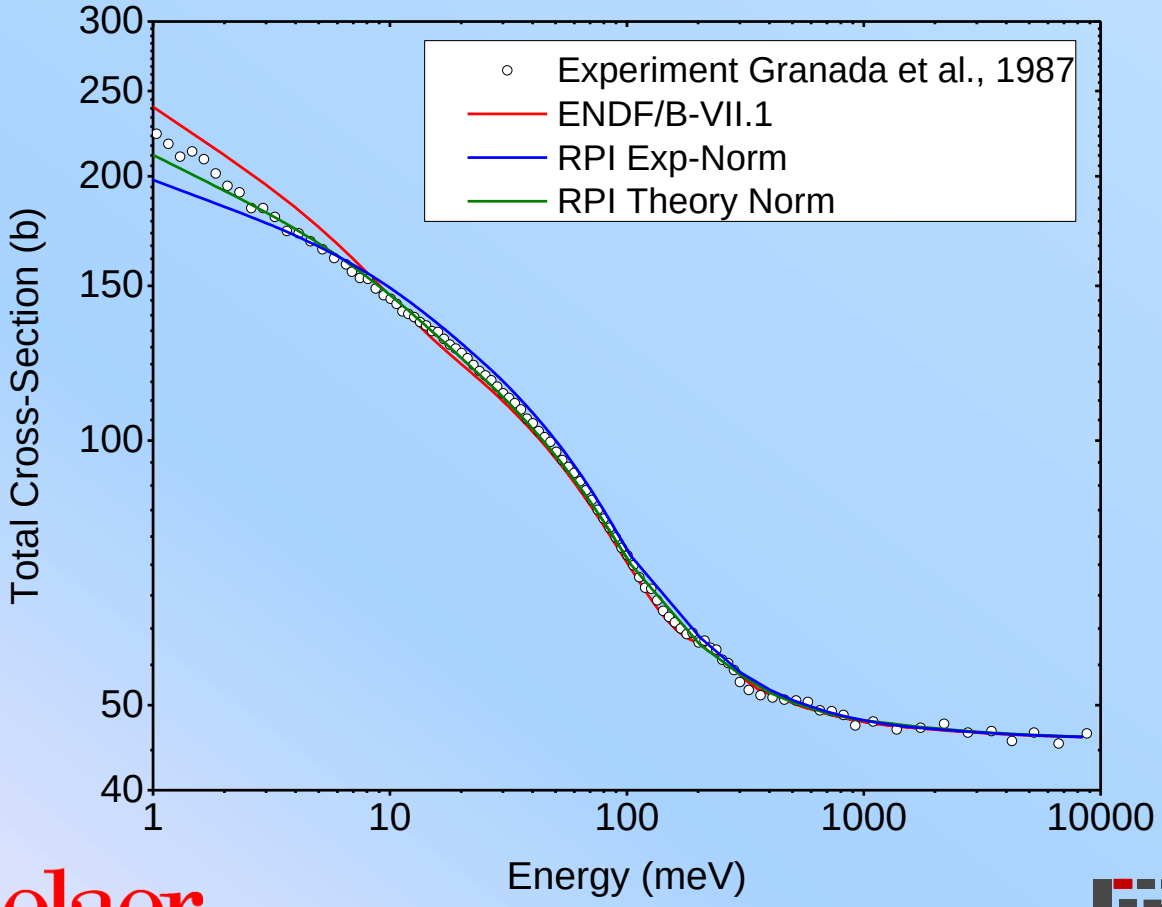

Resonance Scattering
(including up scattering)

^{238}U Resonance Scattering

- From a theoretical point of view, the neutron angular distribution can be calculated from resonance parameters
- Neutron scattering kinematics in the resonance region is normally treated as free gas.
- The derivation of the scattering kernel in most (if not all) Monte Carlo (MC) codes assumes a constant cross section
  - OK in the thermal region, but not for the low lying resonances.
- **Resonance scattering experiments were used to validate an improved model implementation**

Example from MCNP5

If the energy of the neutron is greater than 400 kT and the target is not ^{1}H, the velocity of the target is set to zero. Otherwise, the target velocity is sampled as follows. The free-gas kernel is a thermal interaction model that results in a good approximation to the thermal flux spectrum in a variety of applications and can be sampled without tables. The effective scattering cross section in the laboratory system for a neutron of kinetic energy E is

$$\sigma_s^{eff}(E) = \frac{1}{v_n}\int\int \sigma_s(v_{rel})v_{rel}p(V)dv\frac{d\mu_t}{2} \qquad (2.1)$$

Equation (2.1) implies that the probability distribution for a target velocity V and cosine μ_t is

$$P(V, \mu_t) = \frac{\sigma_s(v_{rel})v_{rel}P(V)}{2\sigma_s^{eff}(E)v_n} .$$

It is assumed that the variation of $\sigma_s(v)$ with target velocity can be ignored. The justification for

the consequences of the approximation will be negligible.

the consequences of the approximation will be negligible. As a result of the approximation, the probability distribution actually used is

MCNP Scattering Kernel Treatment "Sampling the target velocity"

MCNP Manual: "If the energy of the neutron is greater than 400 *kT* and the target is not Hydrogen the velocity of the target is set to Zero" (Asymptotic kernel)

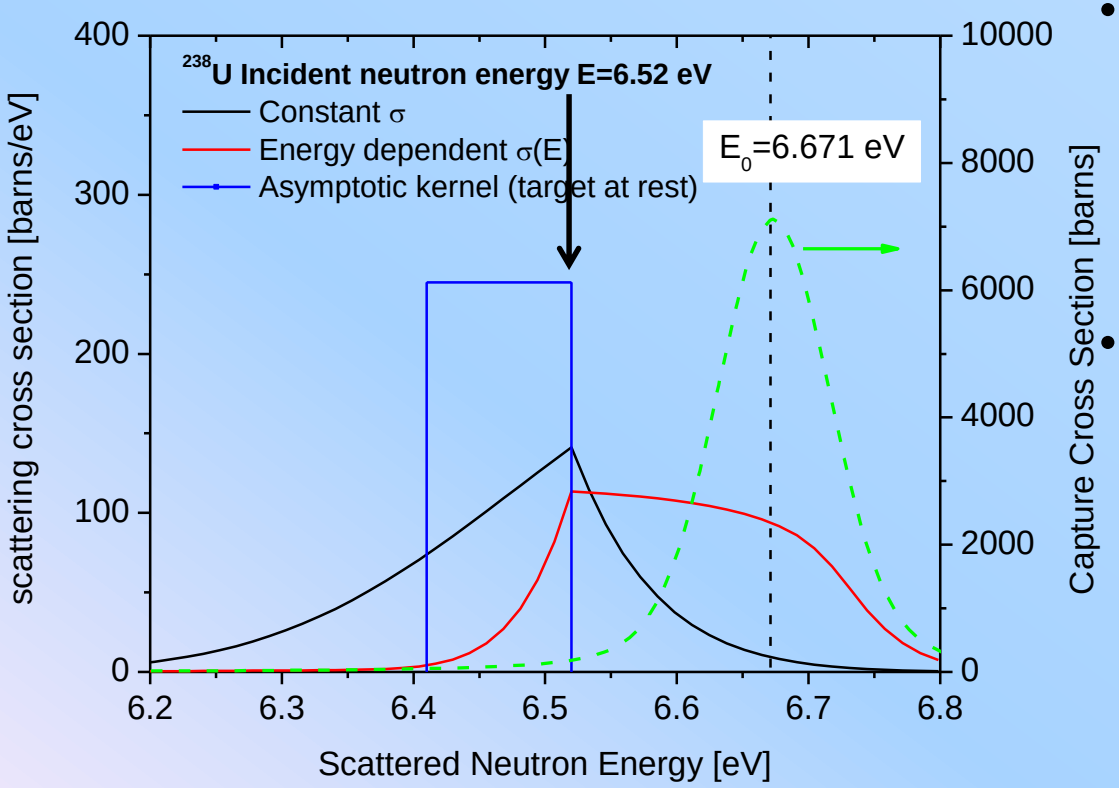

- The 400 *kT* (~10 eV for *T*=300 K) limit can be easily fixed. (but still assume the cross section does not depend on energy)
- In this example, with the correct model neutrons have a higher probability to up-scatter into the 6.671 eV resonance

Effect on Reactor Calculations (HTR)

- B. Becker, R. Dagan, C.H.M. Broeders, G.H. Lohnert, Improvement of the resonance scattering treatment in MCNP in view of HTR calculations, Annals of Nuclear Energy, Volume 36, Issue 3, Pages 281-285, April 2009.

Table 2
Multiplication factor k_{eff} of HTR-10 with standard MCNPX and improved scattering kernel for different fuel temperatures T_F.

T_F	1200 K	1800 K
Standard MCNPX k_{eff}	$1.00841 \pm 21 \times 10^{-5}$	$1.00271 \pm 20 \times 10^{-5}$
With $S(\alpha, \beta)$ k_{eff}	$1.00768 \pm 20 \times 10^{-5}$	$1.00110 \pm 20 \times 10^{-5}$
$\lvert dk/k \rvert$	72 ± 28 pcm	107 ± 28 pcm

Table 3
Multiplication factor k_{eff} of HTTR with standard MCNPX and improved scattering kernel for different fuel temperatures T_F.

T_F	1200 K	1800 K
Standard MCNPX k_{eff}	$1.06657 \pm 39 \times 10^{-5}$	$1.05111 \pm 38 \times 10^{-5}$
With $S(\alpha, \beta)$ k_{eff}	$1.06433 \pm 35 \times 10^{-5}$	$1.04671 \pm 37 \times 10^{-5}$
$\lvert dk/k \rvert$	210 ± 52 pcm	419 ± 853 pcm

Experimental Investigation

- **Dagan**:
  - Implemented the new Kernel in MCNP inputting it as an S(α,β) table.
  - Showed the effect on K_{eff} of different systems.
- **Danon**: find a simple experiment to benchmark the new kernel. Considered:
  - Capture experiments in the ^{238}U scattering resonance at 36.68 eV
  - Can it be done at room temperature (instead of 1200K)?
  - **Design a scattering experiment measuring the detailed spectrum of the scattered neutrons.**

A Simple Neutron Scattering Experiment

- Use the Time-Of-Flight (TOF) method
  - The TOF will correspond to the scattered neutron energy
  - Scattering in forward and backward scattering angles can be measured

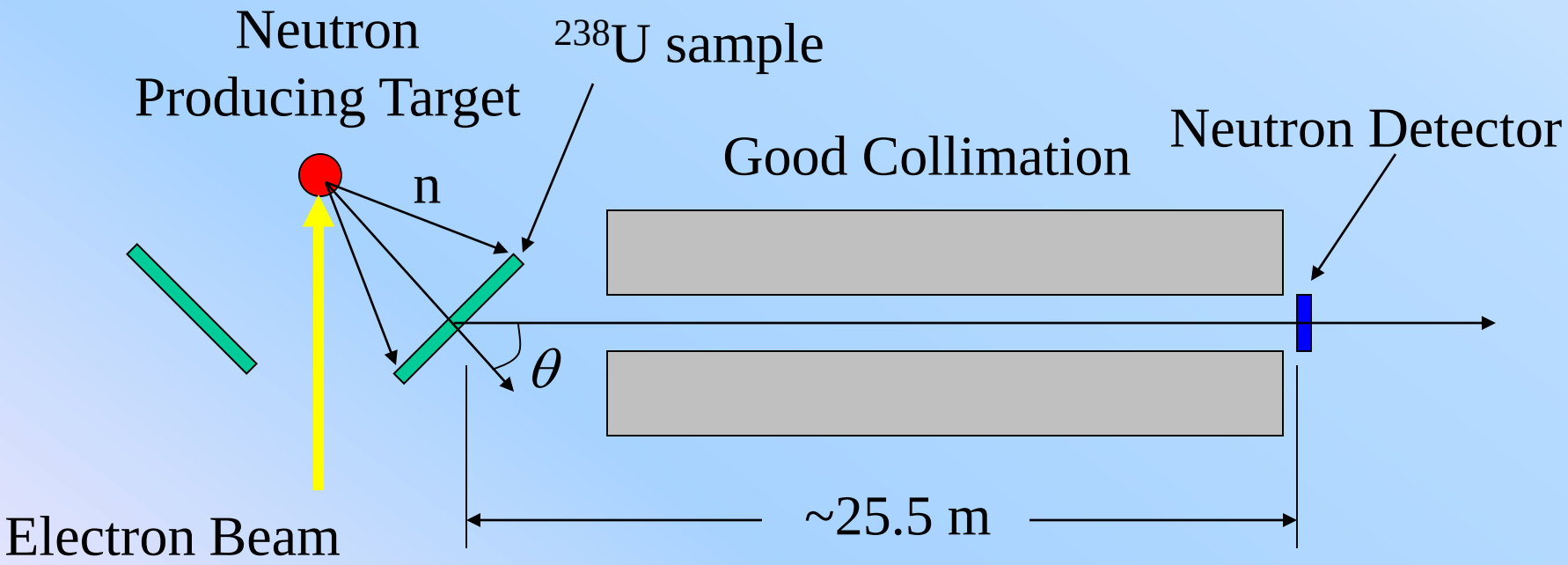

A First Collision Analytical Model

- Consider a simple back scattering geometry

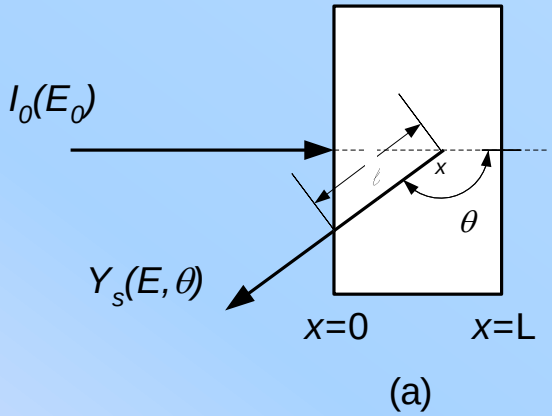

$$dY_s(x,E,\theta) = I_0(E_0)\eta(E)\Sigma_s(E_0,\theta)\cdot dx\cdot e^{\left(\Sigma_t(E)\frac{1}{\cos(\theta)}-\Sigma_t(E_0)\right)x}$$

η(E) - the neutron detection efficiency
Y_s(x,E,θ) - the scattering yield

Use scattering kernel with target at rest

$$E_0 = E\frac{(A+1)^2}{A^2+2A\mu_{cm}+1}$$

E_0 – incident n energy
E – scattered n energy

The scattering yield is given by:

$$Y_s(E,\theta) = I_0(E_0)\eta(E)\frac{\Sigma_s(E_0,\theta)}{\Sigma_t(E)/\cos(\theta)-\Sigma_t(E_0)}\left[e^{\left(\frac{\Sigma_t(E)}{\cos(\theta)}-\Sigma_t(E_0)\right)L}-1\right]$$

Analytical Model and MCNP

- Compare the analytical model to MCNP5
  - Excellent agreement (for first collision)

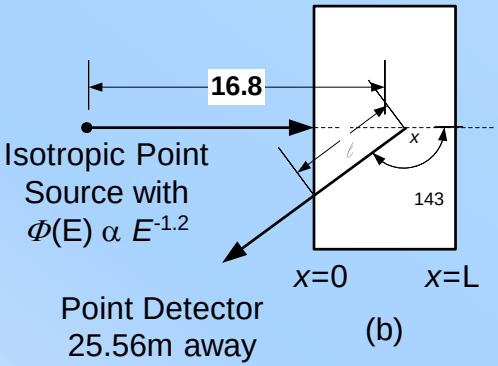

- **Peak location**– Energy loss due to collision with ^{238}U
- **Valley location** – Scattered Neutrons attenuated by the strong 36.68 eV resonance.

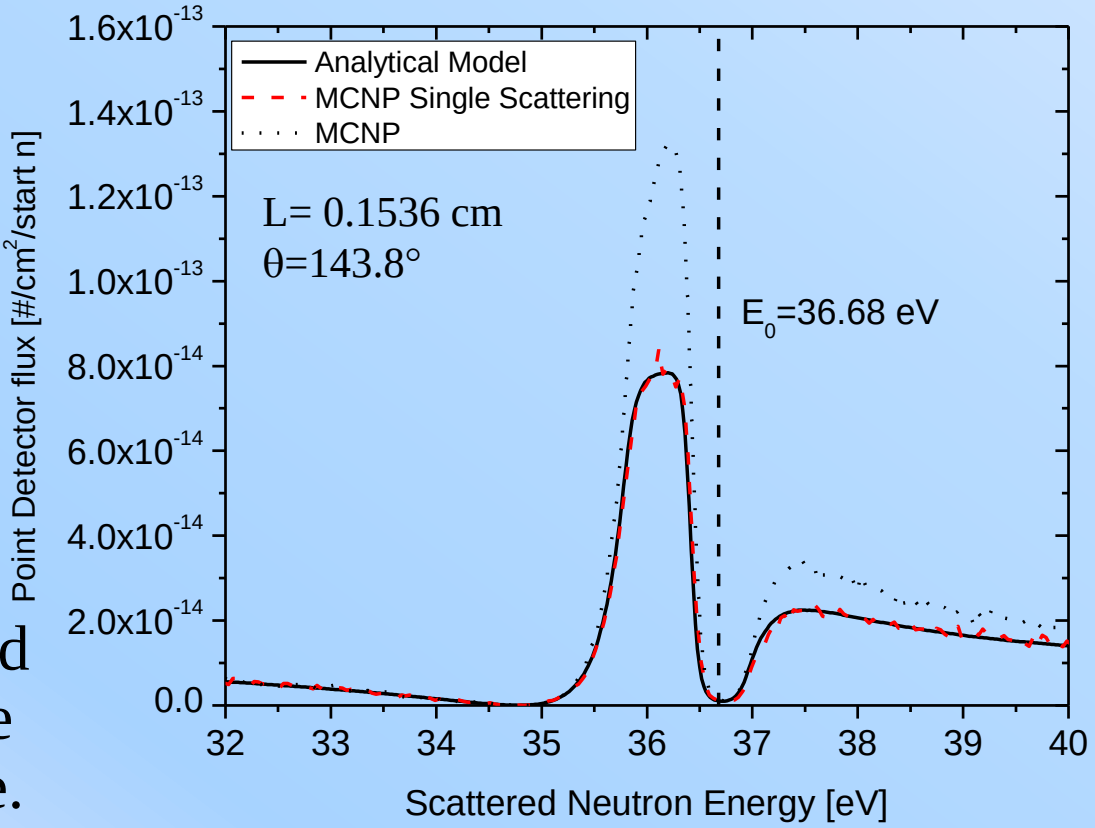

^{238}U Resonance Scattering
Experimental Setup

- Compare forward to backward scattering from depleted ^{238}U samples
- The forward angle **38.9°** is and the backward angle is **143.8°**

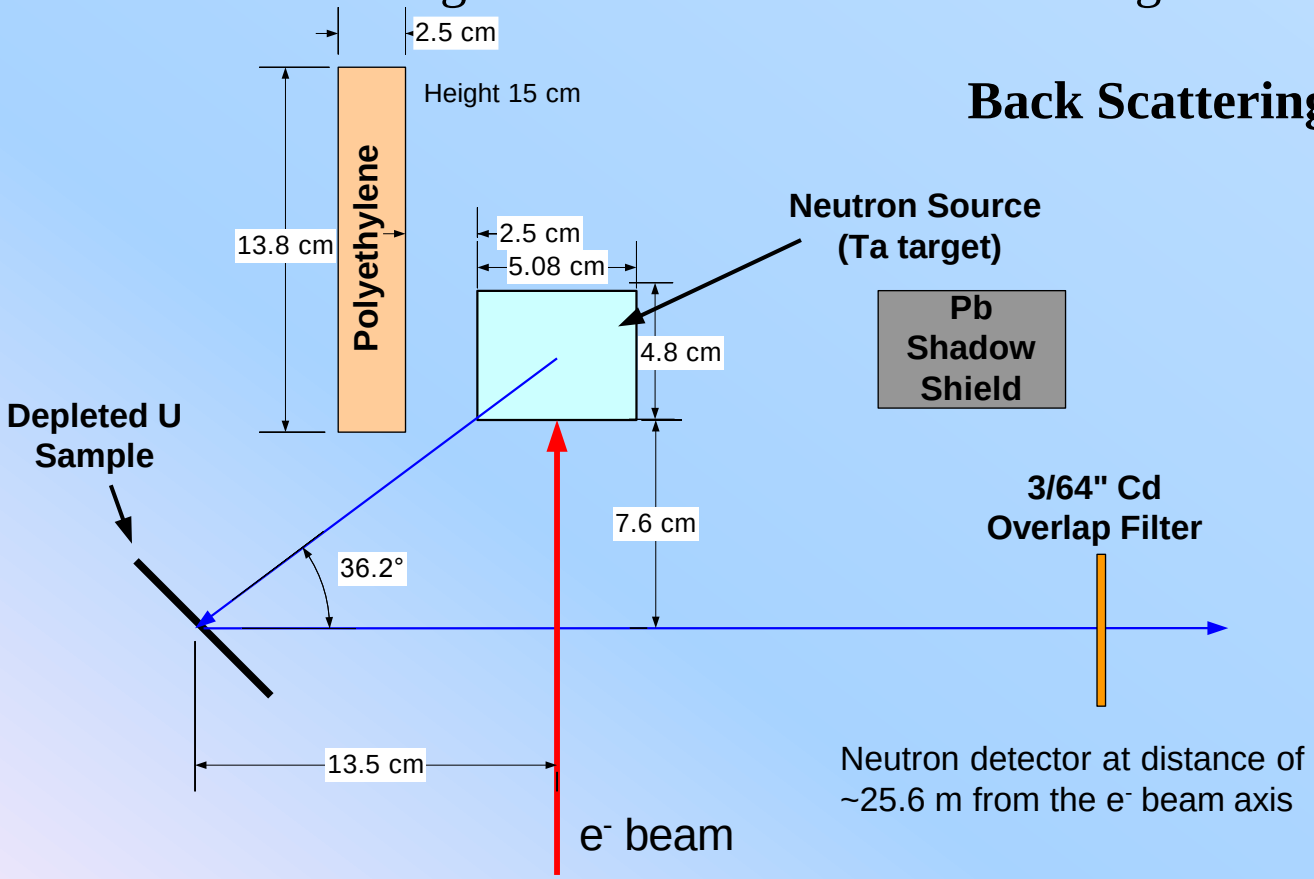

Experimental Setup

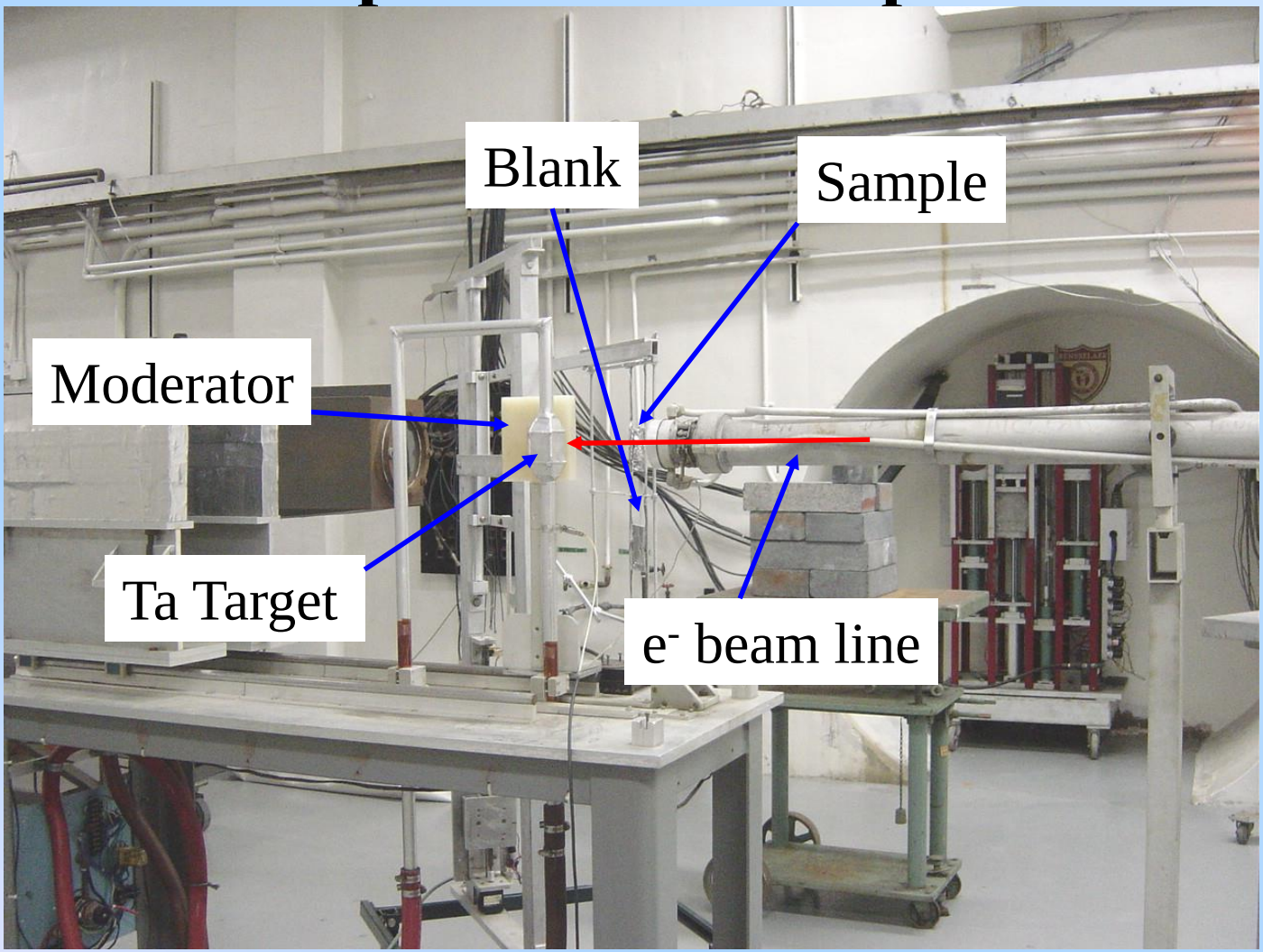

Samples

Sample ID	Width (cm)	Height (cm)	Thickness (cm)	Weight (g)
Thin	7.62 ± 0.05	7.62 ± 0.05	0.1536	169 ± 0.5
Thick	7.62 ± 0.05	7.62 ± 0.05	0.329	362 ± 0.5

Measured Data

- Thick Sample time-of flight spectrum forwards scattering

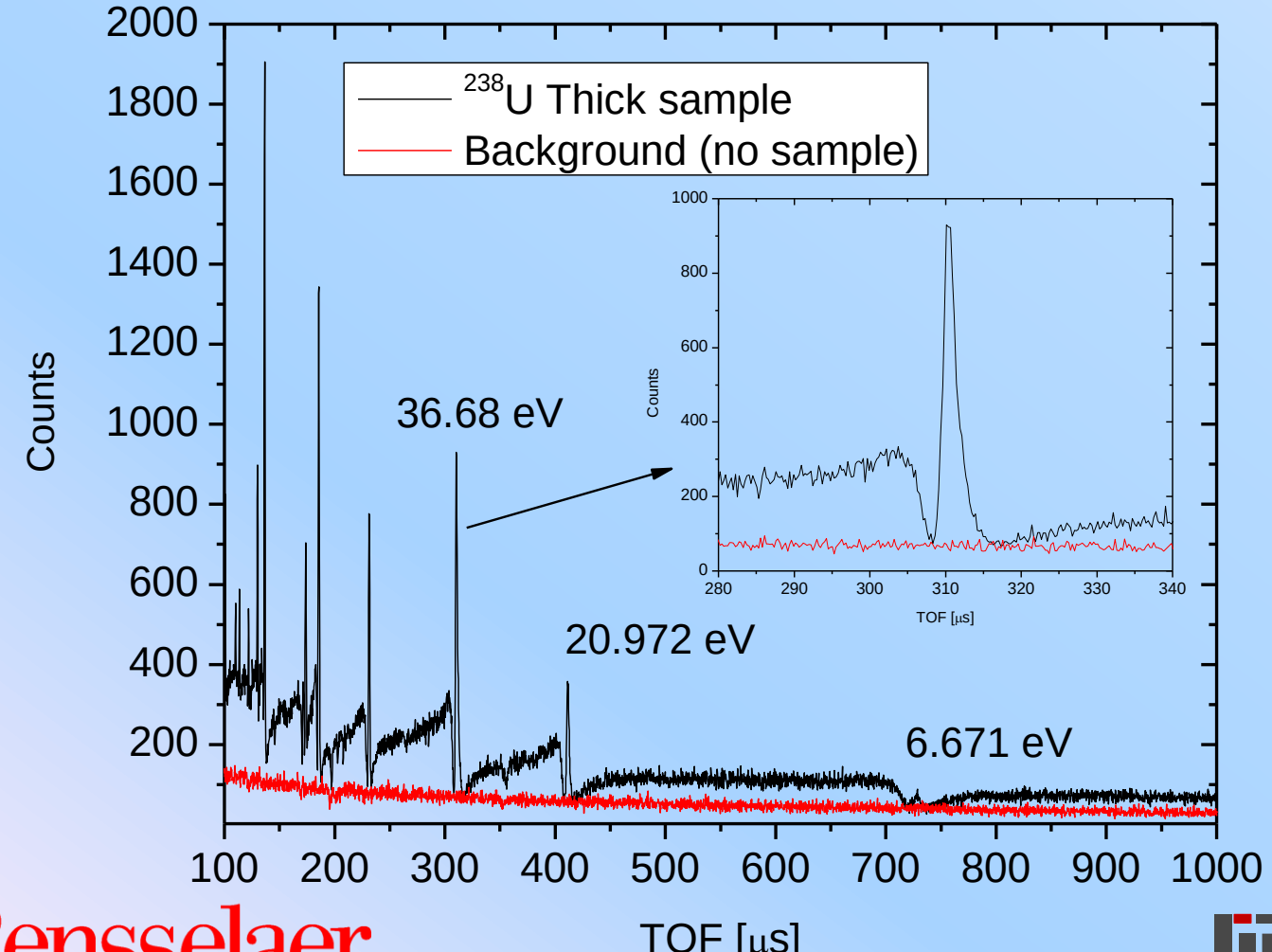

Other Considerations

- In order to compare with calculations:
  - Need good energy calibration
    - Use resonances in the Cd overlap filter
  - Need the neutron flux shape
    - Obtained from an experiment with a Pb Sample
    - The result is the product of the neutron flux shape with the detector energy response $I_0(E_0)\eta(E)$

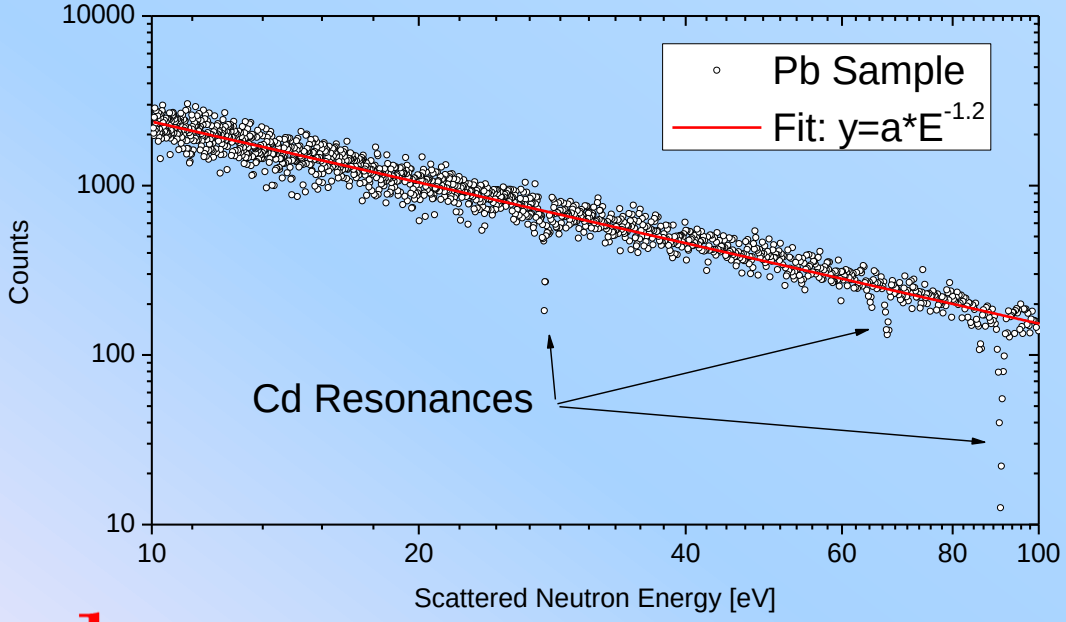

MCNP Simulations

- Source
  - Treat the source as a point source with energy distribution of $\phi(E) \sim E^{-1.2}$
  - Simulate the LINAC 50 ns pulse width
- Tally
  - Use tally F5 for the detector response
  - Tally the flux as a function of time
- Sample
  - Use actual size dimensions
  - Assume pure ^{238}U
- Include the Cd overlap filter in the simulation

Results - ^{238}U Scattering

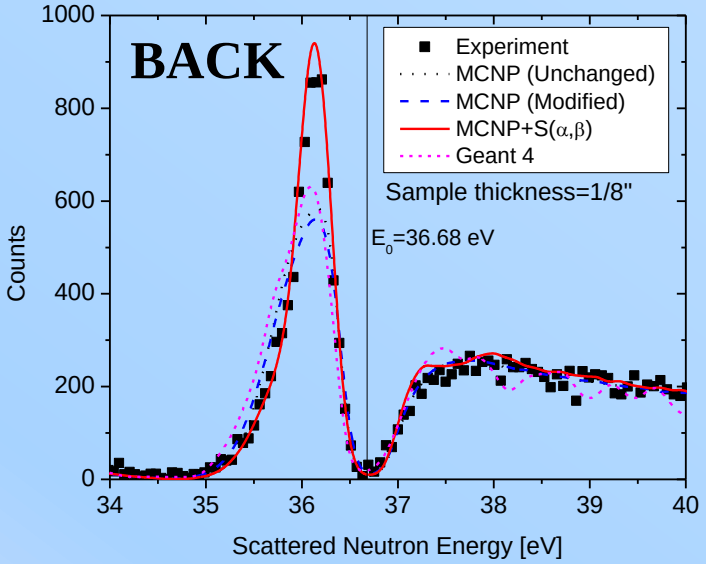

Thick Sample

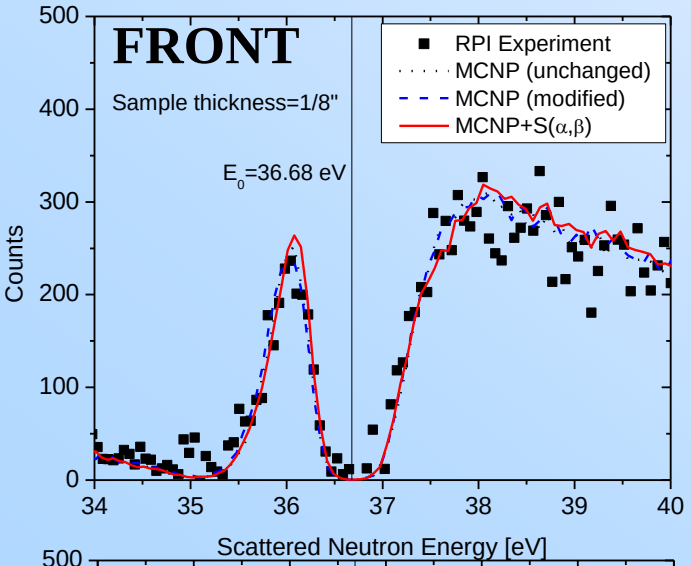

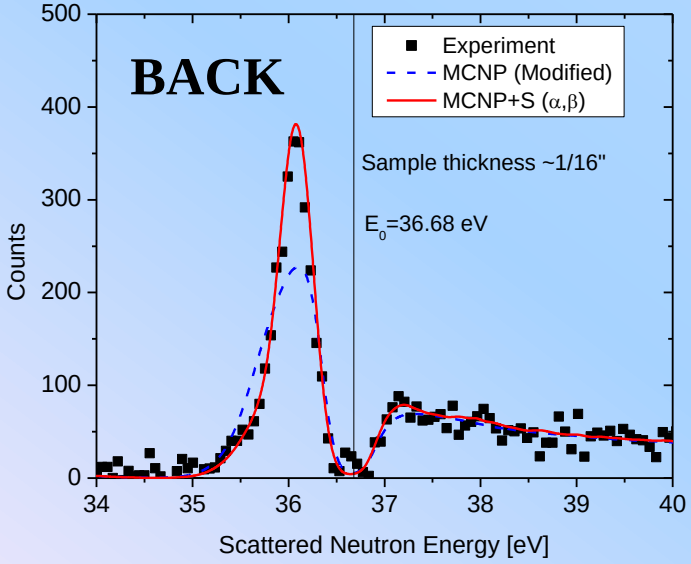

Thin Sample

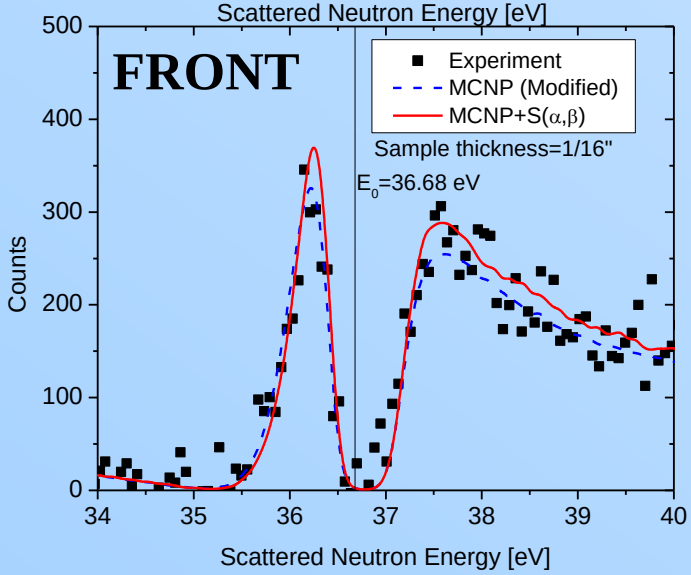

Other Resonances

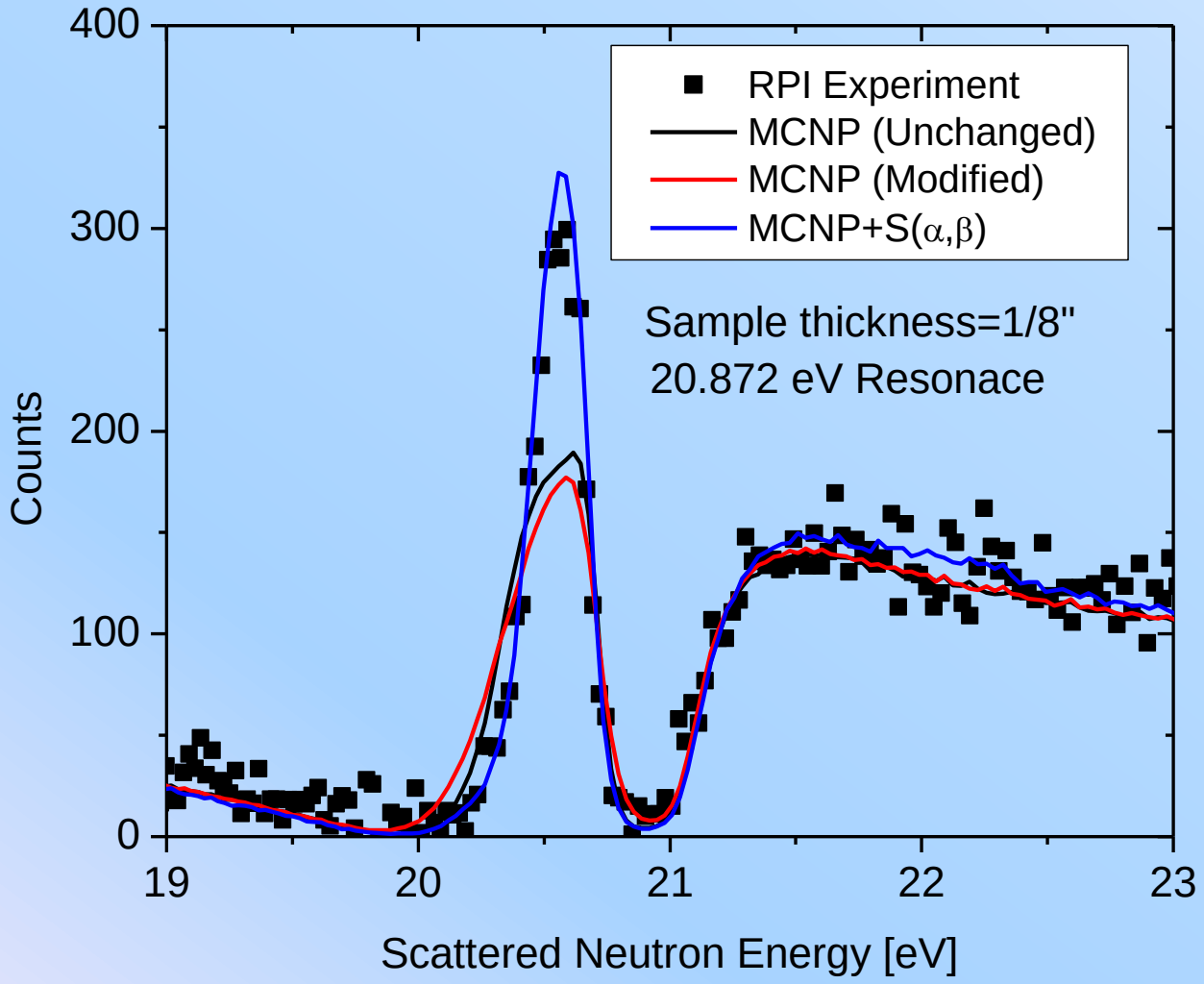

Thorium Scattering Measurements

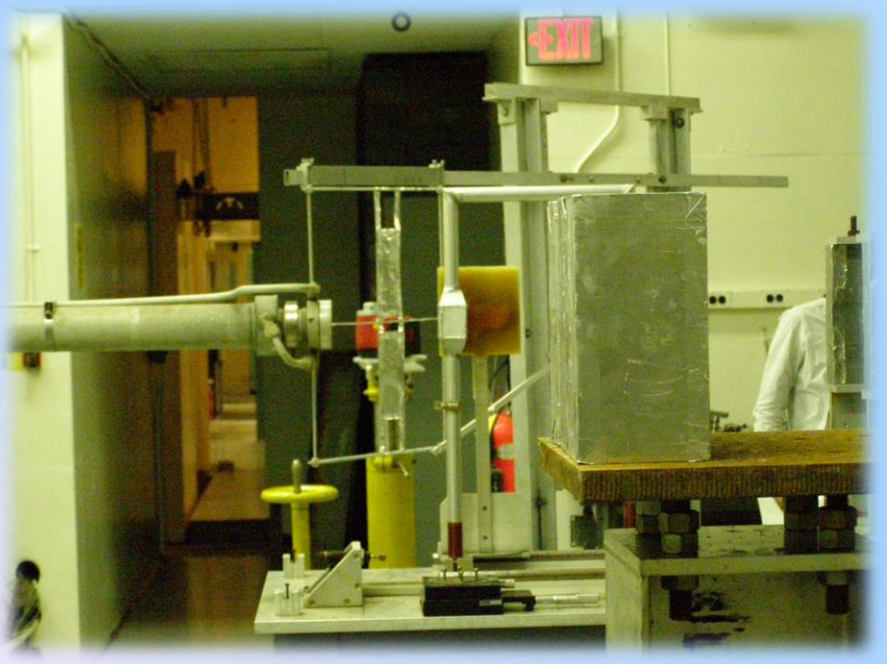

Thorium Backscattering Experimental Results

- Two sample thicknesses were used
- The backscattering angle was 140.8° and no moderator
- Experimental data was compared to current MCNP Doppler broadening and the new Doppler Broadening Rejection Correction (DBRC) method implemented by Dagan in MCNP 5
- The DBRC method is in good agreement with the experiments

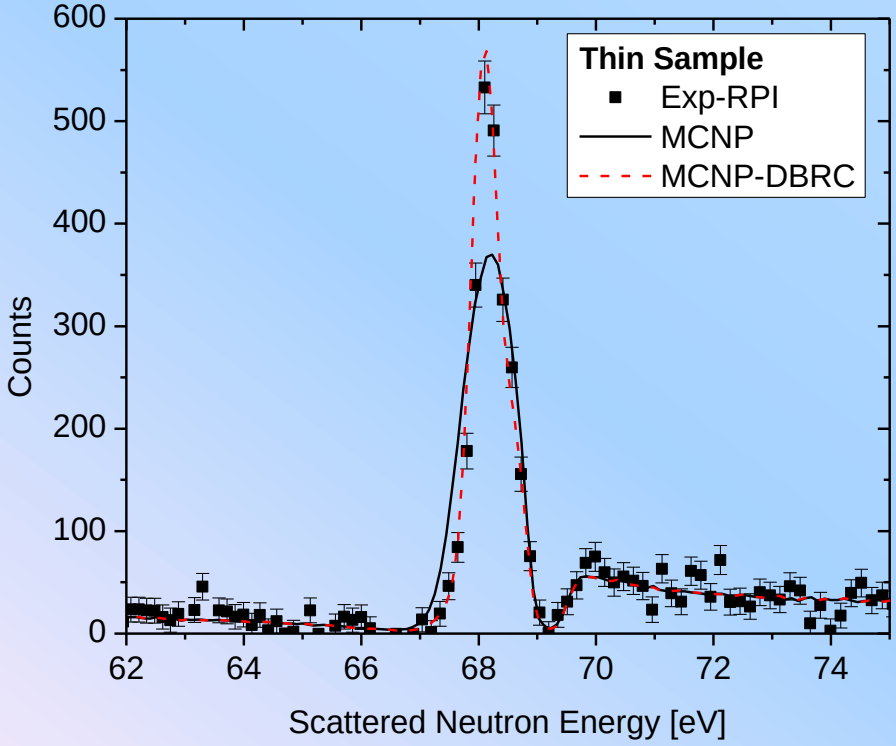

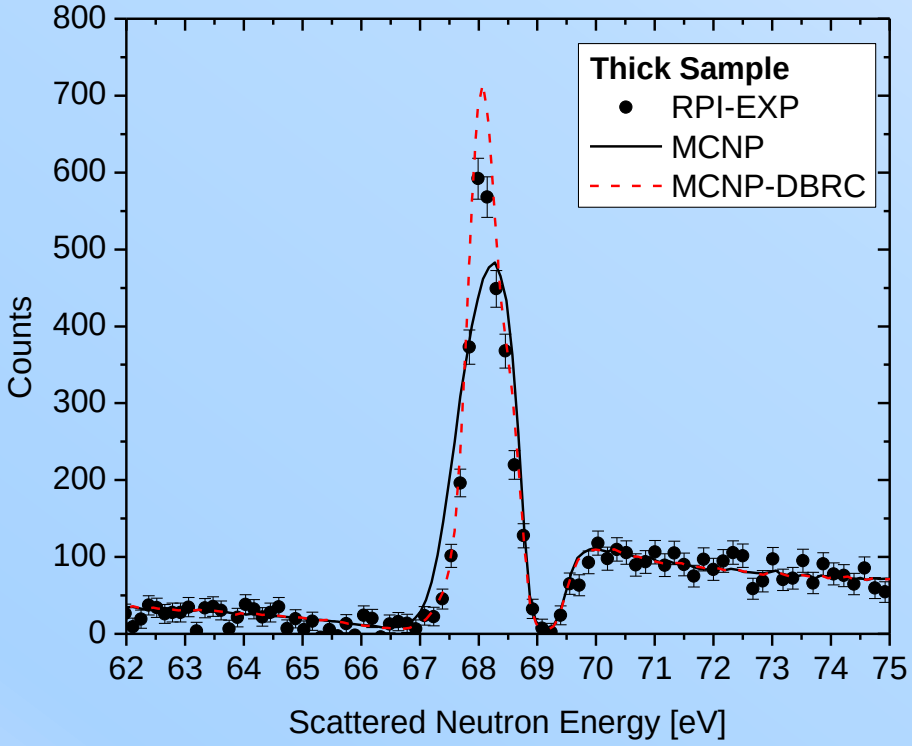

Is There More to the Line Shape?

- Comparing two measurements with different pulse width 300 ns and 150 ns

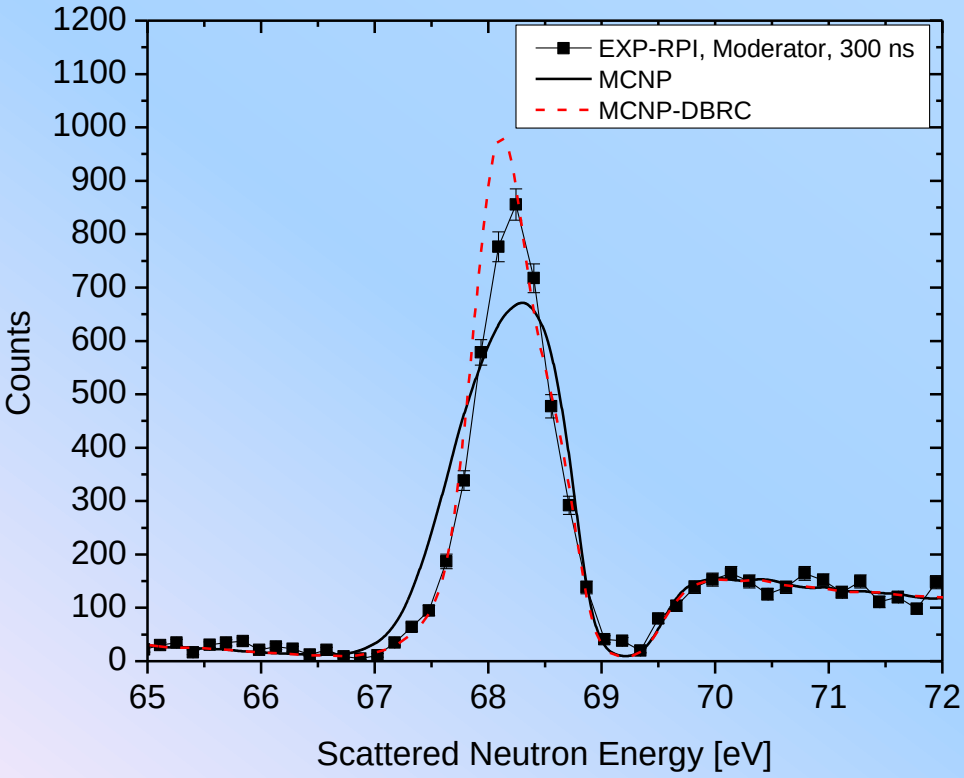

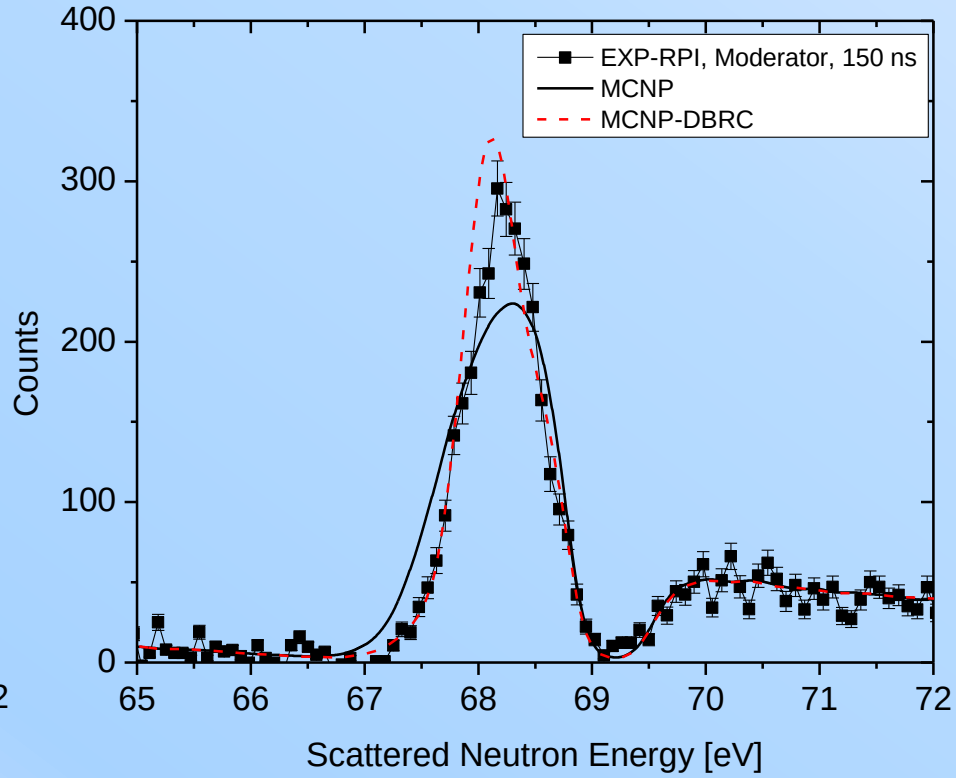

Conclusions

- Neutron resonance scattering of ^{238}U were preformed for forward and backward angles.
- The current versions of MCNP and GEANT 4 under predict the back angle scattering by nearly a factor of 2
- The measurements are in excellent agreement with a new resonance free gas scattering kernel by Dagan.
- More accurate experiments are required in order to validate the model in the forward angle
- Results with Th indicate the model might still be refined.

Fast Neutron Scattering

Differential Scattering measurements

- Use monoenergetic pulsed neutron source
- Measure the TOF spectrum using multiple detectors located around the sample
- Requires thin sample to eliminate multiple scattering
- Example below are form the INL 10 angle spectrometer

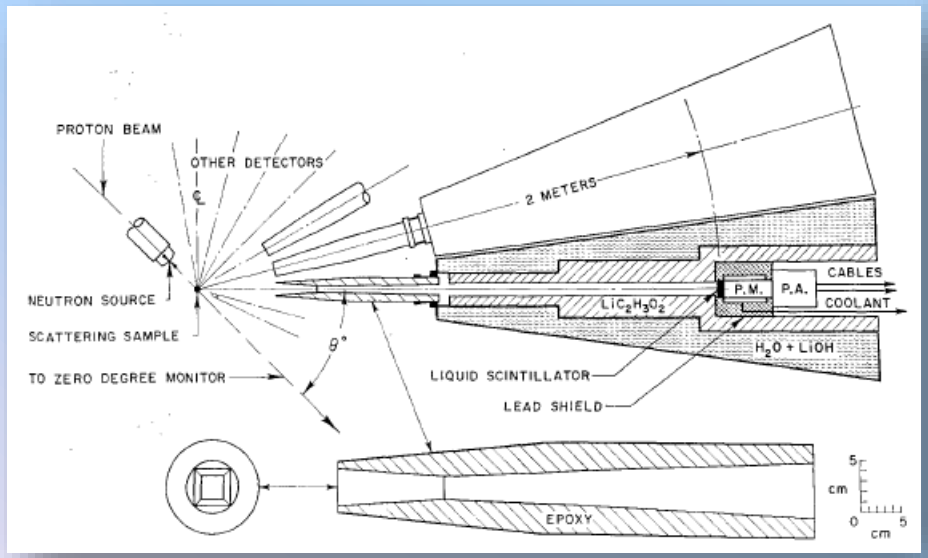

A.B. Smith, P. Guenther, R. Larsen, C. Nelson, P. Walker, J.F. Whalen, Multi-angle fast neutron time-of-flight system, Nuclear Instruments and Methods, Volume 50, Issue 2, Pages 277-291,1 May 1967.

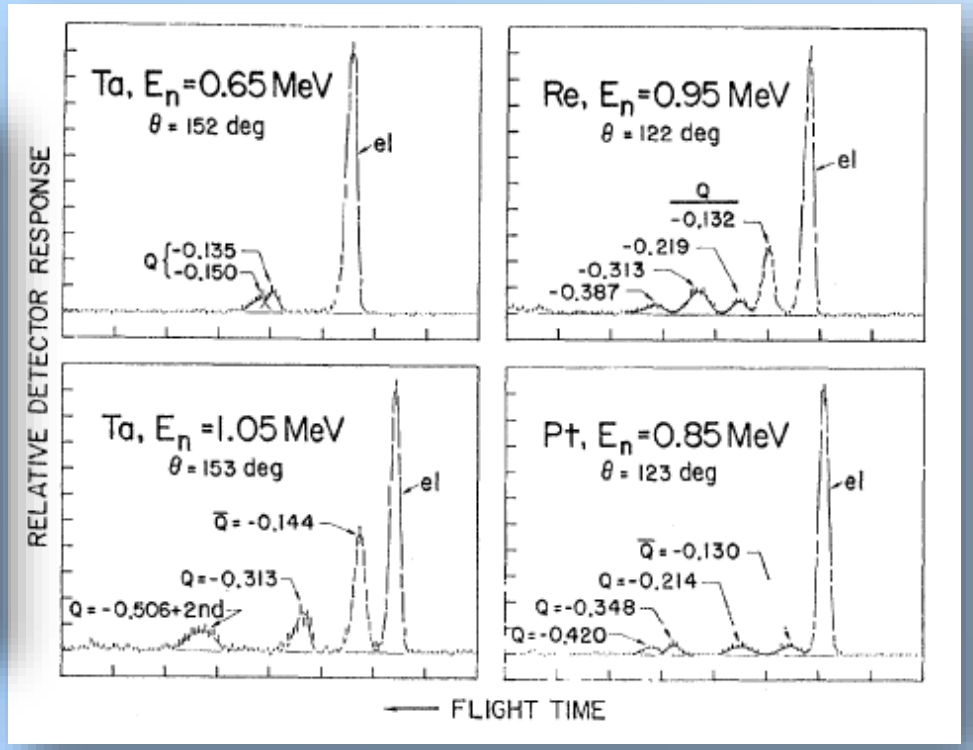

A. B. Smith, P. T. Guenther, and J. F. Whalen Phys. Rev. 168, 1344 – Published 20 April 1968

Inelastic Scattering Cross Section

- Use a high resolution gamma detector to detect gammas following inelastic scattering
- Use gamma branching, detector efficiency, and neutron flux to determine the cross section

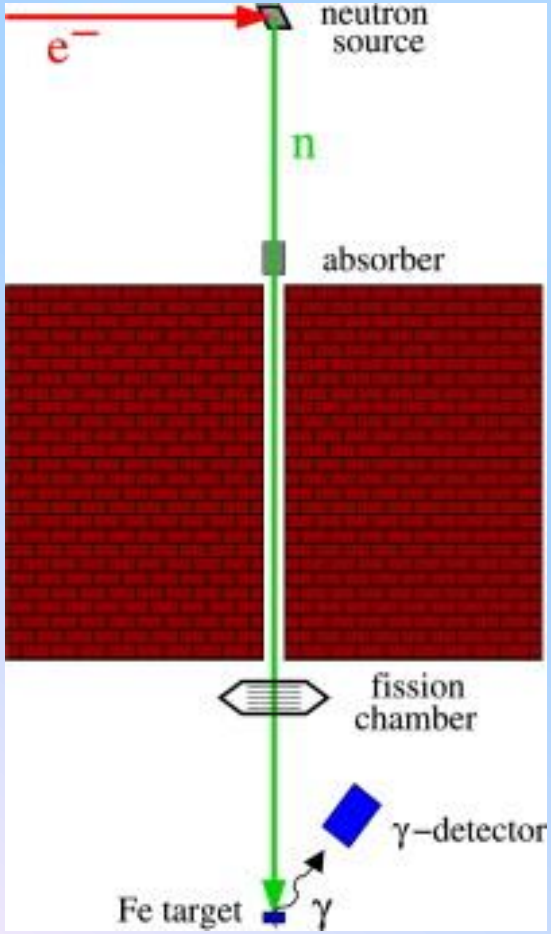

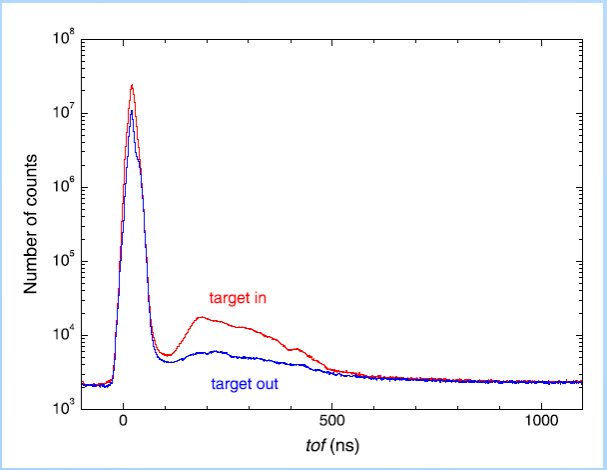

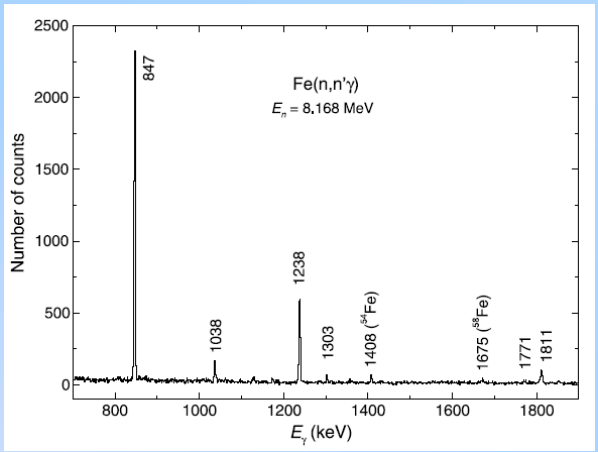

R. Beyer, R. Schwengner, R. Hannaske, A.R. Junghans, R. Massarczyk, M. Anders, D. Bemmerer, A. Ferrari, A. Hartmann, T. Kögler, M. Röder, K. Schmidt, A. Wagner, Inelastic scattering of fast neutrons from excited states in ^{56}Fe, Nuclear Physics A, Volume 927, Pages 41-52, July 2014.

Pulsed sphere measurements

- Use a DT source in the center of a sphere of material
- Measure the leakage from the sphere using liquid scintillator detectors.
- Use as benchmark by comparing with simulations

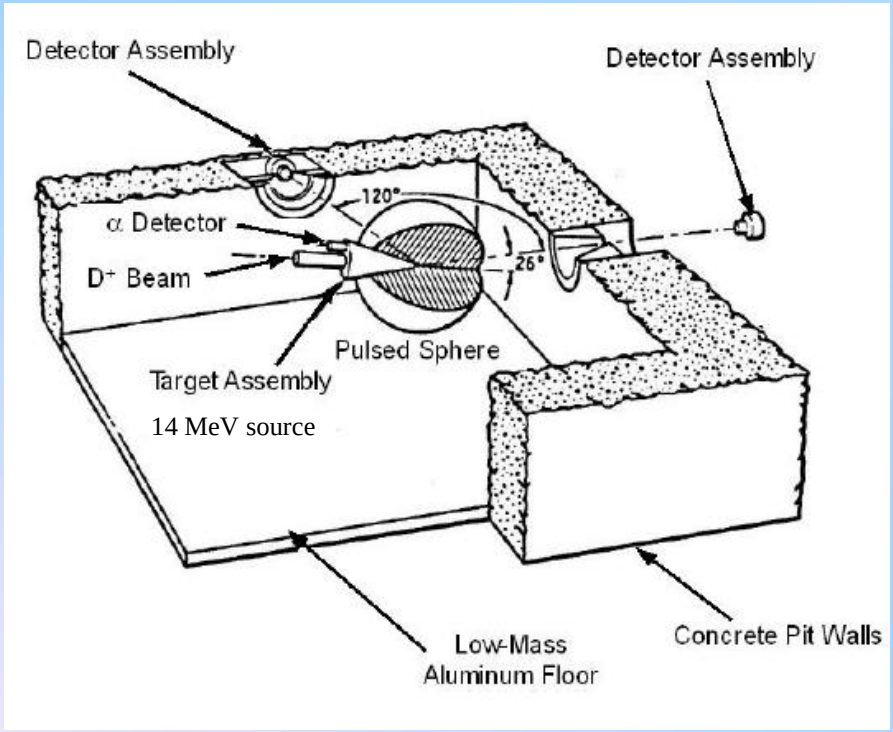

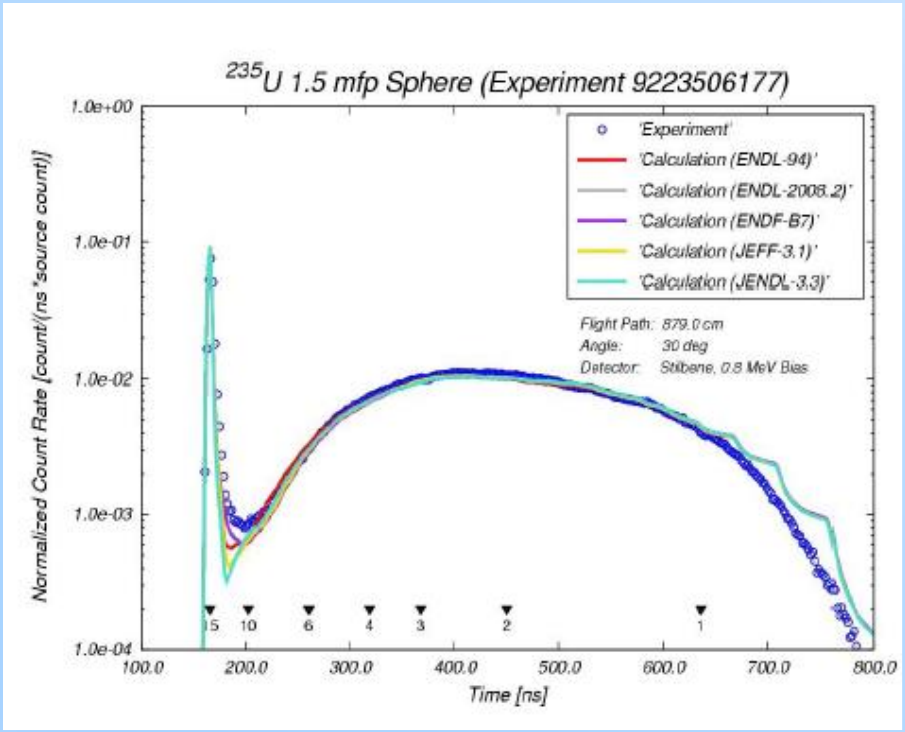

R. J. Procassini, M. S. McKinley, Modern Calculations of Pulsed-Sphere Time-of-Flight Experiments Using the Mercury Monte Carlo Transport Code LLNL-PROC-453212, September 3, 2010

The RPI fast neutron scattering system

- Use a 60 MeV pulse electron LINAC to produce neutrons (white neutron source)
- Use samples with different thicknesses (enhance multiple scattering)
- Use 8 angles, two detectors measure at the same angle.
- Measure all scattered neutrons

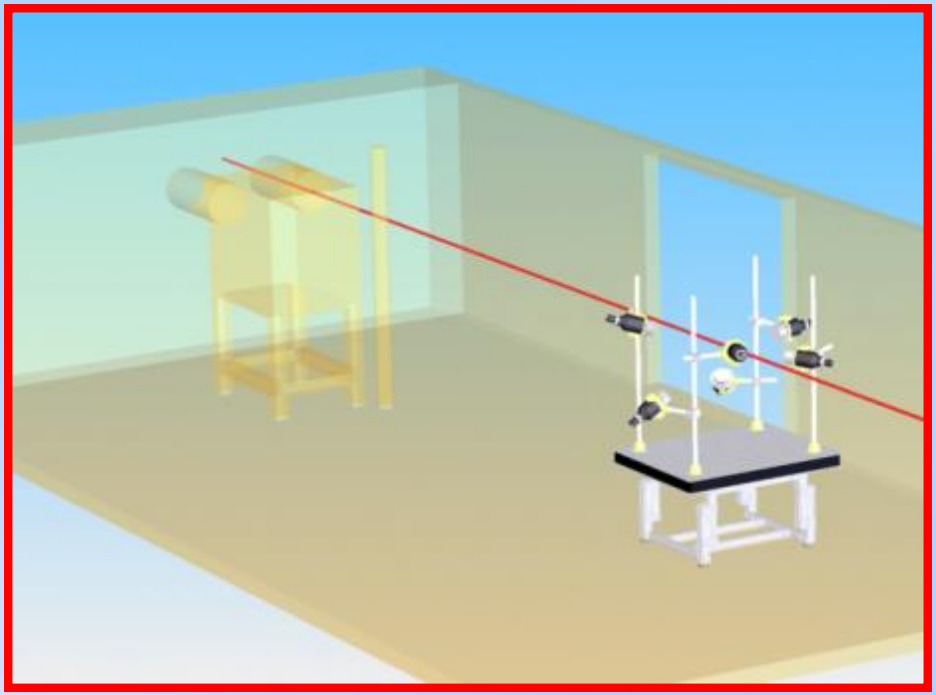

Objectives

- Provide accurate benchmark data for scattering cross sections and angular distributions in the energy range from 0.5 to 20 MeV
- Can be developed to provide differential elastic and inelastic scattering cross section measurements
- Design a flexible system: now also used for fission neutron spectra measurements

Methodology

- Characterize the neutron flux and detector efficiencies
- Measure the neutron scattering distribution at several angles around the sample
  - TOF used to measure the neutron's incident energy
  - Liquid scintillators used to discriminate neutrons from gammas
- Measurements are compared with detailed simulations of the system
  - Different cross section libraries assessed
- Identify energy/angle regions where libraries may be improved by comparing:
  - Total Angular TOF Data
  - Inelastic-to-Elastic Ratios
  - Elastic Angular TOF Data

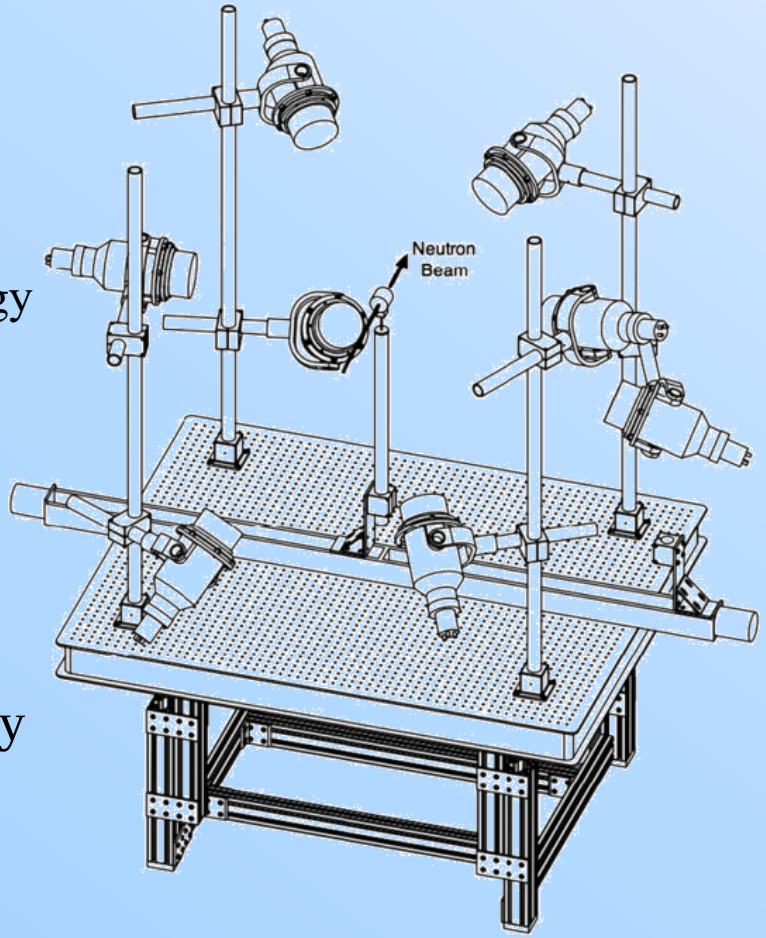

TOF Scattering Yield Measurement

- Measure the total TOF $t=t_1+t_2$
- For all scattering events $E_2<E_1$
- In most cases the energy loss is small $E_1 \sim E_2$
- Since $t_1>>t_2$ and $E_1 \sim E_2$ then for presentation the incident neutron energy E_1 is calculated using t and $L=L_1+L_2$

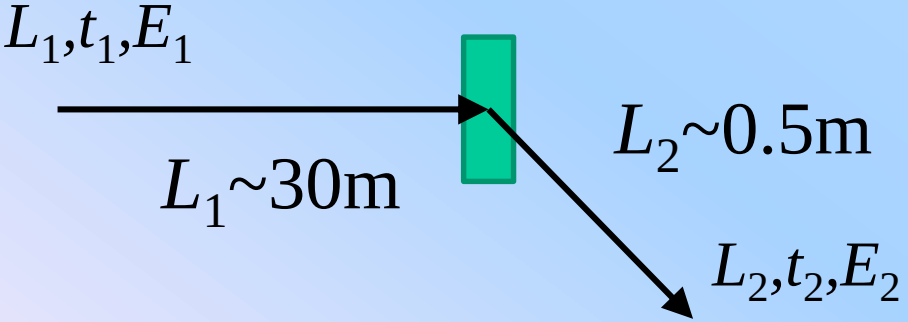

$$E(t) \approx m_n c^2 \cdot \left(\frac{1}{\sqrt{1-\left(\frac{L}{c \cdot t}\right)^2}} - 1 \right)$$

First Order Approximation of the Scattering Yield

Detector Efficiency

Probability to Interact

$$Y(E,\phi) \propto \eta(E')\Phi(E)\left(1-e^{\Sigma_T(E)L}\right)\frac{f(E,\phi)}{2\pi}$$

Incident Flux

Probability to Scatter in direction ϕ

In this approximation multiple scattering is ignored

Experimental Setup Overview

- A well-collimated continuous-energy pulsed neutron beam scatters from a sample and is measured by detectors positioned around the scattering sample

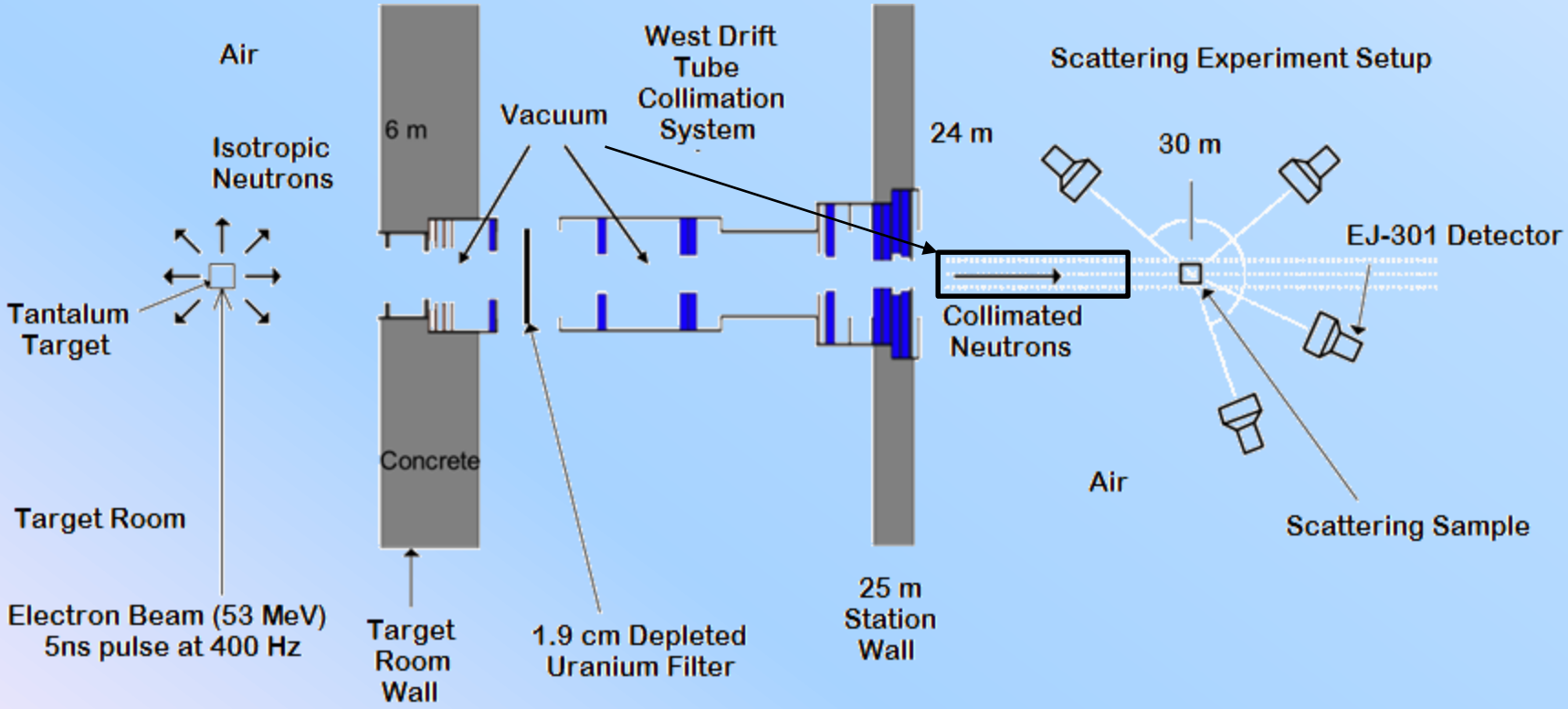

Scattering Detection System: Experimental Setup

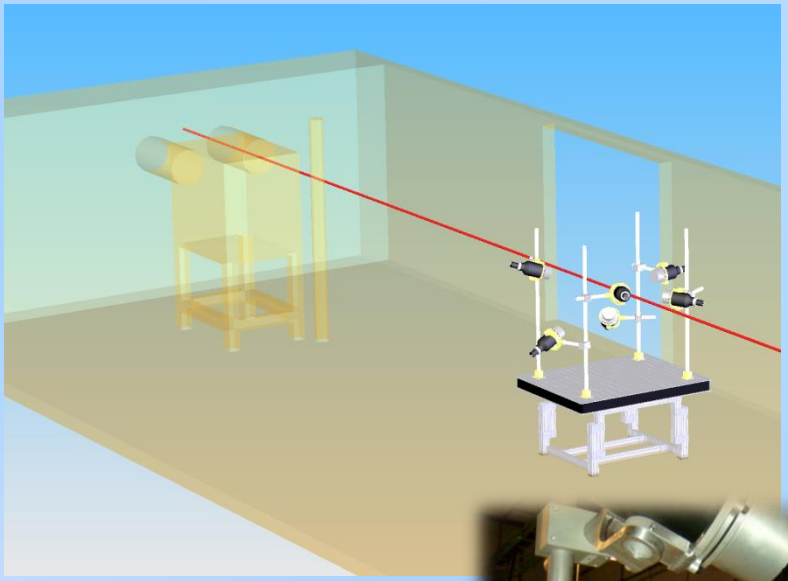

Pioneered the use of Red Bull can for nuclear physics (as low mass sample holder)

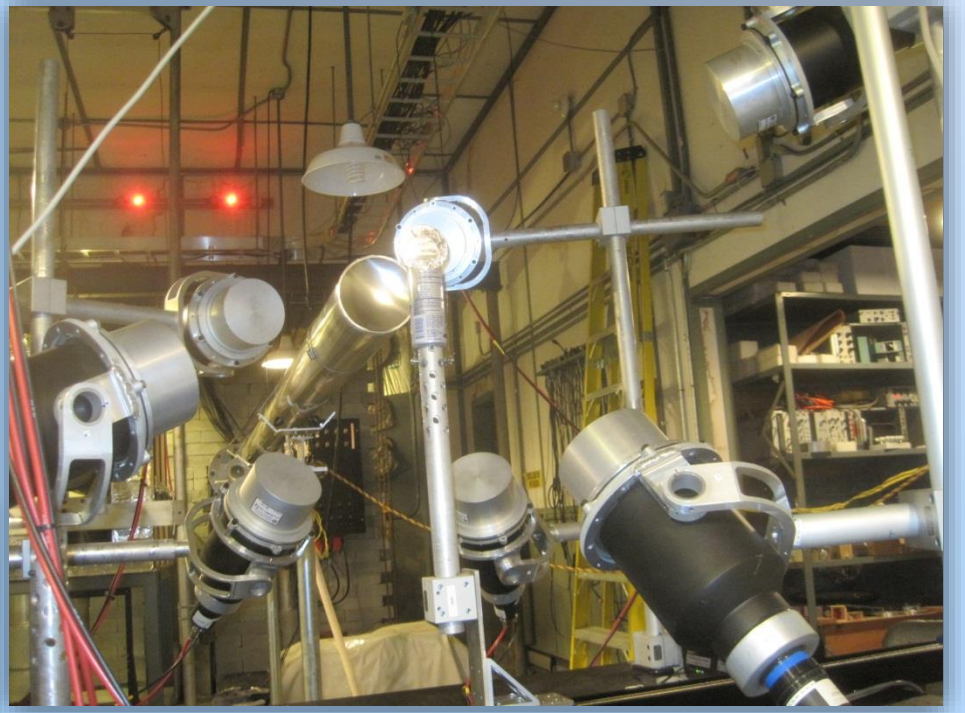

Scattering Detection System: Experimental Setup

- Detector Array
  - 8 EJ301 Liquid Scintillation Detectors
  - 8 A/D channels
  - Pulse Shape discrimination in TOF
- Data Processing System
  - Data Processing Computer (SAL) – Control Room
- Computer Controlled Power Supply
  - Chassis - SY 3527 Board - A1733N
- Sample Holder / Changer

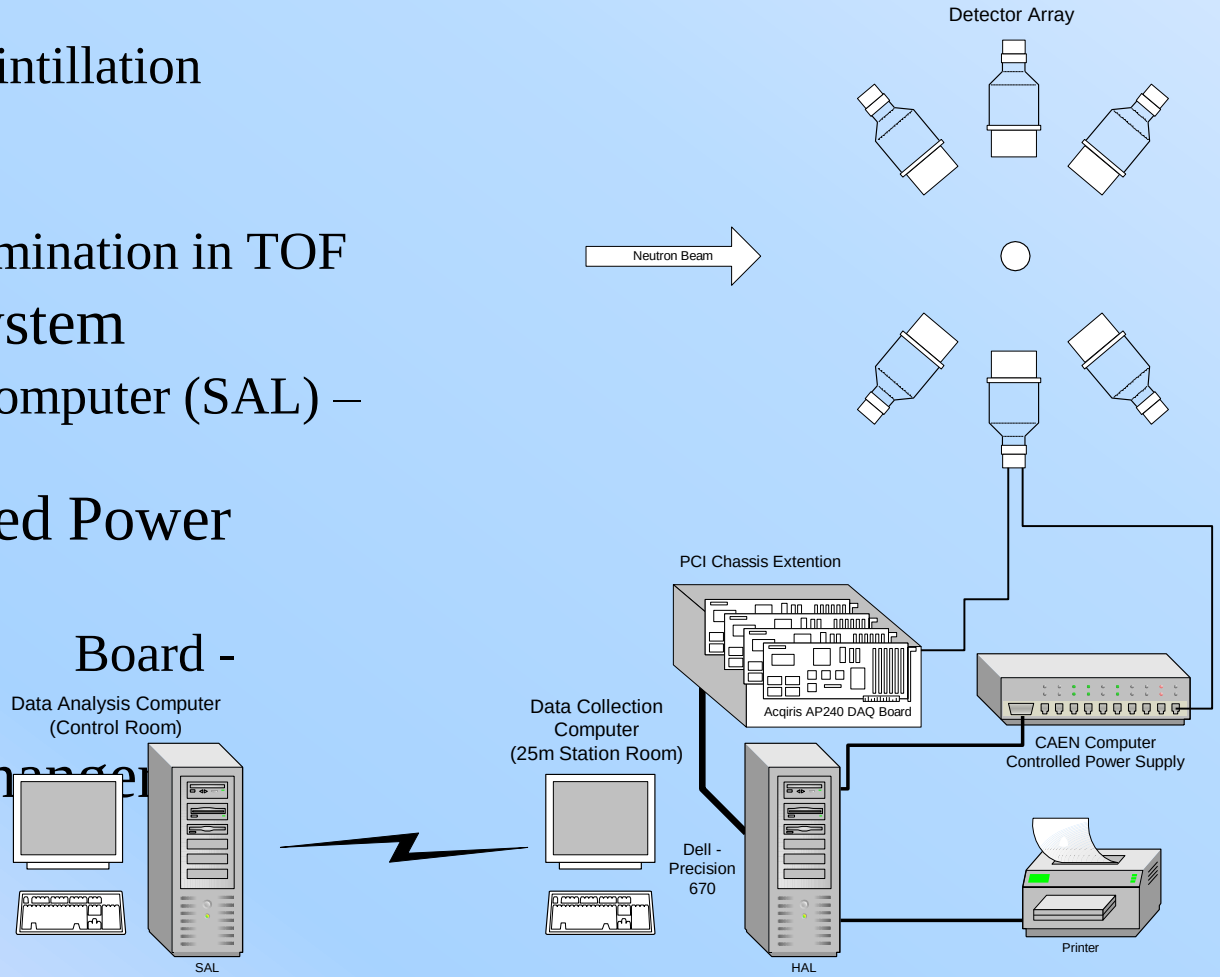

DAQ system

- All DAQ is automated using script based software running under Windows
- Alternate between sample, graphite and open (background) measurements
- Each position is measured for about 10 min
- Fission chamber monitors are used to normalize beam intensity fluctuations.
- Detector/system gain is periodically aligned using ^{22}Na

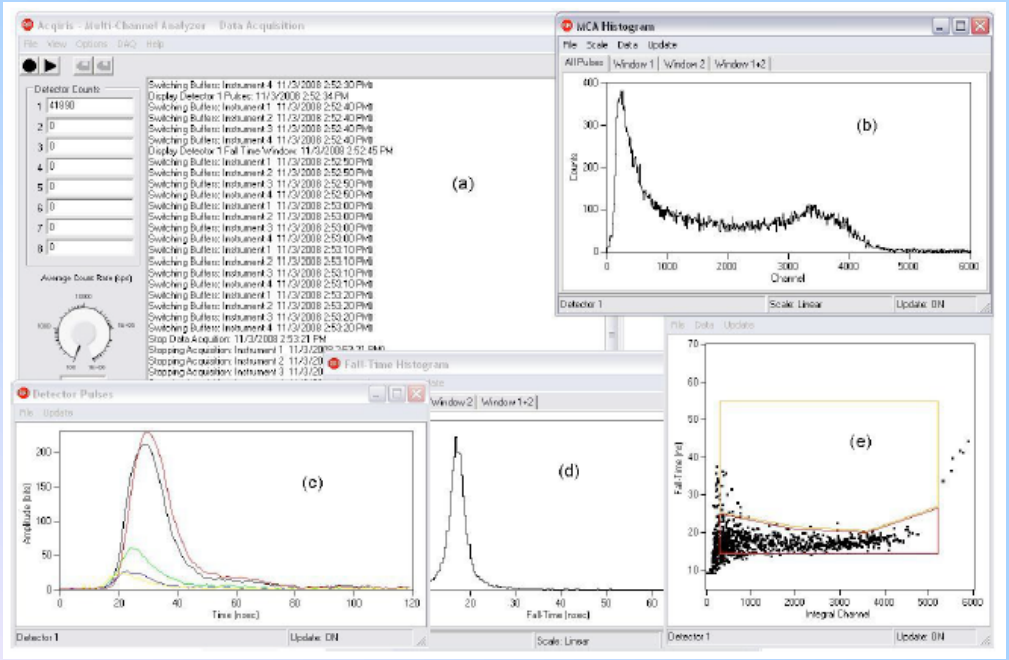

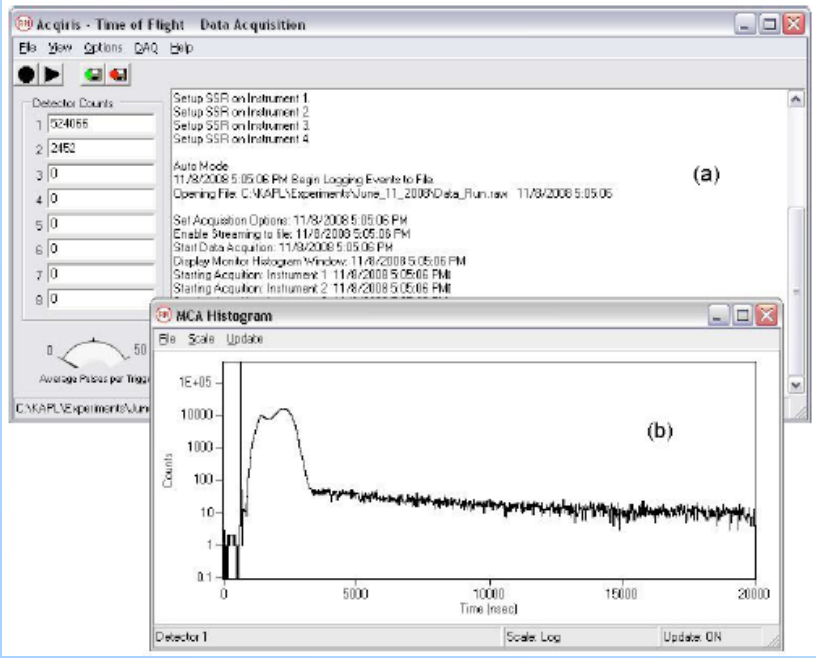

Pulse Shape Analysis – Classification

- EJ-301 (NE-213) liquid scintillator respond to neutrons and gammas
  - Photons interact with electrons via Compton scattering
  - Neutrons interact with protons (^{1}H) via proton recoil

- Percentage of delayed light production varies between the two modes

Pulse Classification Analysis performed to distinguish neutrons from gammas

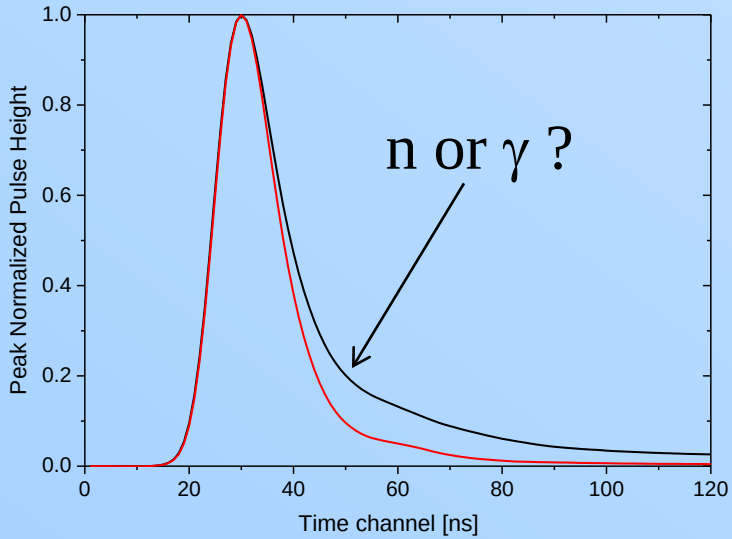

Pulse Classification Analysis – Digital Data

- A collection of gamma and neutron pulses were obtained
  - 5.6 x 10^6 pulses from a ^{137}Cs gamma source (661 keV)
  - 1.9 x 10^6 pulses from a TOF measurement with the graphite reference sample and a detector positioned at 155º (incident neutrons < 4.439 MeV)

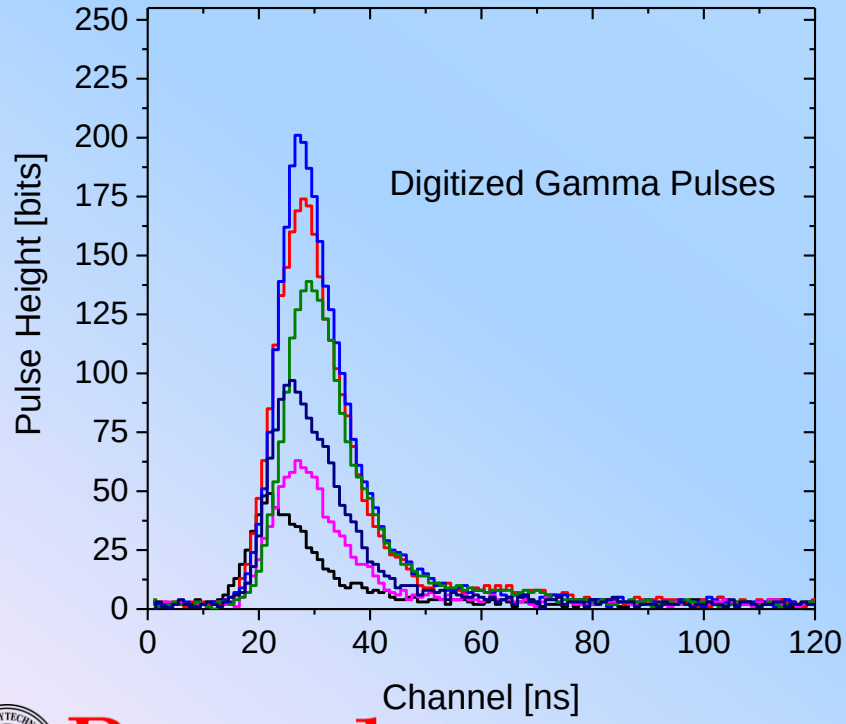

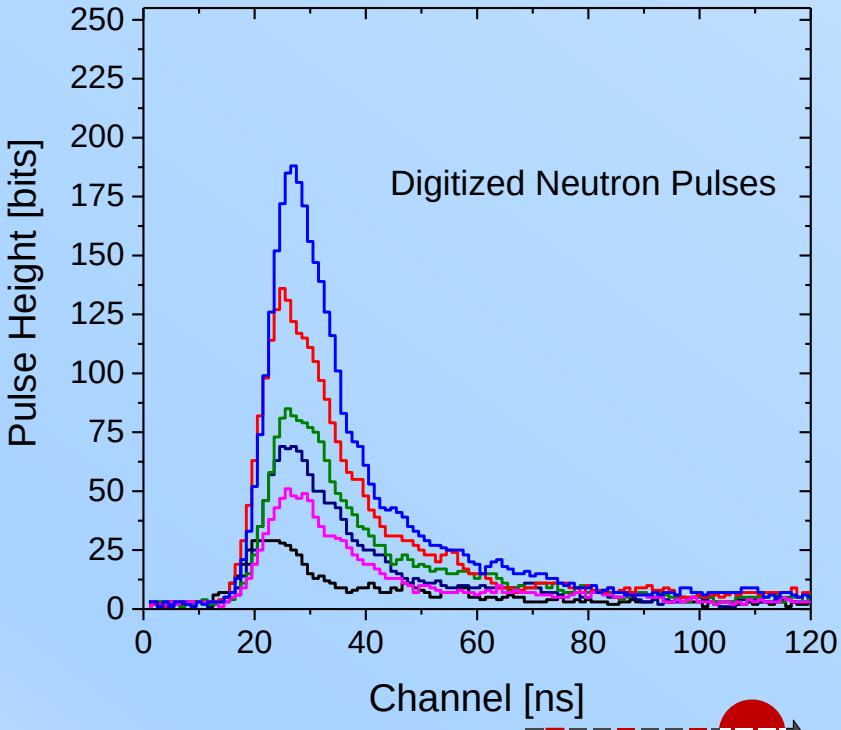

Pulse Classification Analysis – Method

- A reference pulse shape for gamma and neutrons were obtained by:
  1. Averaging pulses with similar integrals (area under pulse) to form representative pulses [Integrals between 300 and 4000]
  2. Peak normalizing the representative pulses
  3. Peak aligning the representative pulses

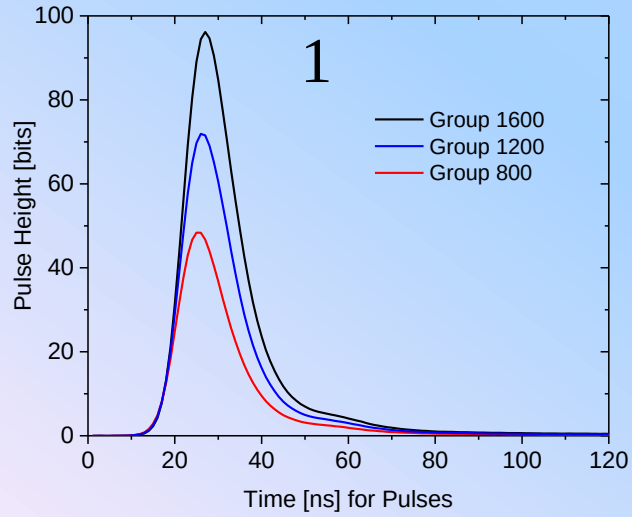

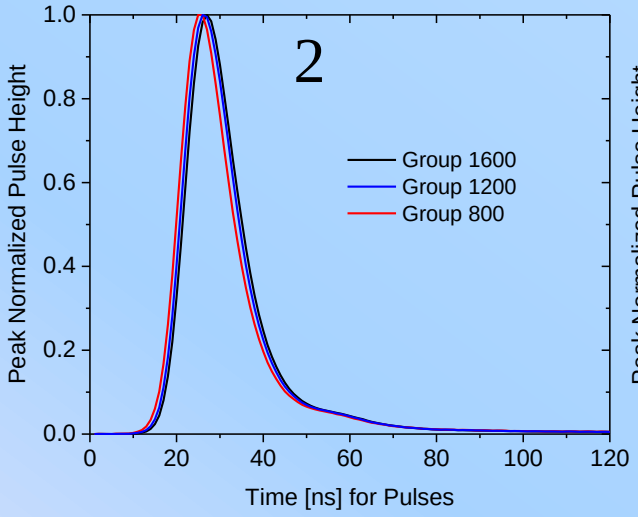

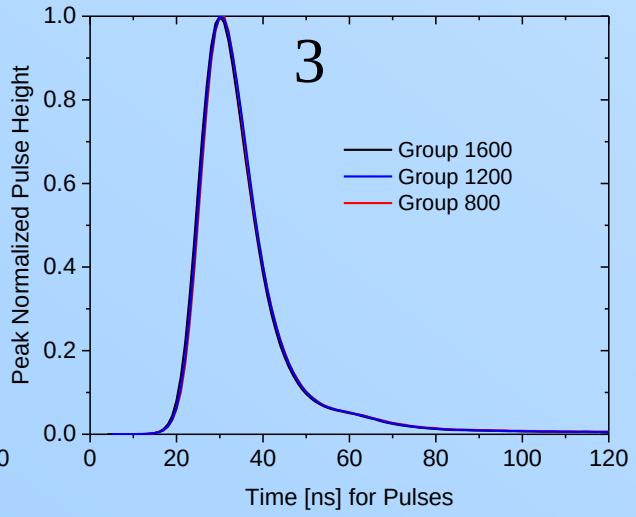

Pulse Classification Analysis – Method

- All representative pulses were averaged to form reference neutron (n^{ref}) and gamma (γ^{ref}) pulse shapes
- Each digitized pulse was smoothed and compared to the n^{ref} and γ^{ref} in the region between 45 and 105 ns

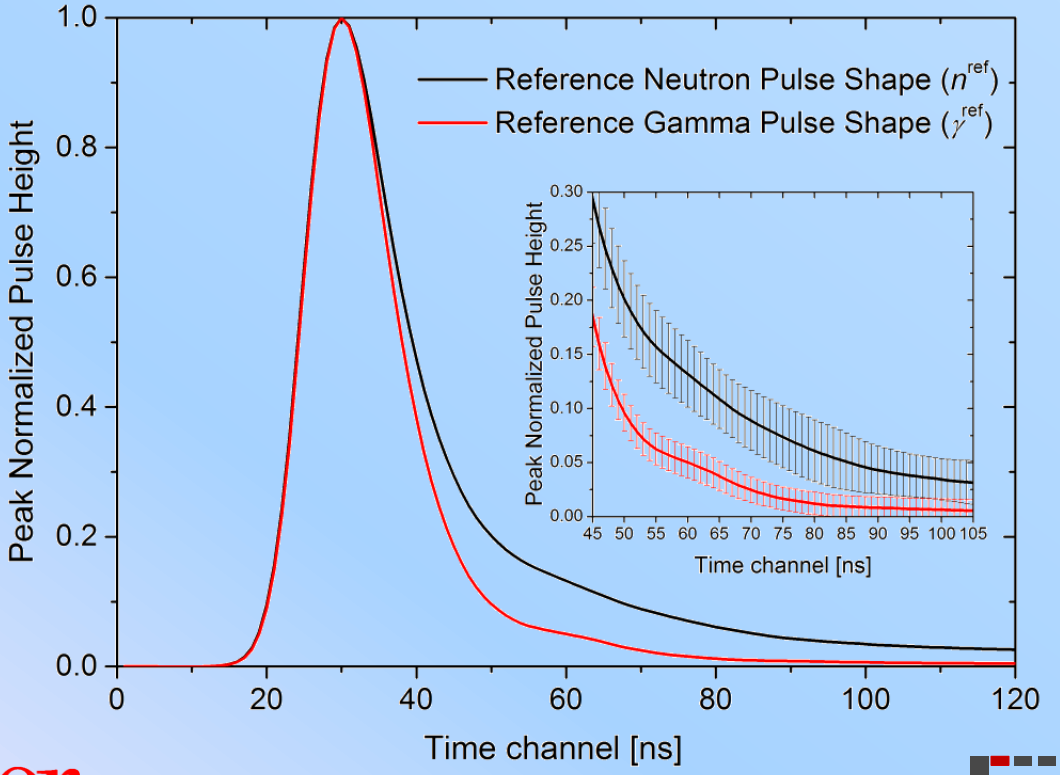

Pulse Classification Analysis

- The ^{137}Cs was examined to quantify how well gammas were classified with PCA method
  - 99% of measured events from the ^{137}Cs (661 keV) and ^{22}Na (0.511 and 1.274 keV) sources were classified as gammas
  - Gammas erroneously classified as neutrons are a concern for pulses with low integrals

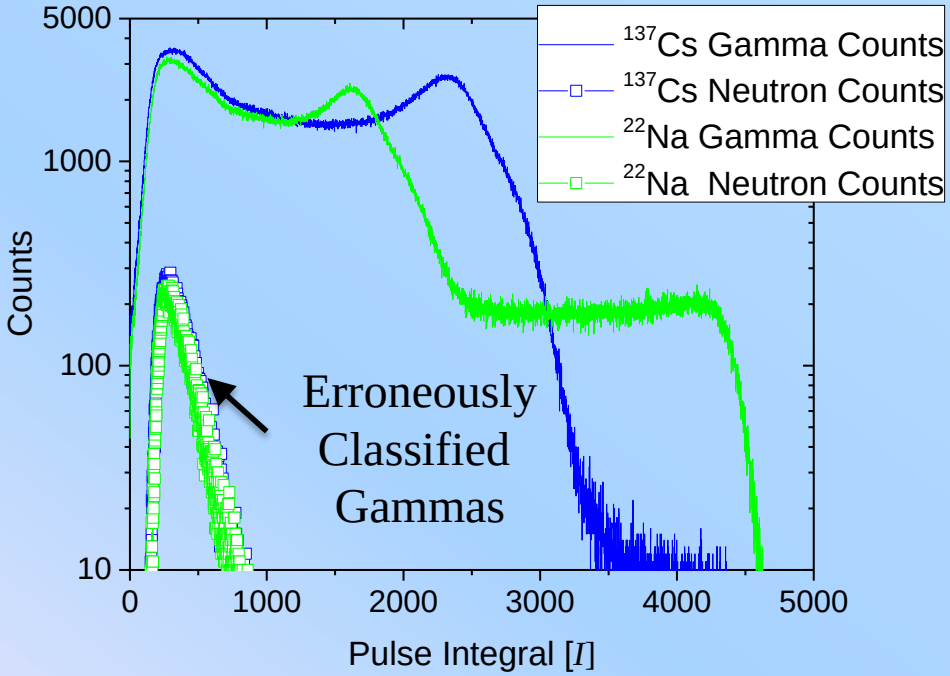

Pulse Classification Analysis – GMC

- Ratio of gammas erroneously classified as neutrons to gamma at each pulse integral bin was found and a pulse function was fit to with Origin 9.1 that has the following form:

$$F(I) = y_0 + A \cdot \left(1 - e^{-\left(\frac{I-I_0}{t_1}\right)}\right)^P \cdot e^{-\left(\frac{I-I_0}{t_2}\right)}$$

  - The GMC relies only on energy deposited **NOT** incident gamma energy
  - The GMC eliminated the neutron contribution for ^{22}Na and ^{137}Cs

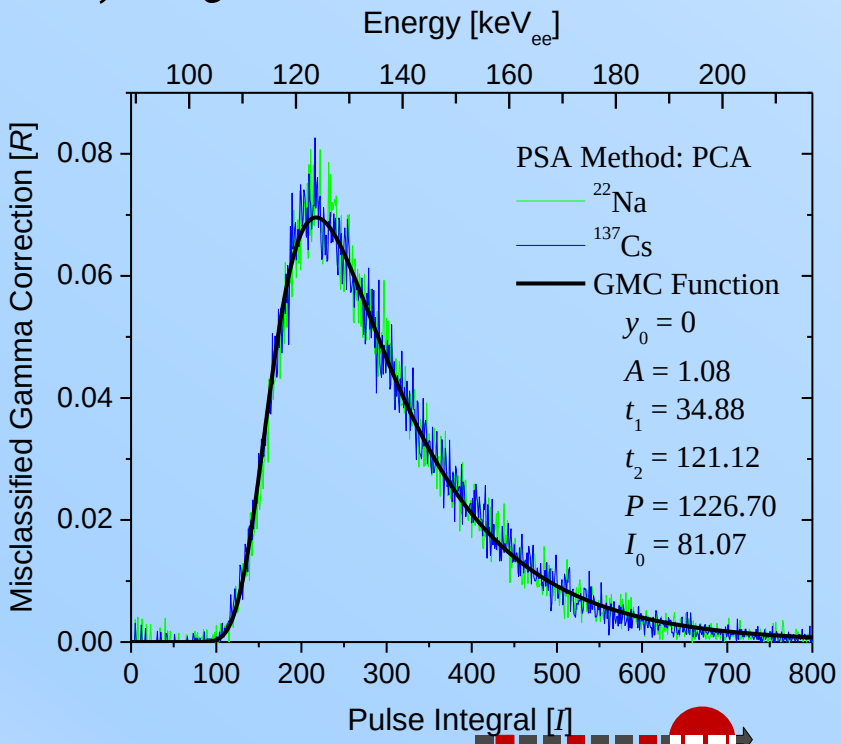

Flux Shape Measurement

- Use a fission chamber with ~391 mg ^{235}U in the sample position
- Use ENDF/B 7.0 fission cross section
- Correct for transmission of all materials between the source and sample
- Compare to a similar measurement using EJ301 and SCINFUL calculated efficiency
- Combine the two data sets using fission for E< 1 MeV

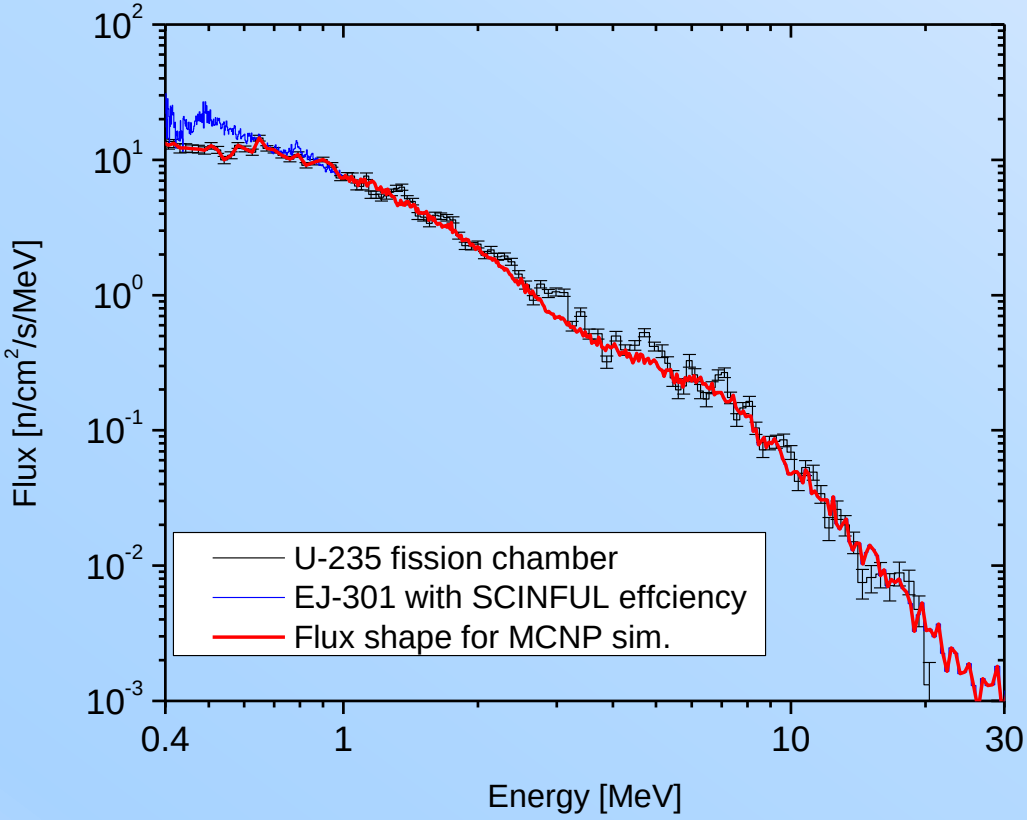

Efficiency as a Function of Energy

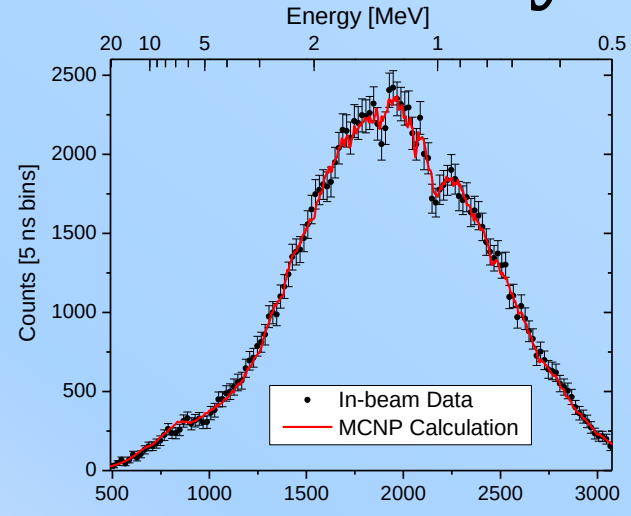

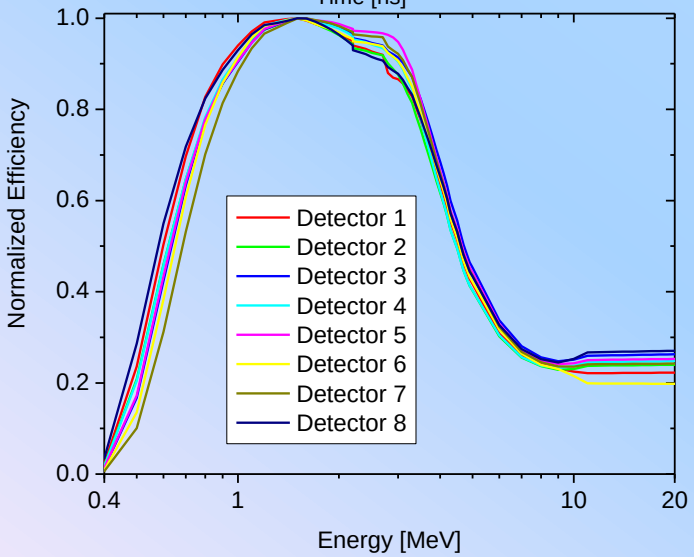

- Objective:
  - MCNP simulation of EJ301 response in the sample position must precisely agree with the measurement
- Methodology:
  - Use the measured flux as a source in MCNP simulation of the in-beam detector response
  - In MCNP set the detector efficiency η=1 (tally only the neutron flux shape)
  - Divide the measured response by the simulation results to get the efficiency $\eta(E)$ for each detector
  - During the experiment periodic gain calibrations are done to minimize gain shift.

Neutron Beam Collimation

- Characterize the collimation system
  - Ensure beam diameter agrees with sample diameter of 7.62 cm
  - Verify measurements and calculations agree

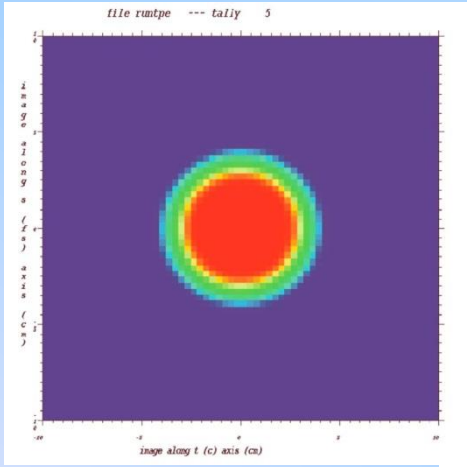

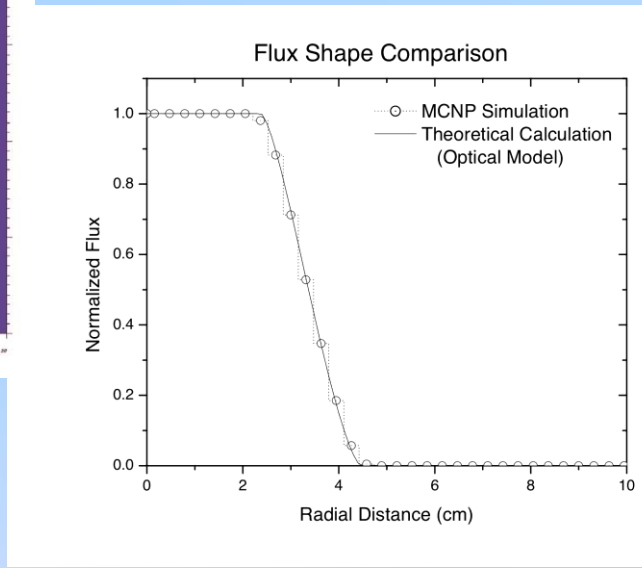

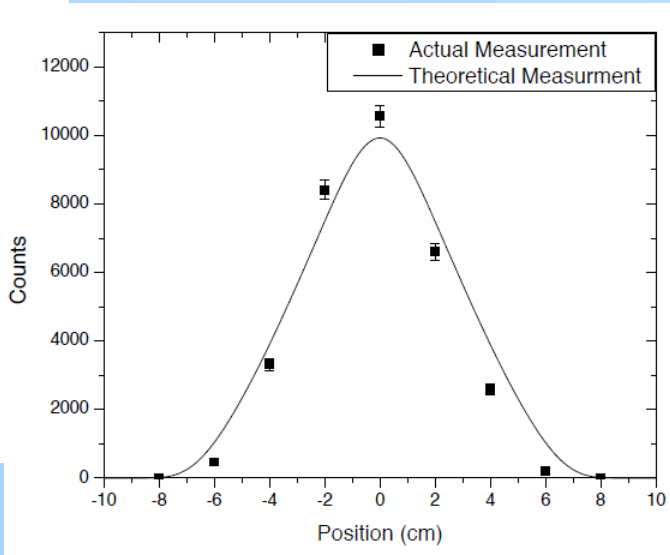

Data Reduction

- Sum all files and dead-time correct.
- The experimental count rate corrected for background, R_i, was obtained by subtracting monitor normalized open data, R_i^O, by sample data, R_i^S, for each channel, i:

$$R_i = R_i^S - \frac{M^S}{M^O} \cdot R_i^O$$

MCNP Simulations

- Objective of the MCNP model is to mimic an experiment
- The MCNP Model includes:
  - Concrete floor, Optical Table, Center beam vacuum tube, Mylar vacuum windows, aluminum vacuum window, depleted uranium filter
  - Neutron flux shape (source term)
  - Tallies convoluted by energy-dependent detector efficiencies
  - Library for scattering sample varied:
    - ENDF/B-VII.1, JEFF-3.2, JENDL-4.0, etc.

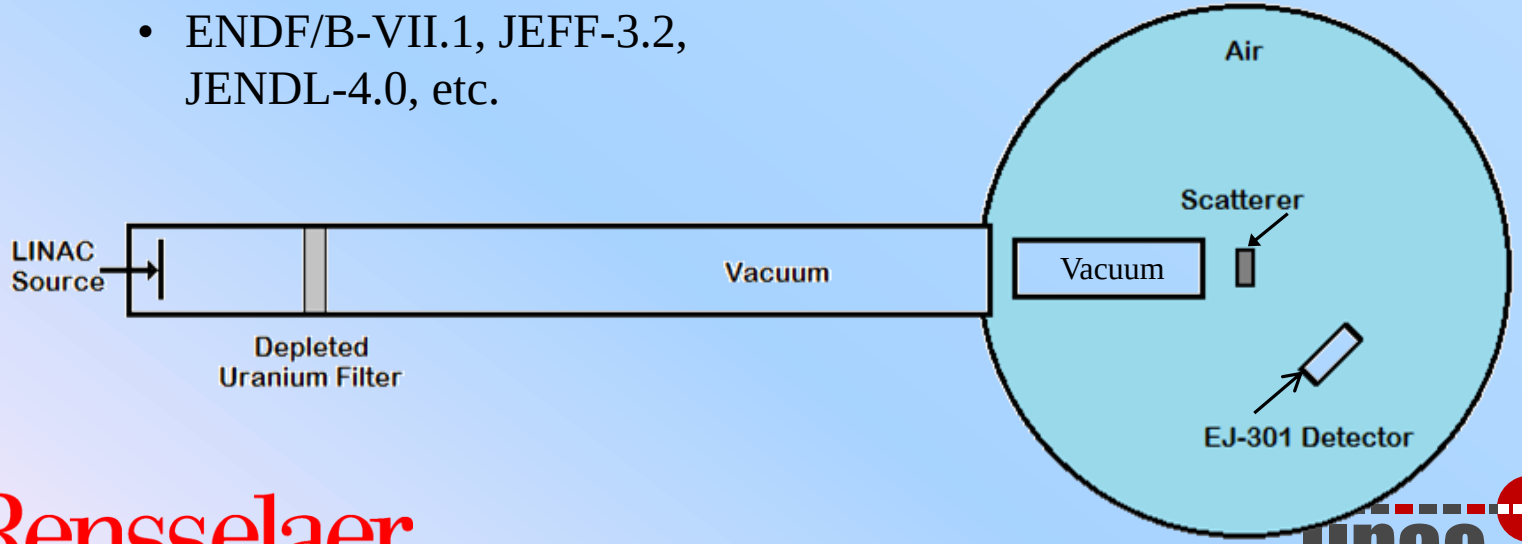

Data Analysis

- Compare the shape (as a function of TOF) between the measurements and simulations
- Use graphite as a reference in all measurements
  - Differences between the measurement and simulation of graphite are considered systematic errors
- Measurements of Be, Mo and Zr
  - The efficiency was derived from SCINFUL calculations
  - Neutron flux shape based on a fit to in-beam measurements with EJ-301 and Li-Glass
  - Used individual detector normalization of the simulation to the experimental data based on graphite measurement
- For ^{238}U experiment
  - Flux was derived from ^{235}U and EJ301 in-beam measurements
  - The efficiency was adjusted to match the MCNP calculations to the in-beam measured data
  - Use one normalization number for all detectors (global normalization)

Carbon Experimental Results

for Be measurement

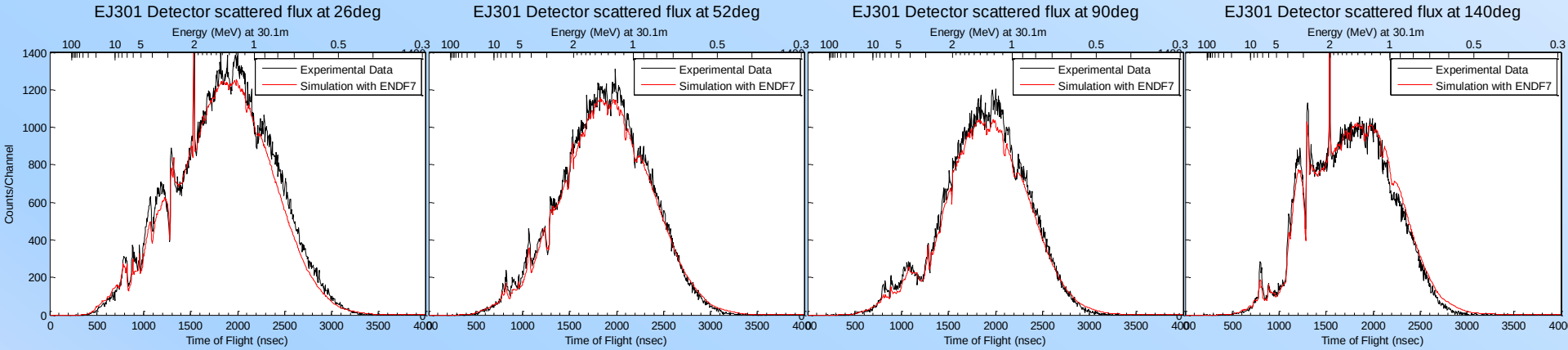

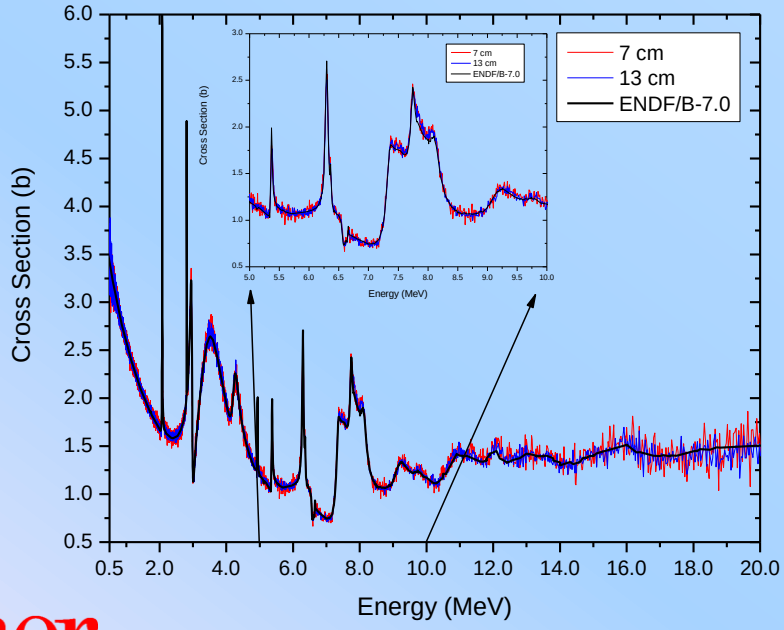

Total cross section

Beryllium Experimental Results

4cm

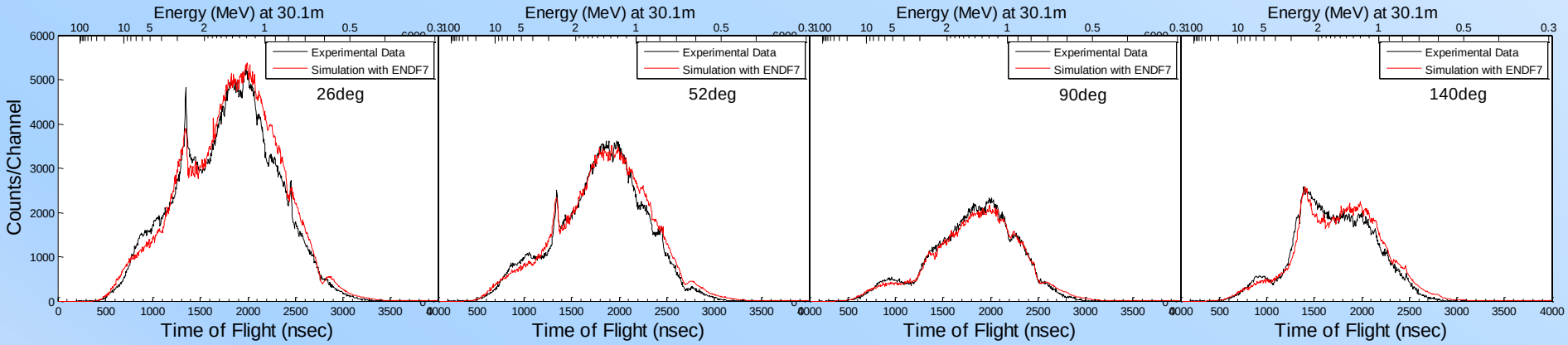

8cm

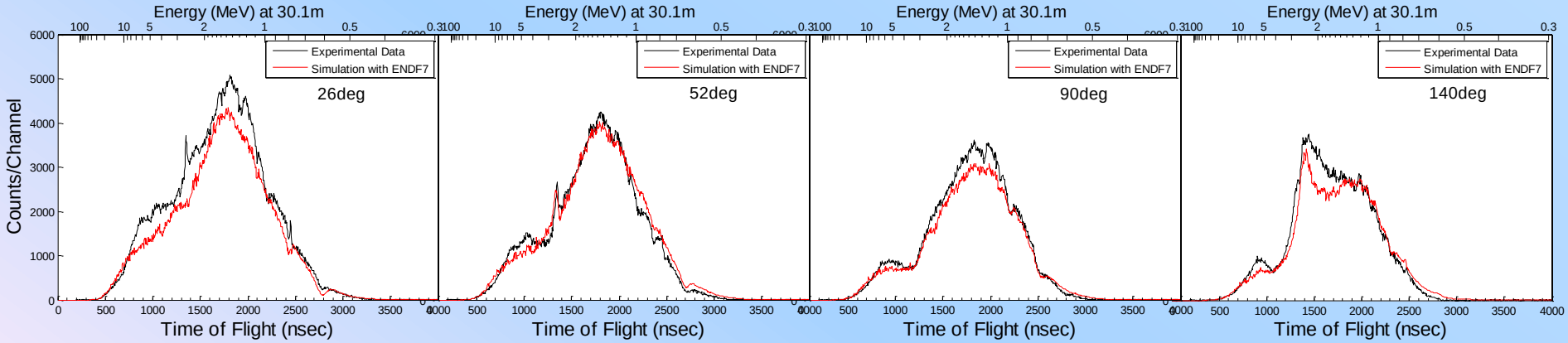

Molybdenum Experimental Results

5cm

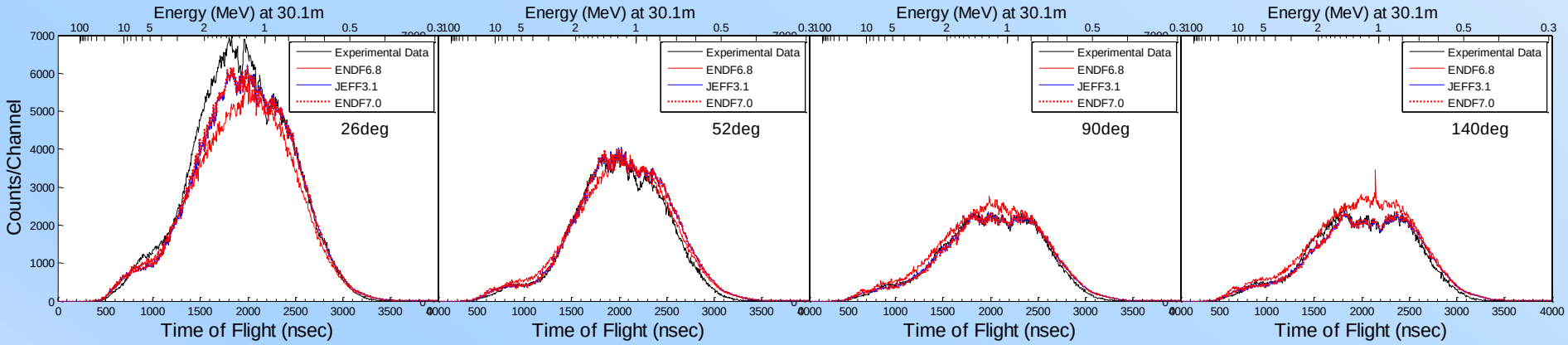

8cm

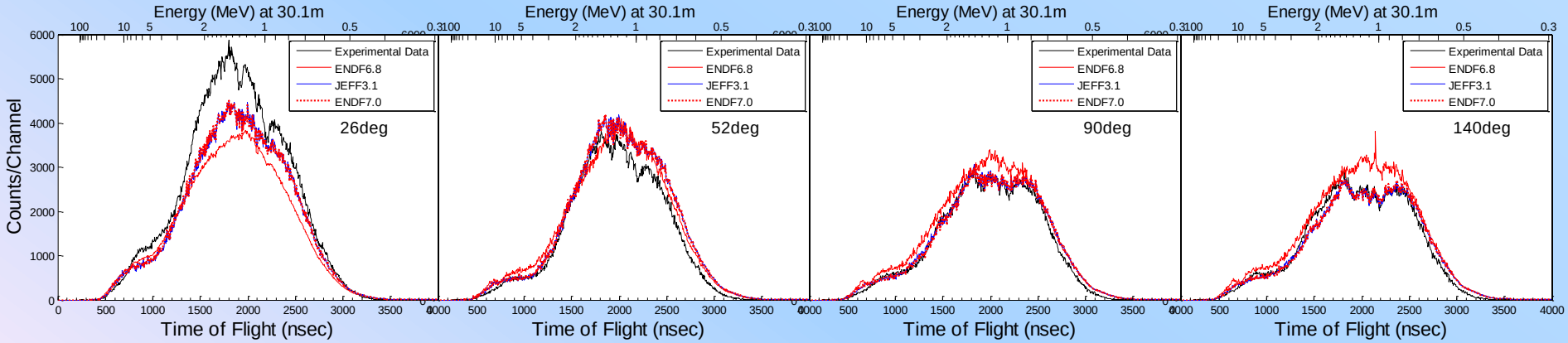

Zr – 6 cm Thick Sample

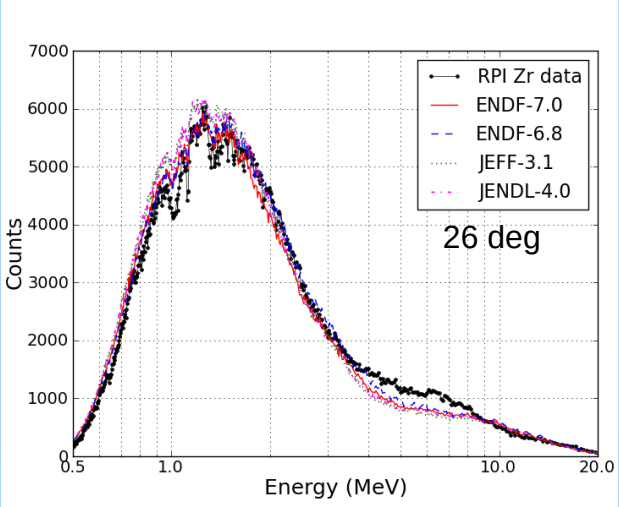

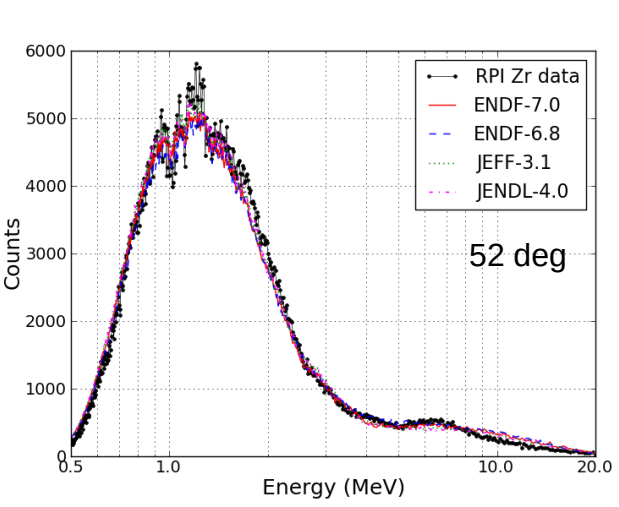

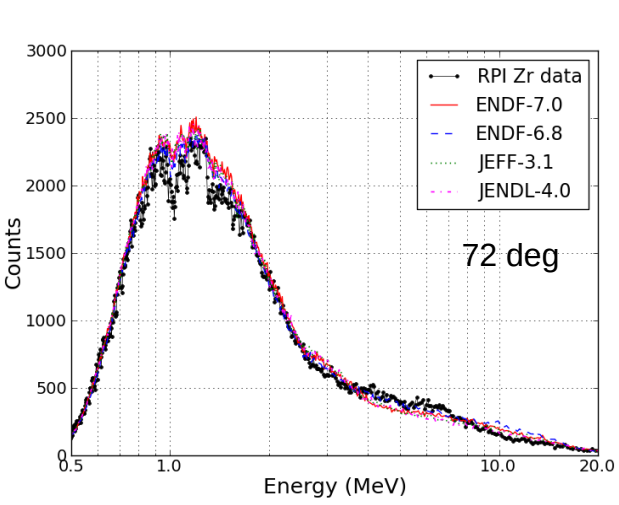

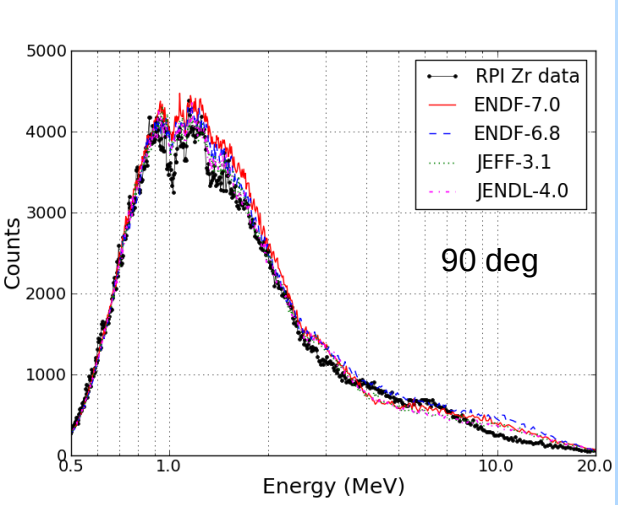

D. P. Barry, G. Leinweber, R. C. Block, and T. J. Donovan, Y. Danon, F. J. Saglime, A. M. Daskalakis, M. J. Rapp, and R. M. Bahran, "Quasi-differential Neutron Scattering in Zirconium from 0.5 MeV to 20 MeV", Nuclear Science and Engineering, 174, 188–201, (2013)

Zr – 10 cm Thick Sample

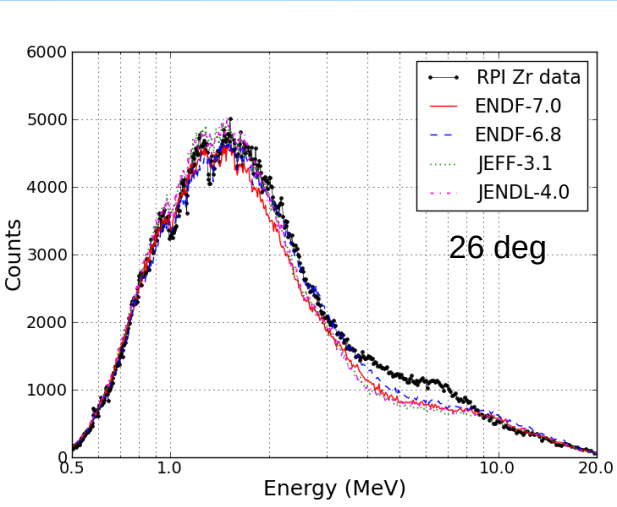

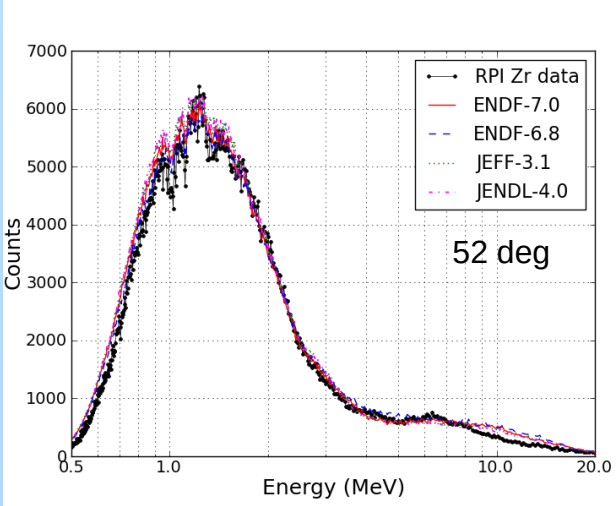

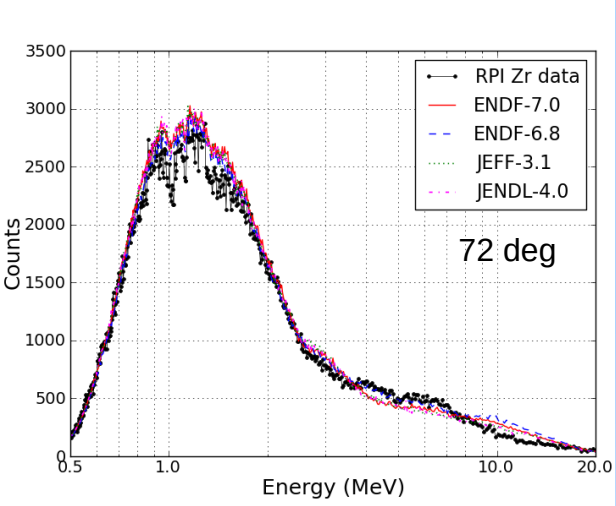

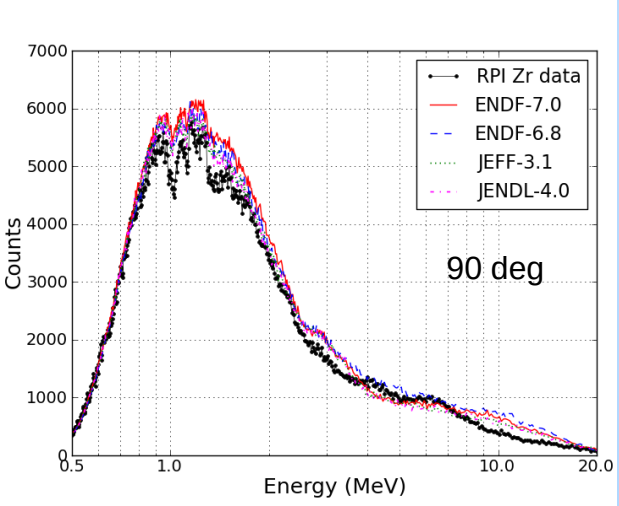

Figure-Of-Merit

- Objective
  - Quantify how well the MCNP simulations match the experimental data
- Methodology
  - Calculate over entire ROI
    - 0.5 to 20 MeV
  - Calculate FOM for each library
    - ENDF/B-VII.1
    - JEFF-3.2
    - JENDL-4.0
  - If FOM > 1 for ^{238}U or ^{Nat}Fe the observed differences are greater than *Ref*

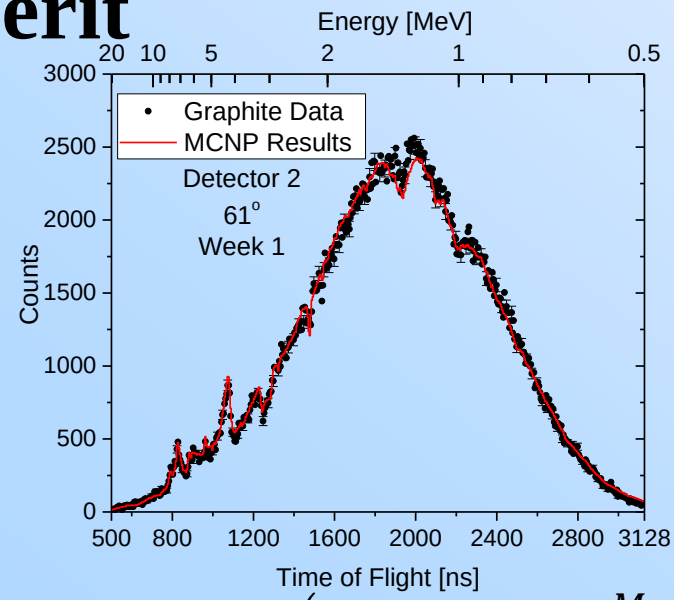

$$\mathrm{FOM} = \frac{1}{\mathrm{I}} \cdot \sum_{i=0.5\ \mathrm{MeV}}^{\mathrm{I=20\ MeV}} \frac{\left(C_i^X - \overline{\mathrm{N}} \cdot \mathrm{MC}_i^X \cdot \frac{M_X}{M_{\mathrm{Ref}}}\right)^2}{\left(\delta C_i^X\right)^2 + \left(C_i^X \cdot \frac{\varepsilon_{sys}}{\overline{\mathrm{N}}}\right)^2}$$

i - Energy (or TOF) bin
C_i^X - Neutron counts from sample
$\overline{\mathrm{N}}$ - Normalization factor
MC_i^X - MCNP counts from sample with specific library
M_X - Monitors counts during sample-in measurement
M_{Ref} - Monitors counts during *Ref* measurement
ε_{sys} - Systematic uncertainty
δC_i^X - Statistical uncertainty for sample
X - *Ref* or sample of interest

†C_i^X and MC_i^X are background subtracted

^{238}U TOF Results

- First three inelastic states are at 0.045, 0.148, and 0.307 keV
- Above 1.5 MeV neutrons from fission contribute to the measured counts
  - "Neutron induced neutron measurement"

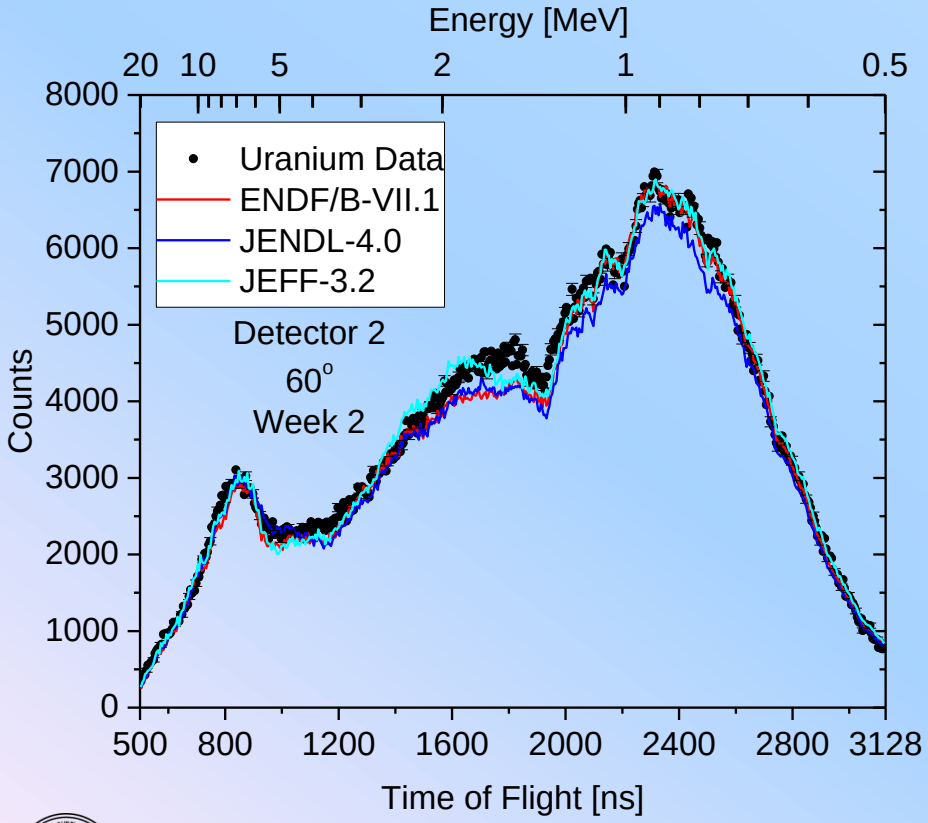

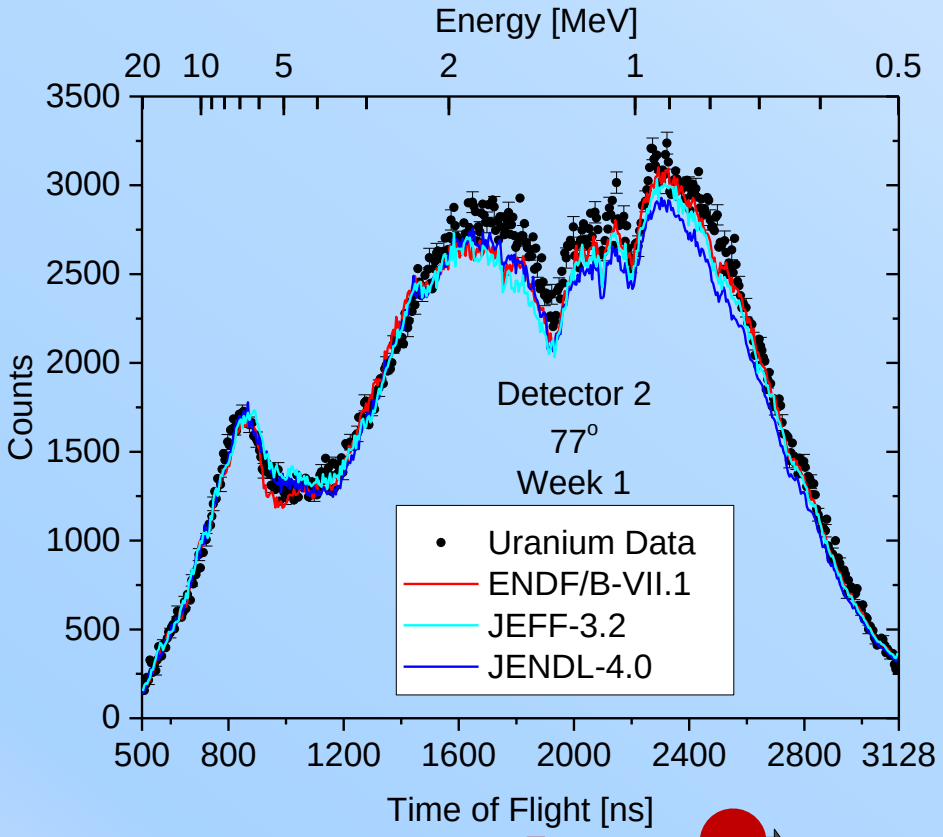

^{238}U TOF Results

- Measurement consistency was confirmed by examining the response from detectors that were not repositioned between experiments
- Observed differences that occur between ^{238}U experimental data and the MCNP simulations can provide evaluators with additional information needed to construct a more accurate ^{238}U library

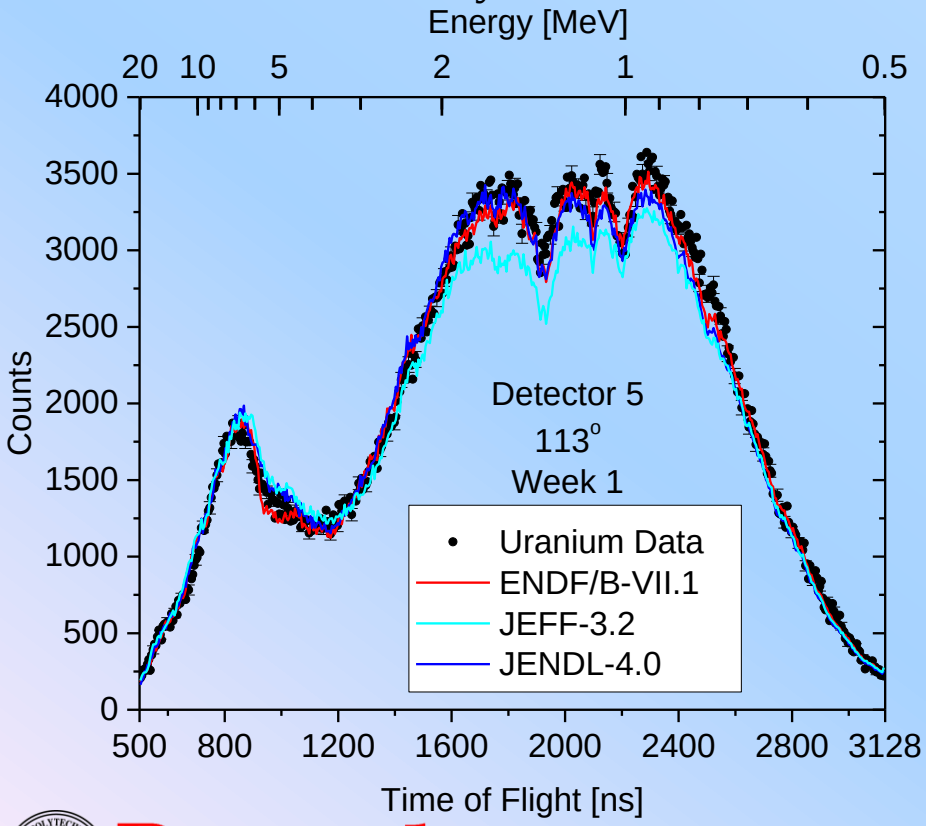

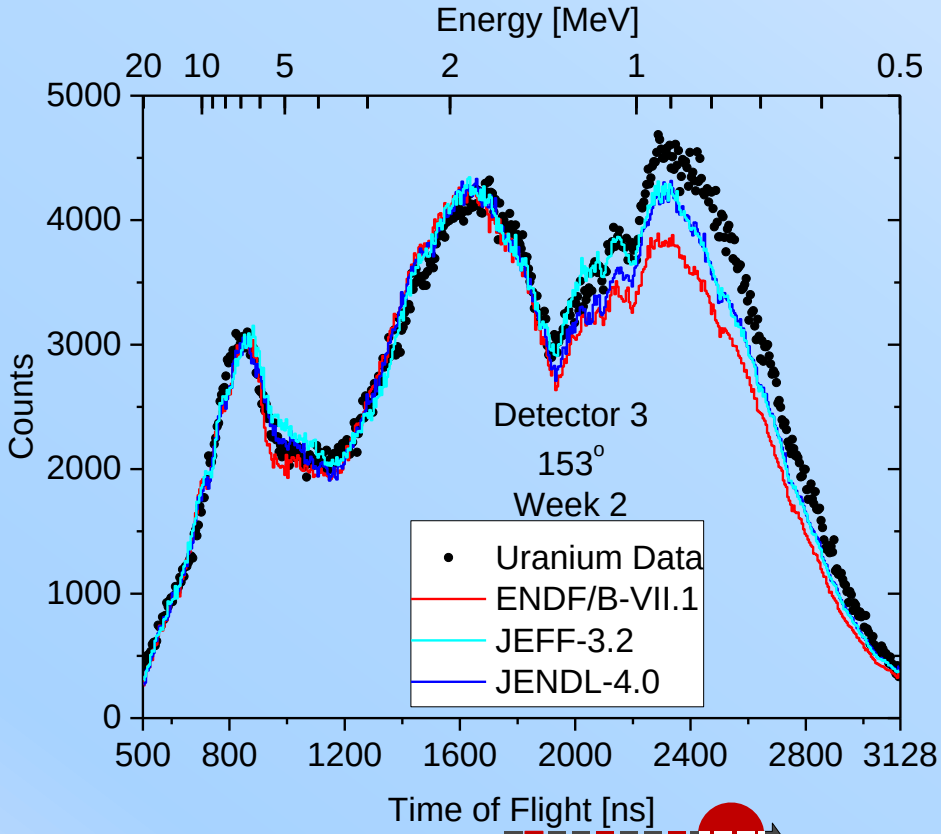

^{238}U TOF Results - FOM

- **FOM:**
  - The JENDL-4.0 ^{238}U library had the best overall agreement with the data; specifically, for detectors positioned at scattering angles greater than 90°
  - The JEFF-3.2 also performed well with detectors at back angles; however, varied greatly with detectors positioned at ≈110° and 130°
  - The ENDF/B-VII.1 library had good agreement with experimental data between 45° to 130° (with the exception of 60°)

Angle	ENDF/B-VII.1	JENDL-4.0	JEFF-3.2
27	1.46	**1.08**	**1.08**
29	3.65	**2.59**	3.04
45	**1.04**	1.59	1.35
60	1.70	2.49	**1.29**
77	**0.87**	1.57	1.21
77	**1.06**	1.32	1.33
112	**0.33**	**0.56**	**0.94**
113	**0.32**	**0.52**	1.09
130	**1.56**	**1.59**	2.28
130	**1.88**	**1.95**	2.65
153	2.15	**0.91**	**0.89**
156	3.54	**1.42**	**1.34**
153	3.20	**1.31**	**1.35**
156	4.28	**1.75**	**1.74**

A.M. Daskalakis, R.M. Bahran, E.J. Blain, B.J. McDermott, S. Piela, Y. Danon, D.P. Barry, G. Leinweber, R.C. Block, M.J. Rapp, R. Capote, A. Trkov, "Quasi-differential neutron scattering from 238U from 0.5 to 20 MeV", Annals of Nuclear Energy, Volume 73, Pages 455-464, November 2014

†Bold values indicate best fitting libraries.
Angles with two bold values indicate that the two libraries were statistically indistinguishable

IAEA ^{238}U Evaluation

- JEFF-3.1.2
- Collaboration with IAEA† on their ^{238}U evaluation
  - Agreement with experimental data provides a means to benchmark their new evaluation

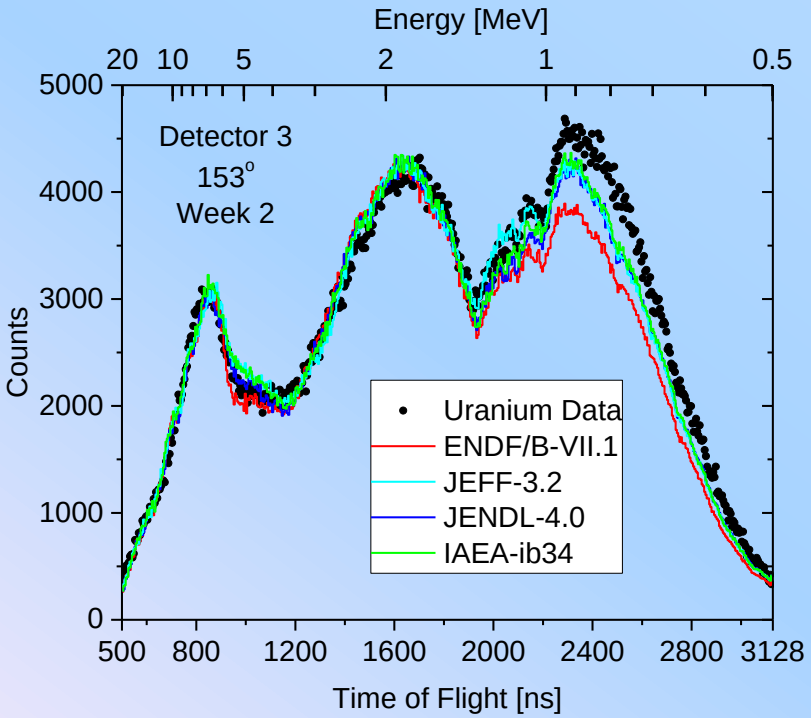

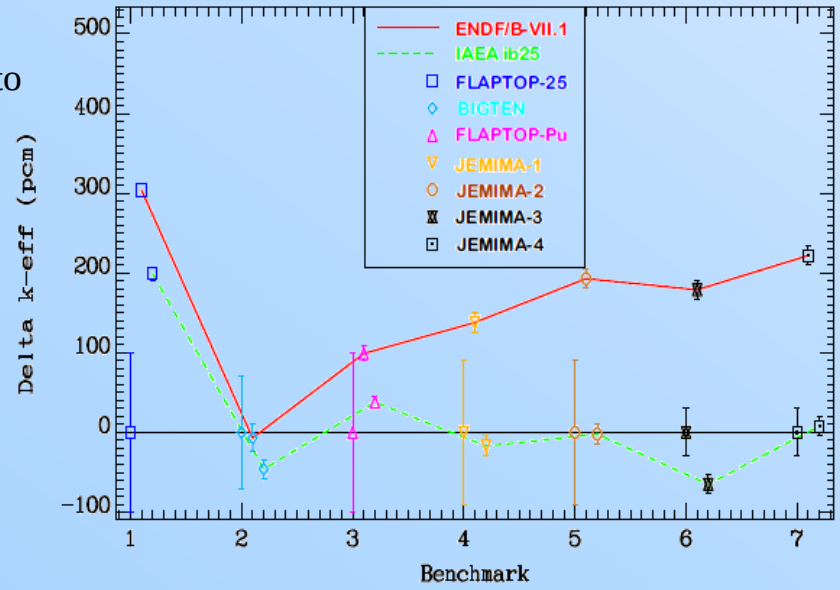

R. Capotea, A. Trkovb, M. Sinc, M. Hermand, A. Daskalakise, Y. Danon, "Physics of Neutron Interactions with ^{238}U: New Developments and Challenges," *Nucl. Data Sheets*, vol. 118, pp. 26-31, Apr. 2014.

†Dr. R. Capote and Dr. A. Trkov

^{Nat}Fe Scattering Experiment Setup

- ^{56}Fe Identified as an isotope of interest for Gen IV reactors and WPEC-SG26
- Iron consists of 4 naturally occurring isotopes:
  - ^{54}Fe (5.845%), ^{56}Fe (91.754%), ^{57}Fe (2.119%), and ^{58}Fe (0.282%)
- TOF experiments for ^{Nat}Fe were performed similar to ^{238}U experiments:
  - 7 angles were measured
  - Detectors at ≈155° were not repositioned
  - Three sets data were collected:
    - ^{Nat}Fe, *Ref*, Open Beam
  - Beam monitors recorded fluctuations in neutron intensity

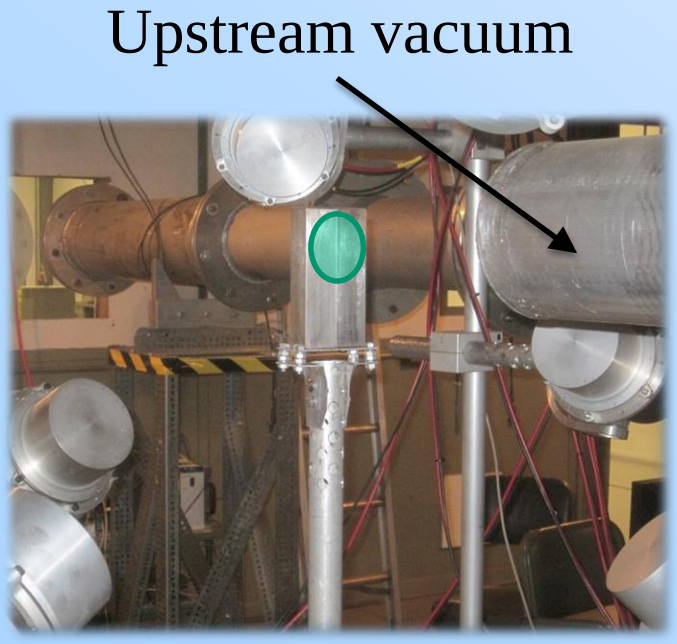

^{Nat}Fe TOF Results - Forward angle

- Resonance structure visible from 0.5 to ≈3 MeV
- Below 1.3 MeV only elastic neutrons were measured
  - ^{56}Fe first inelastic state is 0.847 MeV

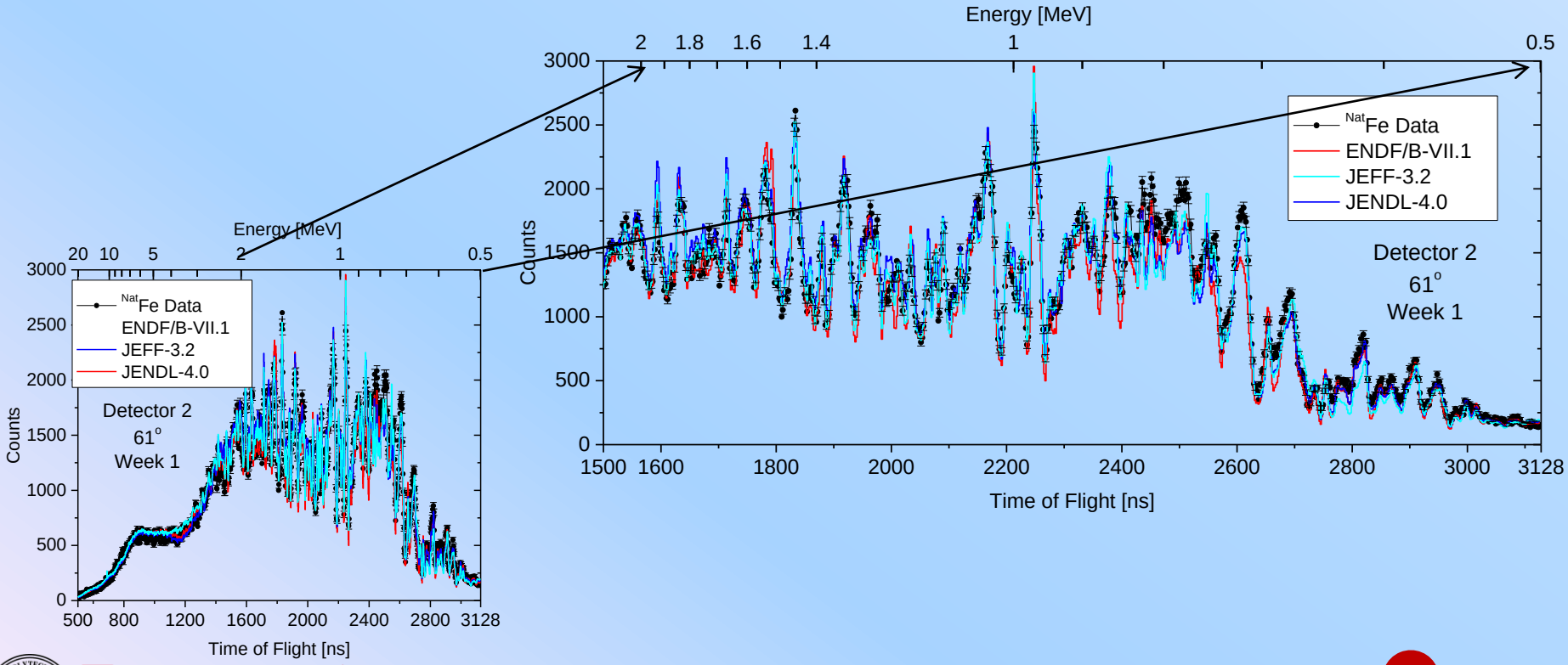

^{Nat}Fe TOF Results – Back angle

- Measurement consistency was again confirmed
- Structure at back angles was more prominent in the data than MNCP simulation

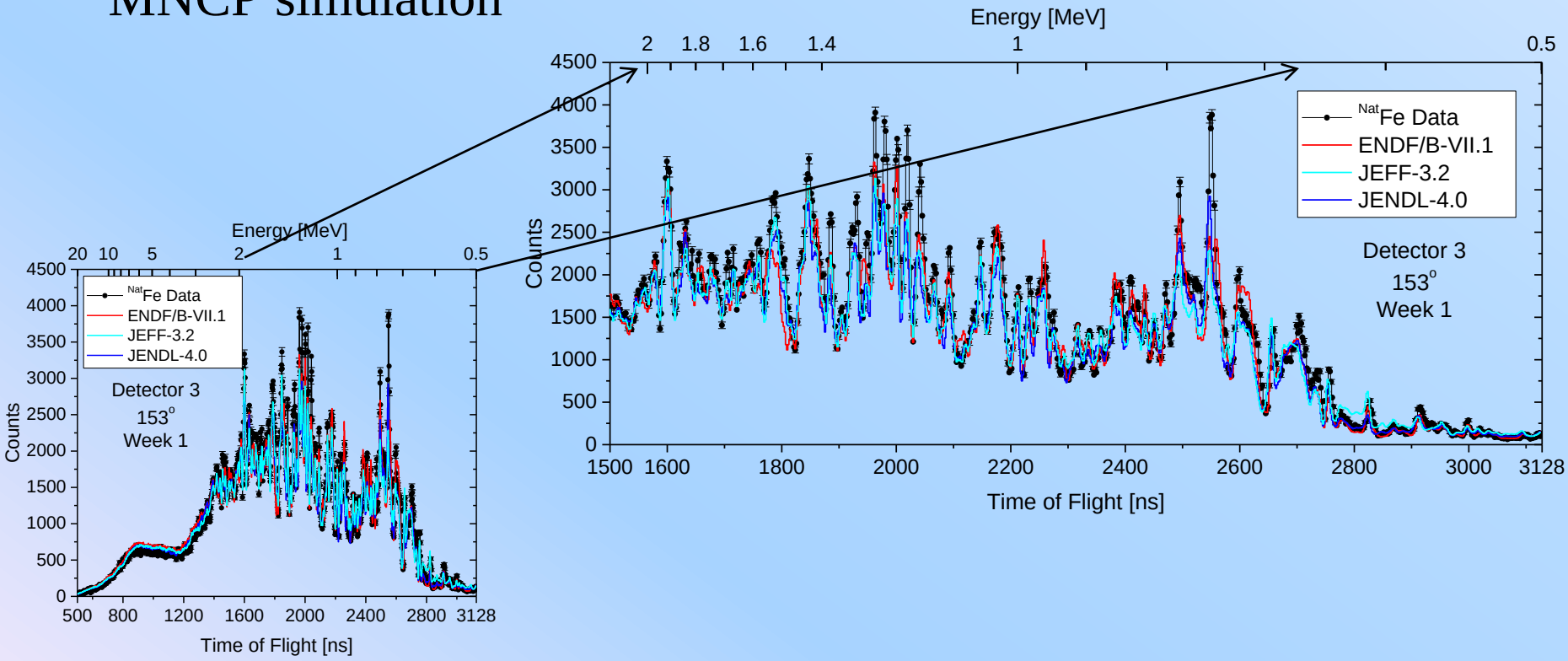

^{Nat}Fe TOF Results - FOM

- **FOM:**
  - The JENDL-4.0 ^{238}U library had the best agreement with the data
  - The ENDF/B-VII.1 library had good agreement with detectors positioned at back angles of 155º
  - The JEFF-3.2 had the worst agreement of the three evaluations examined

Angle	ENDF/B-VII.1	JENDL-4.0	JEFF-3.2
30	6.68	**5.36**	13.54
45	5.80	**4.27**	7.43
61	7.22	**6.41**	7.28
77	**6.14**	**6.34**	7.26
111	4.68	**3.30**	4.94
109	5.12	**3.28**	4.89
130	3.11	**2.16**	4.03
130	4.82	**3.72**	6.51
153	**5.44**	**5.60**	7.32
153	5.26	**4.75**	8.09
156	**4.85**	**5.02**	6.27
156	**5.51**	**5.64**	9.10

†Bold values indicate best fitting libraries.
Angles with two bold values indicate that the two libraries were statistically indistinguishable

Response Function Development

- Provide an additional way to assess evaluations with experimental data
  - Specifically, provide a measured quantity related to elastic and inelastic scattering
- At each TOF bin near mono-energetic neutrons were measured
- Response Function (RF) Development:
  - Isolate a narrow energy region and record each pulse's integral, *I* (area under pulse)
    - Distribution for a particular neutron energy
  - 23 RF were developed for neutron energies between 0.5 and 3.2 MeV
    - 0.1 MeV intervals up to 2.0 MeV
    - 0.2 MeV intervals between 2.0 and 3.2 MeV
  - Unique for each detector

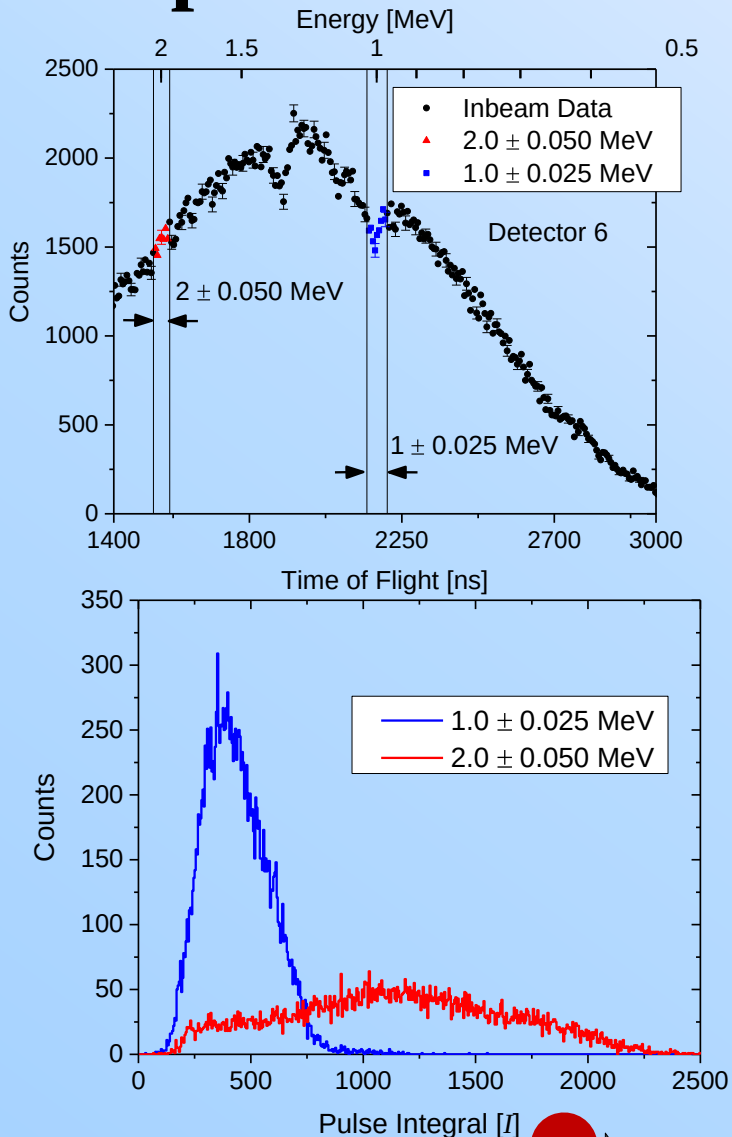

Inelastic-to-Elastic Ratios

- I/E range from 1.4 to 2 MeV
  - Only two energies are expected:
    - Elastic scattering
    - Inelastic from ^{56}Fe†

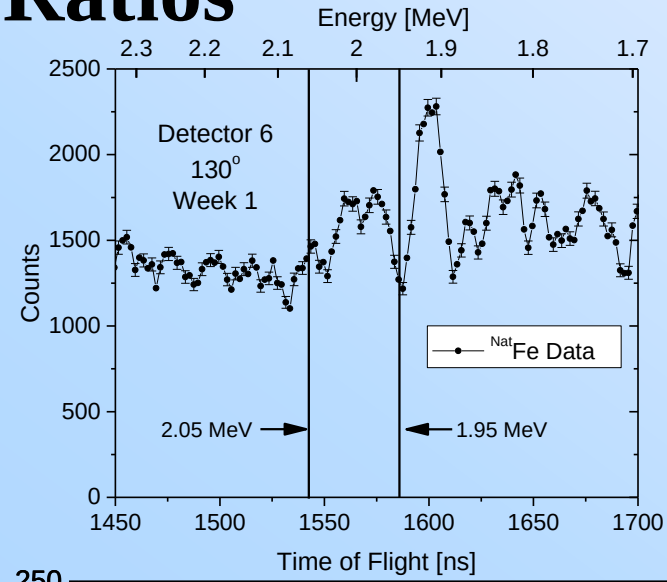

- RF with energies corresponding to elastic and inelastic scattering are fit to the scattering data

$$C(\mathrm{E}_n) = A \cdot \mathrm{R}(\mathrm{E}_{el}) + (1 - A) \cdot \mathrm{R}(\mathrm{E}_{inl})$$

- Ratio of inelastic-to-elastic was calculated

$$\mathrm{I/E} = \frac{(1 - A)}{A}$$

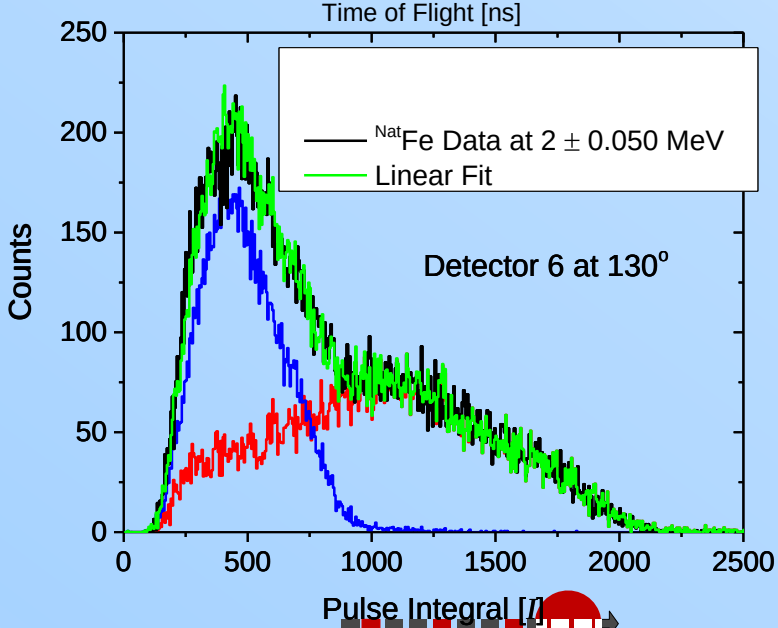

†^{54}Fe, ^{57} 1st state ≈1.4 and ≈ 0.12 MeV, ^{58}Fe only 0.282%

‡Not differential XS ratios (multiple scattering)

^{Nat}Fe I/E Results

- **Results – Forward Angles:**
  - Forward detectors underestimate I/E ratios
  - The I/E ratio was greater than 1 for detectors close to 90º at energies near 2.0 MeV indicating sensitivity to inelastic scattering

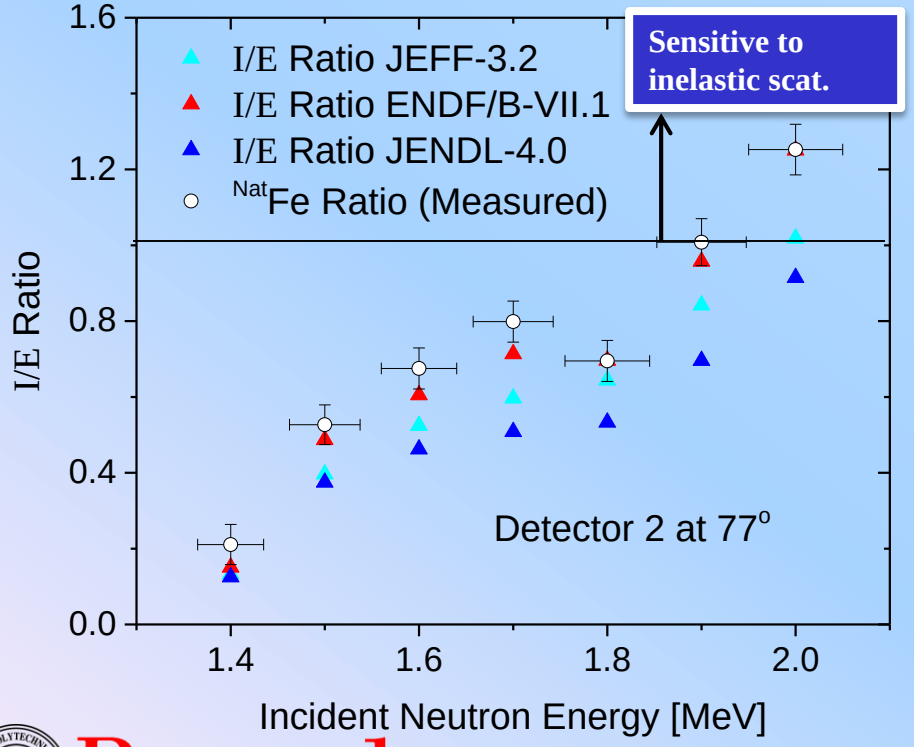

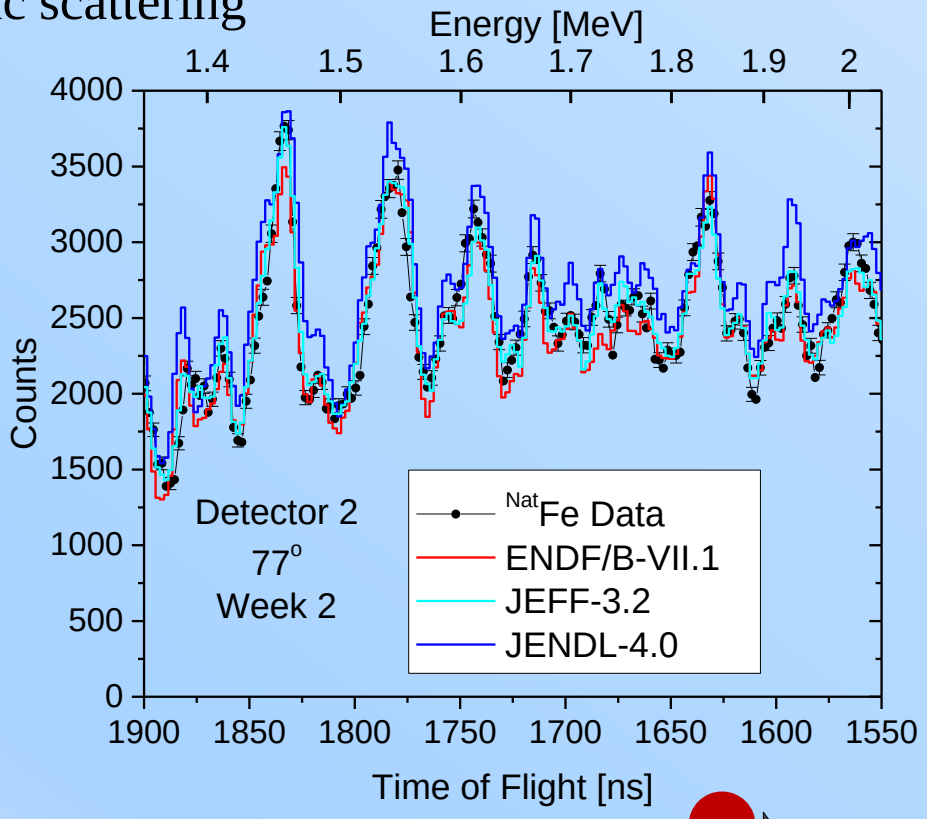

^{Nat}Fe I/E Results

- **Results – Back Angles:**
  - All evaluations had good agreement up to 2.0 MeV where ENDF/B-VII.1 overestimates the I/E ratio

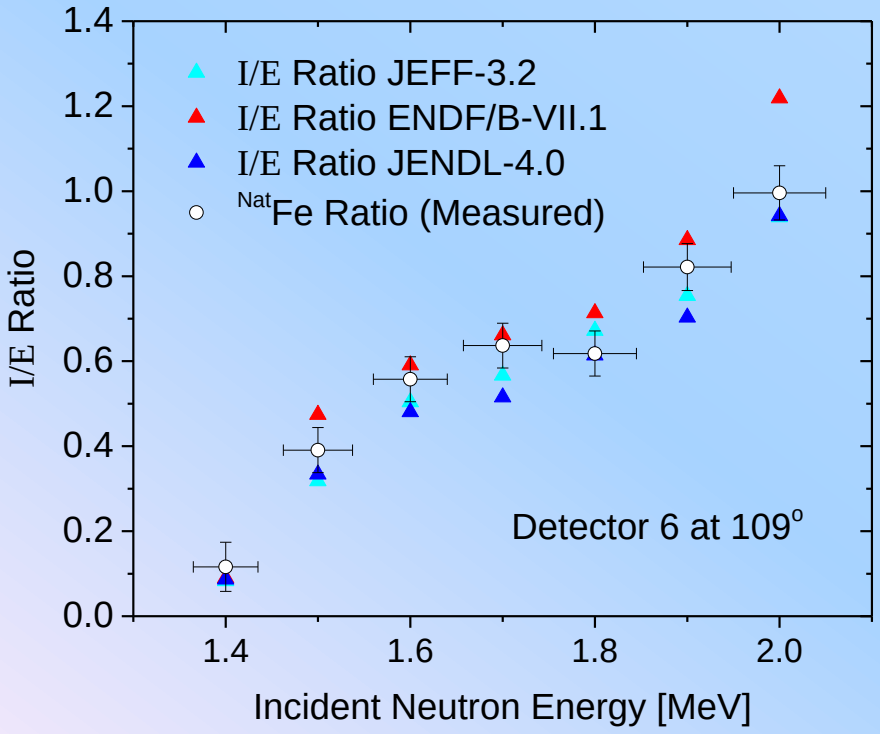

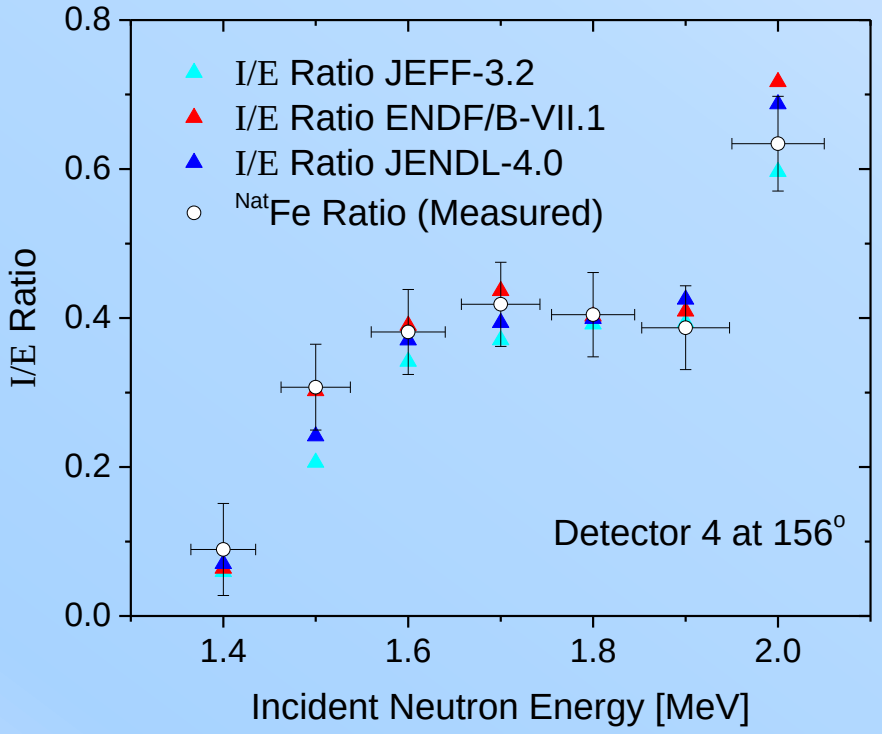

^{Nat}Fe I/E Results

- **Forward scattering angles:**
  - The ENDF/B-VII.1, JEFF-3.2, and JENDL-4.0 evaluations were in agreement with 9, 5, and 5 energy bins, respectively (28 total energy bins).
- **Back scattering angles:**
  - The ENDF/B-VII.1, JEFF-3.2, and JENDL-4.0 evaluations were in agreement with 41, 37, and 39 energy bins, respectively (56 total energy bins).
- **I/E and TOF:**
  - Although I/E ratios may be in good agreement with the experimental values this should be used in parallel with TOF results to assess the accuracy of an evaluation.

- To separate elastic and inelastic events in TOF another method that uses RF was developed

Moving Window Discriminator

- Locate “end point” location for each measured RF
- TOF used to determine elastic and inelastic energies
  - Set discriminator to max pulse integral for inelastic neutrons
  - ***Correct for missing elastic contribution (next slide) to preserve the detection efficiency***

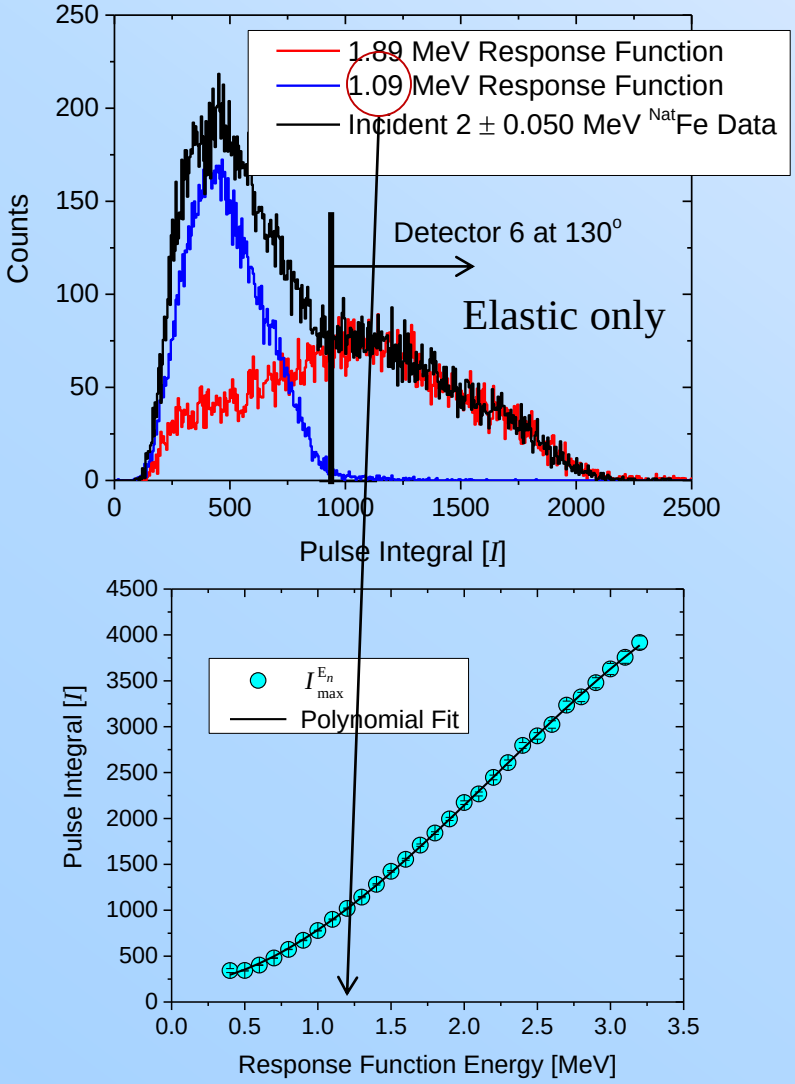

Moving Window Discriminator

- At each TOF the fraction of the elastic RF above the discriminator was calculated and the measured counts were corrected
- High statistical uncertainties come from limited counts present in RF and scattering experiments

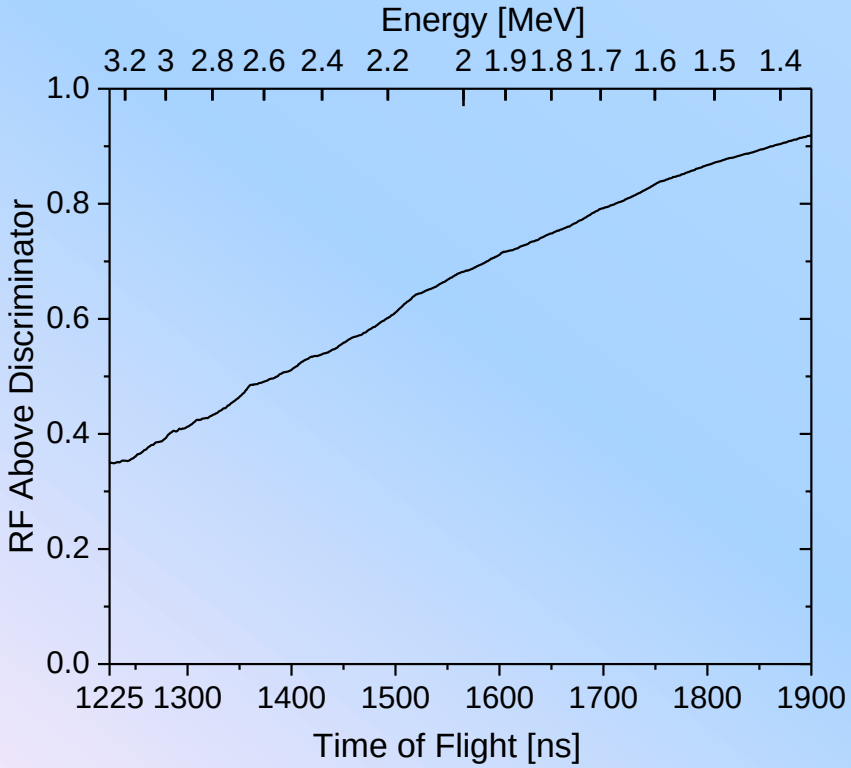

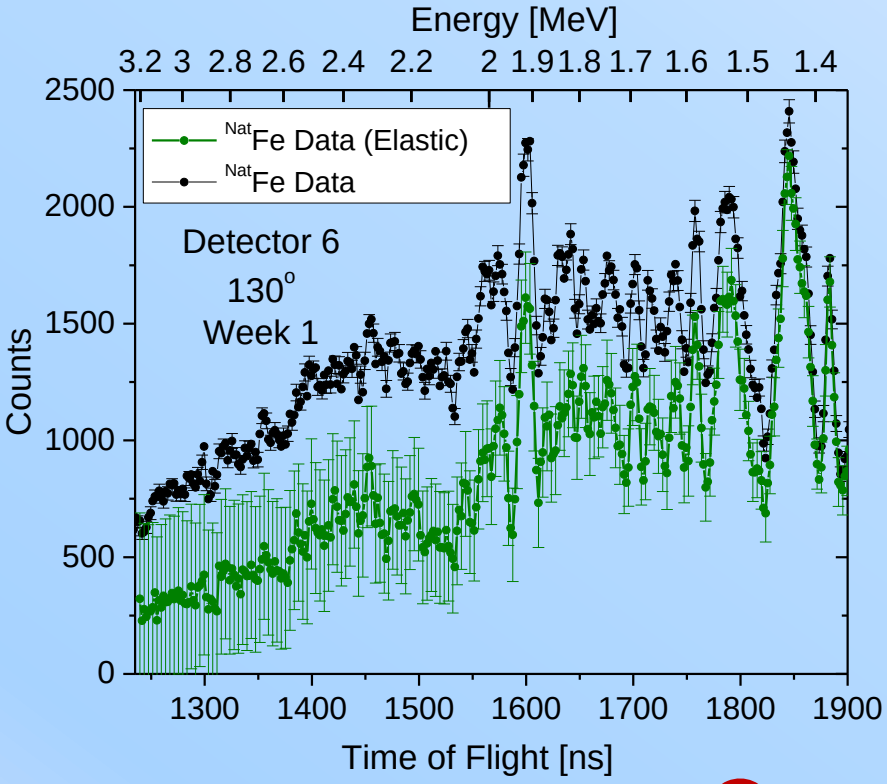

^{Nat}Fe Elastic Scattering

- The JENDL-4.0 evaluation overestimated the elastic signal at 77°
- It seems that the I/E ratio for JENDL is low because the elastic scattering is too high.

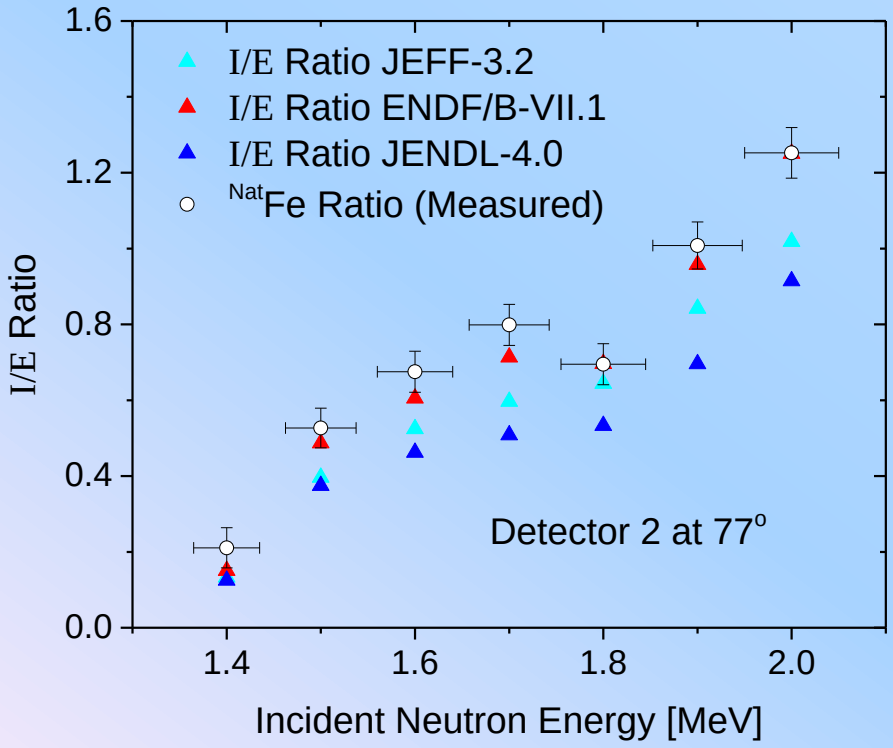

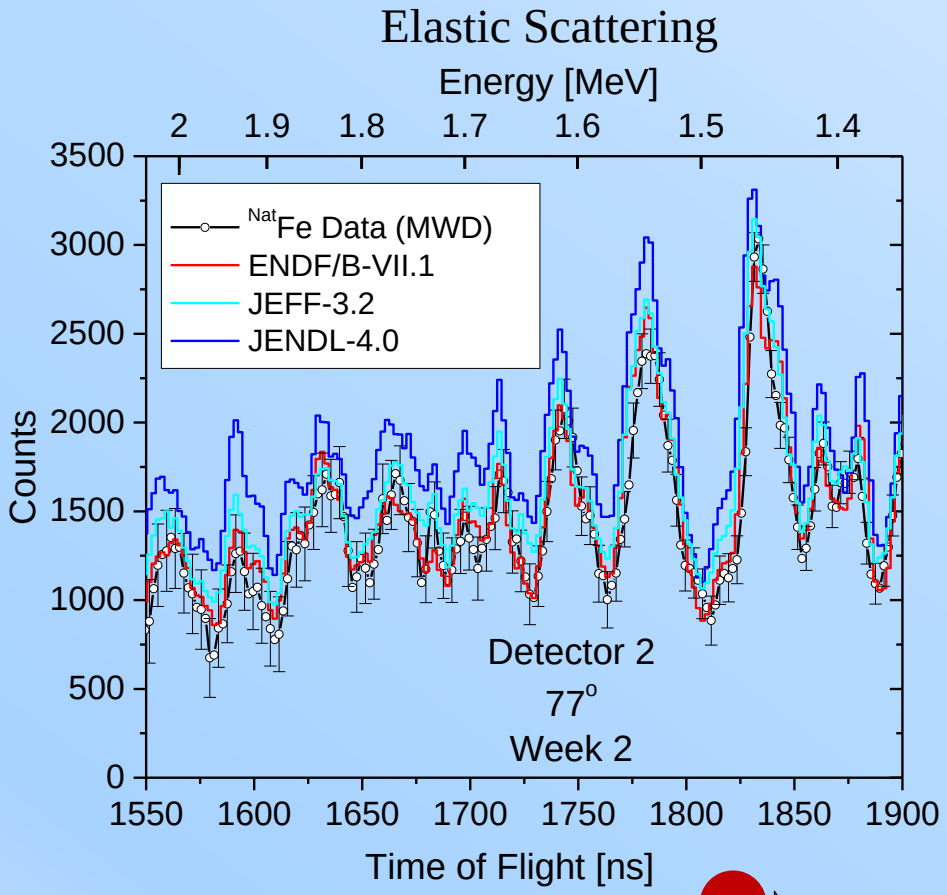

^{Nat}Fe FOM - Elastic only (1.4 - 2 MeV)

- The JEFF-3.2 evaluation had the best agreement with the elastic only experimental data and the ENDF/B-VII.1 evaluation had the least
- This technique was used to assess only elastic scattering
- Future improvements to RF could reduce uncertainties above 2.0 MeV

Angle	ENDF/B-VII.1	JENDL-4.0	JEFF-3.2
30	20.38	22.61	**6.64**
45	11.07	7.11	**6.64**
61	**4.30**	9.58	5.15
77	**4.20**	34.65	9.23
111	10.60	4.36	**2.94**
109	3.81	**1.26**	**1.10**
130	1.72	**0.82**	**0.29**
130	3.20	1.12	**0.58**
153	5.49	4.93	**2.45**
153	12.74	9.99	**4.33**
156	2.70	2.66	**1.13**
156	6.18	5.24	**1.92**

Conclusions

- Measurements at RPI include: thermal, resonance , and fast neutron scattering
- The fast neutron detector array measures the neutron scattering yield and fission neutron emission from a sample
- Simulation of the system with different libraries shows differences from the experimental data
  - Can be used to benchmark evaluations
  - Can be used to improve evaluations
- The accuracy of the experiments is sufficient to provides:
  - A recommendation of which evaluated library is best for treatment of neutron scattering
  - Pinpoint the differences in angle and energy and provide information to evaluators.
- Future outlook
  - Expand the system to neutrons below 0.5 MeV
  - Perform similar measurements at LANL with the Chi Nu fast detector array.

Some Related RPI Publications

- **Journal**
  - A.M. Daskalakis, R.M. Bahran, E.J. Blain, B.J. McDermott, S. Piela, Y. Danon, D.P. Barry, G. Leinweber, R.C. Block, M.J. Rapp, R. Capote, A. Trkov, "*Quasi-differential neutron scattering from 238U from 0.5 to 20 MeV*", Annals of Nuclear Energy, Volume 73, Pages 455-464, November 2014.
  - R. Dagan, B. Becker, Y. Danon, F. Gunsing, S. Kopecky, C. Lampoudis, O. Litaize, M. Moxon, P. Schillebeeckx, "*Impact of the Doppler Broadened Double Differential Cross Section on Observed Resonance Profiles*", Nuclear Data Sheets, 118, 179–182 (2014).
  - R. Capote, A. Trkov, M. Sin M. Herman, A. Daskalakis, and Y. Danon, "*Physics of Neutron Interactions with ^{238}U: New Developments and Challenges*", Nuclear Data Sheets 118, 26–31, (2014).
  - D. P. Barry, G. Leinweber, R. C. Block, and T. J. Donovan, Y. Danon, F. J. Saglime, A. M. Daskalakis, M. J. Rapp, and R. M. Bahran, "*Quasi-differential Neutron Scattering in Zirconium from 0.5 MeV to 20 MeV*", Nuclear Science and Engineering, 174, 188–201, (2013).
  - R.Dagan, B. Becker, Y. Danon, "*A complementary Doppler Broadening formalism and its impact on nuclear reactor simulation*", Kerntechnik 3, Page 185-189, (2011).
  - Frank J. Saglime III, Yaron Danon, Robert C. Block, Michael J. Rapp, Rian M. Bahran, Greg Leinweber, Devin P. Barry, Noel J. Drindak, and Jeffrey G. Hoole, "*A system for differential neutron scattering experiments in the energy range from 0.5 to 20 MeV*", Nuclear Instruments and Methods in Physics Research Section A, 620, Issues 2-3, Pages 401-409, (2010).
  - Tae-Ik Ro, Yaron Danon, Emily Liu, Devin P. Barry and Ron Dagan, "*Measurements of the Neutron Scattering Spectrum from ^{238}U and Comparison of the Results with a Calculation at the 36.68-eV Resonance*", Journal of the Korean Physical Society, Vol. 55, No. 4, , pp. 138-1393, October 2009.
- **Conference Proceedings**
  - Y. Danon, L. Liu, E.J. Blain, A.M. Daskalakis, B.J. McDermott, K. Ramic, C.R. Wendorff, D.P. Barry, R.C. Block, B.E. Epping, G. Leinweber, M.J. Rapp, T.J. Donovan, "*Neutron Transmission, Capture, and Scattering Measurements at the Gaerttner LINAC Center*", Transactions of the American Nuclear Society, Vol. 109, p. 897-900, Washington, D.C., November 10–14, 2013
  - Adam M. Daskalakis, Rian M. Bahran, Ezekial J. Blain, Brian J. McDermott, Sean Piela, Yaron Danon, Devin P. Barry, Greg Leinweber, Robert C. Block, Michael J. Rapp, "*Quasi-Differential Neutron Scattering Measurements of ^{238}U*", ANS Winter Meeting and Nuclear Technology Expo, American Nuclear Society, San Diego CA. November 11-15, 2012.
  - Frank J. Saglime III, Yaron Danon, Robert C. Block, Michael J.Rapp, and Rian M. Bahran, Devin P. Barry, Greg Leinweber, and Noel J. Drindak, "*High Energy Neutron Scattering Benchmark of Monte Carlo Computations*", International Conference on Mathematics, Computational Methods & Reactor Physics (M&C 2009), Saratoga Springs, New York, May 3-7, 2009, on CD-ROM, American Nuclear Society, LaGrange Park, IL (2009).
  - Frank J. Saglime III, Yaron Danon, Robert Block, "*Digital Data Acquisition System for Time of Flight Neutron Beam Measurements*", The American Nuclear Society's 14th Biennial Topical Meeting of the Radiation Protection and Shielding Division, p. 368, Carlsbad New Mexico, USA. April 3-6, 2006.